Design and Application of Dextran Based Cross-linked Networks

Proefschrift

ter verkrijging van

de graad van Doctor aan de Universiteit Leiden,

op gezag van Rector Magnificus Prof. mr. C.J.J.M. Stolker,

volgens besluit van het College voor Promoties

te verdedigen op donderdag 18 oktober 2018

klokke 10:00 uur

door

Yue Gao

geboren op 15 Januari 1986 te Jilin, China

Promotiecommissie:

Promoter:	Prof. dr Alexander Kros
Co-promotor:	Dr. Roxanne Kieltyka
Overige leden:	Prof. Dr. H.S. Overkleeft (voorzitter)
	Prof. Dr. J. Brouwer (secretaris)
	Prof. Dr. J. Bouwstra
	Prof. Dr. J van der Gucht, Wageningen Universiteit
	Dr. T. Vermonden, Universiteit Utrecht

TABLE OF CONTENTS

CHAPTER 1	General introduction	5
CHAPTER 2	Thiolated human serum albumin crosslinked dextran hydrogel as a macroscale delivery system	19
CHAPTER 3	Dual-crosslinked human serum albumin-polymer hydrogels for affinity-based drug delivery	37
CHAPTER 4	Zebrafish embryo toxicity assay using a cyclodextrin-modified dextran-PEG polymeric drug carrier	61
CHAPTER 5	Chemically crosslinked polymer networks assist the formation of giant unilamellar vesicles	81
CHAPTER 6	The effect of coiled-coil peptide conjugation on dextran self-assembly	107
CHAPTER 7	Summary and perspectives	137
	Samenvatting	143
	List of abbreviations	147
	Curriculum Vitae	149
	List of publications	150

Chapter 1

General Introduction

DEXTRAN

Polymers such as proteins and polysaccharides, abundantly exist in nature and are major components of plants, animals and micro-organisms.[1] Polysaccharides are polymers composed of monosaccharide units connected through glycosidic bonds.[2, 3] The glycosidic bonds are formed by a condensation reaction between the anomeric carbon (C1) of one monosaccharide unit and an oxygen atom from a hydroxyl group on another monosaccharide unit. Since hydroxyl groups present on C2, C3, C4 and C6 carbons, the generated glycosidic bonds can be 1→2, 1→3, 1→4, or 1→6 linked providing linear to highly branched chains. Polysaccharides can be categorized into two groups: (1) mammalian polysaccharides such as hyaluronan, chondroitin sulfate, and heparin; (2) non-mammalian polysaccharides such as alginate, chitin, and dextran (Scheme 1).

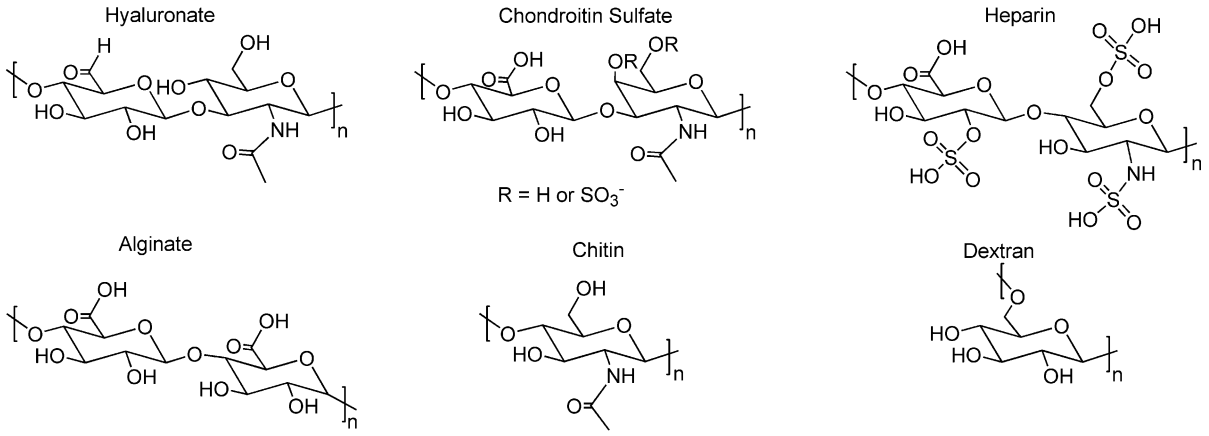

Scheme 1. *Main structures of repeating units of some polysaccharides widely investigated in biomaterials applications. Top row: mammalian polysaccharides; bottom row: nonmammalian polysaccharides.*

Dextran is a neutral and hydrophilic polysaccharide consisting of an α-(1→6) linked D-glucose main chain with a relatively low level of α-(1→3) branched linkages.[4, 5] The molecular weight of dextran chains can vary from 1 to 2 000 kilodaltons (kDa). Although physiochemical properties of each dextran polymer depend on its particular structure (e.g. molecular weight and degrees of branching), the glycosidic bonds of dextran provide relatively high chain mobility and solubility, while the three pendant hydroxyl groups provide handles for its functionalization.[6-8] Moreover, dextran is biologically inert due to the α-(1→6) glycosidic bonds making it resistant to cleavage by most endogenous cellular glycosidases, but it is degradable by dextranase[9] which exists in mammalian (including human) tissues. Dextran is also non-immunogenic,[10-14] making it an attractive polymer for the design of novel biomaterials.

Dextran and dextran derivatives are already successfully commercialized in the biomedical field. Examples of dextrans used pharmaceutically include those of molecular weight 70 kDa

(Macrodex®) and 40 kDa (Rheomacrodex®) for plasma expansion.[15-17] Furthermore fluorescent dye-dextran conjugates (Molecular Probes®) are widely applied in numerous biological studies.[18] Dextran can also be crosslinked by epichlorohydrin to form hydrogel beads, which are used for separations of molecules based on differences in molecular weight (e.g. Sephadex®).[19] Dextran-based materials are also used in wound healing (e.g. Debrisan®).[20]

Due to their hydrophilicity, long shelf-life, relative stability, biocompatibility and biodegradable properties, dextrans have been studied as a starting material for drug delivery carriers. Cargo that was delivered in these studies included low molecular weight drugs, proteins/enzymes, and imaging agents by either direct attachment or through a linker since the 1980s.[11, 21-23] Degradation of linkages between dextran and the conjugated drug results in the delivery of therapies. Dextran conjugation was also used to overcome problems such as limited solubility of the drug, short plasma half-life high toxicity and/or undesired interactions with tissues. For example, the solubility of paclitaxel increased >2000 fold upon conjugation to aminated dextran (M_w = 70 000). Furthermore, modification of the dextran-paclitaxel conjugates with folate increased the uptake 2-3 folds in human oral carcinoma KB cells.[24] The *in vivo* biodistribution and circulation time can also be altered upon dextran conjugation. For example, prolonged circulation time and decreased uptake in kidney were observed for dextran-mouse epidermal growth factor (mEGF) conjugates, wherein mEGF was attached to aldehyde group functionalized dextran polymers *via* the formation of imine bonds which was further stabilized by reducing to secondary amide bonds with $NaCNBH_3$.[25, 26]

HYDROGELS

Hydrogels are a class of soft materials that possess a hydrophilic three-dimensional (3D) network hold together *via* chemical and/or physical bonds (i.e. crosslinks). Upon contact with water, the 3D-network swells and the (physically) entrapped molecules diffuse out of the network and the kinetics of release depend on both the properties of the encapsulated molecule as well as the physical characteristics of the hydrogel. The viscoelastic properties are similar to soft tissues and combined with the water-rich environment making these hydrogels an attractive biomaterial with potential applications in the fields of tissue engineering and regenerative medicine.[27, 28] These hydrogels can be synthesized from various precursors over a large molecular weight range. In this thesis the formation of hydrogels comprised of dextran covalently crosslinked by proteins is described.

In the last two decades, *in situ* forming hydrogels have been extensively investigated since they can be delivered to patients in a minimally invasive fashion.[29, 30] *In situ* forming hydrogels allow premixing of drug compounds or cells,[31] followed by injection of the formulation with its non-toxic gelation due to polymer crosslinking in the target tissues in a therapeutically relevant time

period. To this end, extensively applied chemoselective ligations for *in situ* gelation include Michael addition,[32] azide-alkyne Click reactions,[33, 34] Schiff base formation[35] and disulfide exchange.[36] Moreover, physical crosslinking methods with suitable gelation kinetics can also be used to form *in situ* hydrogels.[37] The physical crosslinks can consist of hydrogen bonds, hydrophobic interactions, π-π interactions or host-guest inclusion, to endow the hydrogels with dynamic, reversible and self-healing properties.[38]

Hydrogels have been studied as a biomaterial for the localized and sustained release of therapeutic agents in order to decrease the number of drug administrations, to prevent rapid drug degradation or to prolong therapeutic drug concentrations.[39] Typical drug release mechanisms applied in drug delivery systems include diffusion controlled drug release[40], degradation controlled drug release,[41] stimuli triggered drug release,[42] and affinity-based drug release. The affinity-based drug release mechanism uses non-covalent interactions between the therapeutic agents and hydrogel platform, such as electrostatic, hydrophilic-hydrophobic, hydrogen bonding, or van der Waals interactions, to control the release of the therapeutic.[43] These materials can improve drug loading, stability and release. Affinity-based carriers include specific host molecules such as cyclodextrin,[44-48] serum albumin[49-52] and heparin[53-55], or cavities formed within the solid polymer material by the molecular imprinting technique.[56, 57]

DEXTRAN GELS

Since the 1990s, hydrogels composed of dextran have been developed for macroscale therapeutics delivery and 3D cell culture.[58, 59] Chemically crosslinked dextran hydrogels can be prepared from a functionalized dextran precursor. For example, Hennink and co-workers prepared degradable dextran hydrogels by free radical polymerization of aqueous solutions of glycidyl methacrylated dextran or hydroxyethyl methacrylated dextran for the delivery of proteins.[9, 60-62] Liu et al. used UV-light exposure to initiate the crosslinking between dextran functionalized with both methacrylate and lysine groups and methacrylamide modified gelatin in presence of a photoinitiator and cells to obtain a 3D smooth muscle cell culture.[63]

To improve the biocompatibility of the gelation process and the obtained hydrogels, crosslinked dextran hydrogels can be prepared from a pair of polymeric precursors that can react with each other under physiological condition. Hiemstra et al. synthesized thiol modified dextrans and vinyl-sulfone modified dextrans to induce hydrogel formation *via* a Michael type addition reaction.[64] Wei et al. synthesized fulvene modified dextran and dichloromaleic-acid modified poly(ethylene glycol) to develop self-healing dextran hydrogel *via* reversible Diels–Alder reaction.[65] Supramolecular dextran hydrogels have also be developed *via* specific non-covalent interactions. For example, Huh et al. established a thermo-reversible hydrogel system with poly(ethylene glycol) grafted dextrans

and α-cyclodextrins which was crosslinked by the inclusion complex formation between poly(ethylene glycol) and α-cyclodextrins.[66] De Jong et al. established another thermo-reversible hydrogel system with L-oligo(lactic acid) grafted dextran and D-oligo(lactic acid) grafted dextran which was crosslinked by the stereocomplex formation between enantiomers.[67]

Besides macroscopic dextran hydrogels, various emulsification approaches were applied to obtain chemically crosslinked dextran microgels (also called as microspheres or microcapsules) and nanogels. Using a cyclohexane inverse miniemulsion, crosslinked nanogels with an averaged diameter below 100 nm were prepared starting from alkyne-dextran and azide-dextran.[68] To avoid the use of organic solvents, "water-in-water" emulsions were used to synthesize microgels. Aqueous mixtures of dextran and polymers such as polyethylene glycol (PEG) or poly(vinyl alcohol) (PVA) can form an aqueous two-phase system at elevated concentrations, which can be emulsified to obtain a water-in-water emulsion. De Geest et al. emulsified an aqueous solution containing dextran azide and dextran alkyne in an external aqueous PEG phase. $CuSO_4$ and sodium ascorbate were added afterward to obtain dextran microgels *via* Huisgen click reaction.[69] Similarly, Ghugare et al. prepared dextran microgels with an averaged diameter around 1000 nm using ultrasound assisted "water-in-water" emulsification. The emulsion contained dextran methacrylate, photoinitiator and PVA was crosslinked under UV-light afterwards.[70]

Additionally, charged dextrans, such as dextran sulfate, dextran phosphate and dextran amine, have been used to prepare polyelectrolyte complex. For example, positively or negatively charged colloids were obtained from non-stoichiometric polyelectrolyte complexes of dextran sulfate and chitosan.[71] Dextran sulfate and protamine were constructed to microcapsules for enzyme delivery by a layer-by-layer approach using a removable melamine formaldehyde template.[72] Complexes formed by cationized dextran amine and plasmid DNA enhanced gene expression *in vitro*, showing its potentials for gene delivery.[73]

GENERAL OUTLINE OF THE THESIS

In the present thesis, several dextran-based hydrogel systems are synthesized and characterized for biomedical applications. To prepare dextran polymers for crosslinking, the backbone is initially functionalized with maleimides or vinyl sulfones, which are able to form covalent bonds with nucleophilic thiols *via* a thiol-Michael addition reaction. These reactive groups (i.e. maleimides or vinyl sulfones) were coupled to the hydroxyl groups of dextran *via* an ester or an ether linkage. The stability of linkages strongly affected the properties and applications of the prepared hydrogel systems as described in the following chapters.

Human serum albumin (HSA), the most abundant protein in human plasma, strongly binds various

types of (hydrophobic) low molecular weight molecules. Inspired by this natural carrier, a covalently crosslinked dextran-albumin hydrogel system was developed in **Chapter 2** to explore the potential of HSA as a hydrophobic-drug cavity and crosslinker for affinity-based drug delivery. Native HSA was modified with 2-iminothiolane (2-IT) to introduce thiol groups at the lysine residues. Circular dichroism spectroscopy revealed that the conformation of thiolated HSA (sHSA) is mostly maintained showing that sHSA was capable of simultaneously being a drug carrier and the crosslinker in the hydrogel system. The hydroxyl groups of dextran were modified with maleimide groups through the formation of ester linkages resulting in functionalized dextran (i.e. Dex-Mal). Next, sHSA was added to Dex-Mal resulting in gelation of the mixture under physiological conditions in a relatively fast manner. The resulting dextran-albumin (**Dex-Mal-sHSA**) hydrogel was characterized by oscillatory rheology experiments. *In vitro* release profiles of three hydrophobic drugs (i.e., ibuprofen, paclitaxel and dexamethasone) from the dextran-albumin hydrogel were recorded, showing high drug loading efficiency and demonstrating sustained release of the corresponding guest molecule.

To improve the stability and to gain control over the properties of the abovementioned dextran-albumin hydrogel system (Dex-Mal-sHSA), two new affinity-based drug delivery hydrogel systems were developed in **Chapter 3**. Firstly, a fraction of the dextran hydroxyl groups were modified with vinyl sulfone. The effect of reaction temperature, reaction time and dextran molecular weight was studied to control degree of vinyl sulfone modification of dextran (i.e. Dex-VS). In comparison to the Dex-Mal polymer in Dex-Mal-sHSA hydrogels used in Chapter 2, the obtained vinyl sulfone functionalized dextran polymers (Dex-VS) showed to be more stable against hydrolysis. Next, a new dextran-albumin hydrogel system (**Dex(VS)-sHSA**) with improved stability was developed by reacting Dex-VS with sHSA. However, the vinyl sulfone groups show relatively slower reaction kinetics towards thiol groups than the maleimide groups. To accelerate the gelation process while maintaining the concentration of albumin constant, a third macromolecular precursor, poly(ethylene glycol) dithiol (PEG-DT), was introduced into the dextran-albumin hydrogel. By balancing the number of reactive vinyl sulfone groups from Dex-VS and thiol groups from both sHSA and PEG-DT for the thiol-Michael addition reaction, the covalently dual-crosslinked **Dex(VS)-sHSA-PEG** hydrogel system was prepared where sHSA acts both as a drug carrier and crosslinker. Three Dex-sHSA-PEG hydrogels with different weight concentrations were studied by oscillatory rheology experiments and swelling tests and compared to the corresponding Dex(VS)-sHSA and Dex-VS-PEG hydrogels. By introducing the PEG crosslinker the gelation kinetics and the mechanical properties of the resulting three-component Dex-sHSA-PEG hydrogels could be more easily controlled in comparison to the other two dextran-albumin hydrogels. The capacity of the network to release a drug molecule, Doxorubicin, in a sustained manner was validated through *in vitro* studies using MCF-7 breast cancer cells.

Cyclodextrins are able to form a reversible host-guest complex with suitable hydrophobic molecules. In **Chapter 4** the potential of cyclodextrin-modified dextran based drug carriers in a zebrafish embryo toxicity assay was explored. Zebrafish embryos have become a promising model organism for developmental and reproductive toxicity screening studies.[17, 19, 74] However, ineffective uptake of certain compounds by zebrafish embryos was reported raising concerns of the predictive capacity of zebrafish embryo based toxicity assays.[75] It was reported that zebrafish embryos show a weaker than expected sensitivity for neurotoxic compounds with respect to acute toxicity.[76] Here, a previously reported β-cyclodextrin decorated dextran-poly(ethylene glycol) **Dex-CD/PEG** drug carrier system[45] was used to enhance the uptake of the model drug valproate in the zebrafish embryo toxicity assay. The polymeric drug carrier was synthesized by crosslinking maleimide modified dextran with poly(ethylene glycol) dithiol, wherein cyclodextrins were conjugated to the dextran backbone to ensure binding of valproate through the formation of a non-covalent host-guest complex. The uptake of fluorescent labelled Dex-CD/PEG drug carriers into the gastrointestinal tract of zebrafish embryos was observed by fluorescent microscopy. Comparison of zebrafish embryos exposed to valproate or valproate loaded Dex-CD/PEG carrier showed that the Dex-CD/PEG carrier improves the valproate uptake *via* the gastrointestinal tract. Correlations between the composition of Dex-CD/PEG carriers and the viability of 4-dpf zebrafish embryos after 48-hour exposure to valproate loaded Dex-CD/PEG carrier were also studied to investigate the role of Dex-CD/PEG carriers in the toxicity assay.

In **Chapter 5**, the capacity of hydrogels to guide the formation of giant unilamellar vesicles is explored. Giant unilamellar vesicles (GUVs) are widely used cell membrane model systems for biophysical measurements.[77-79] Recently, it was reported that GUVs can be prepared through hydration of a lipid film on a hydrogel consisting of agarose, which was more straightforward and rapid to generate GUVs in solutions of physiologic ionic strength.[80] However, using agarose for the hydrogel film results in contamination of the vesicles due to its dissolution during the hydration process. To address this issue, the chemically crosslinked polymer system **Dex-Mal-PEG** was covalently anchored to a glass slide as a substrate for GUV formation. Using this method, polymer and additive-free GUVs can be prepared rapidly in high yield under physiological ionic strength conditions. Moreover, by varying physiochemical properties of Dex-Mal-PEG hydrogels through controlling the molar ratio of the maleimide and thiol groups, the molecular weight of PEG-DT and the degrees of substitution of Dex-Mal and PEG-DT, the effect of the network on the yield and size distribution of the prepared GUVs was investigated.

In **Chapter 6**, an attempt was made to direct the assembly of dextran polymers *via* specific coiled-coil interactions. The coiled-coil motif is one of the basic folding motifs in natural proteins, which is a left-handed superhelix formed through the winding of two or more right-handed α-helical peptides around each other.[81, 82] Peptide **E** (amino acid sequence: $(EIAALEK)_3$) and peptide **K** (amino acid sequence: $(KIAALKE)_3$), able to assemble into heterodimeric coiled coils, were grafted

to dextran-vinyl sulfone polymers to obtain multivalent peptide-dextran conjugates. Two pairs of dextran-peptide **E** and dextran-peptide **K** bioconjugates were synthesized, wherein the dextran polymer was attached at either the N- or C-terminus of the peptides. The effect of conjugation on peptide conformation and the interaction between complementary dextran-peptide conjugates was studied by circular dichroism spectroscopy, fluorescence spectroscopy and dynamic light scattering measurements.

Finally in **Chapter 7**, the findings and conclusions of this thesis are summarized and possibilities for future research are presented.

REFERENCES

1. Malafaya P. B., Silva G. A. and Reis R. L., Natural-origin polymers as carriers and scaffolds for biomolecules and cell delivery in tissue engineering applications, *Advanced Drug Delivery Reviews*, 2007, **59**, 207-233.
2. Yang L. and Zhang L., Chemical structural and chain conformational characterization of some bioactive polysaccharides isolated from natural sources, *Carbohydrate Polymers*, 2009, **76**, 349-361.
3. Mizrahy S. and Peer D., Polysaccharides as building blocks for nanotherapeutics, *Chemical Society Reviews*, 2012, **41**, 2623-2640.
4. Heinze T., Liebert T., Heublein B.*, et al.*, Functional polymers based on dextran, *Advances in Polymer Science*, 2006, **205**, 199-291.
5. Purama R. K., Goswami P., Khan A. T.*, et al.*, Structural analysis and properties of dextran produced by leuconostoc mesenteroides nrrl b-640, *Carbohydrate Polymers*, 2009, **76**, 30-35.
6. Ioan C., Aberle T. and Burchard W., Structure properties of dextran. 2. Dilute solution, *Macromolecules*, 2000, **33**, 5730-5739.
7. Ioan C., Aberle T. and Burchard W., Structure properties of dextran. 3. Shrinking factors of individual clusters, *Macromolecules*, 2001, **34**, 3765-3771.
8. Antoniou E. and Tsianou M., Solution properties of dextran in water and in formamide, *Journal of Applied Polymer Science*, 2012, **125**, 1681-1692.
9. Franssen O., Vos O. P. and Hennink W. E., Delayed release of a model protein from enzymatically-degrading dextran hydrogels, *Journal of Controlled Release*, 1997, **44**, 237-245.
10. Larsen C., Dextran prodrugs—structure and stability in relation to therapeutic activity, *Advanced Drug Delivery Reviews*, 1989, **3**, 103-154.
11. Mehvar R., Dextrans for targeted and sustained delivery of therapeutic and imaging agents, *Journal of Controlled Release*, 2000, **69**, 1-25.
12. Heinze T., Liebert T., Heublein B.*, et al.*, in *Polysaccharides ii*, Springer, 2006, pp. 199-291.
13. Khandare J. and Minko T., Polymer–drug conjugates: Progress in polymeric prodrugs, *Progress in Polymer Science*, 2006, **31**, 359-397.
14. Naessens M., Cerdobbel A., Soetaert W.*, et al.*, Leuconostoc dextransucrase and dextran: Production, properties and applications, *J Chem Technol Biot*, 2005, **80**, 845-860.
15. Hill A. J., Teraoka H., Heideman W.*, et al.*, Zebrafish as a model vertebrate for investigating chemical toxicity, *Toxicol Sci*, 2005, **86**, 6-19.
16. Peterson R. E., Theobald H. M. and Kimmel G. L., Developmental and reproductive toxicity of dioxins and related compounds: Cross-species comparisons, *Critical Reviews in Toxicology*, 1993, **23**, 283-335.
17. Strahle U., Scholz S., Geisler R.*, et al.*, Zebrafish embryos as an alternative to animal experiments. A commentary on the definition of the onset of protected life stages in animal welfare regulations, *Reproductive Toxicology*, 2012, **33**, 128-132.
18. Mccollum C. W., Ducharme N. A., Bondesson M.*, et al.*, Developmental toxicity screening in zebrafish, *Birth Defects Research Part C-embryo Today-reviews*, 2011, **93**, 67-114.
19. He J., Gao J., Huang C.*, et al.*, Zebrafish models for assessing developmental and reproductive toxicity, *Neurotoxicology and Teratology*, 2014, **42**, 35-42.
20. Basu S. and Sachidanandan C., Zebrafish: A multifaceted tool for chemical biologists, *Chemical reviews*, 2013, **113**, 7952-7980.
21. Larsen C., Dextran prodrugs - structure and stability in relation to therapeutic activity, *Advanced Drug Delivery Reviews*, 1989, **3**, 103-154.

22. Wasiak I., Kulikowska A., Janczewska M*., et al.*, Dextran nanoparticle synthesis and properties, *PLOS ONE*, 2016, **11**.
23. Varshosaz J., Dextran conjugates in drug delivery, *Expert Opinion on Drug Delivery*, 2012, **9**, 509-523.
24. Nakamura J., Nakajima N., Matsumura K*., et al.*, Water-soluble taxol conjugates with dextran and targets tumor cells by folic acid immobilization, *Anticancer Research*, 2010, **30**, 903-909.
25. Zhao Q., Gottschalk I., Carlsson J*., et al.*, Preparation and purification of an end to end coupled megf-dextran conjugate, *Bioconjugate Chemistry*, 1997, **8**, 927-934.
26. Zhao Q., Tolmachev V., Carlsson J*., et al.*, Effects of dextranation on the pharmacokinetics of short peptides. A pet study on megf, *Bioconjugate Chemistry*, 1999, **10**, 938-946.
27. Hoffman A. S., Hydrogels for biomedical applications, *Annals of the New York Academy of Sciences*, 2001, **944**, 62-73.
28. Cabral J. D. and Moratti S. C., Hydrogels for biomedical applications, *Future Medicinal Chemistry*, 2011, **3**, 1877-1888.
29. Van Tomme S. R., Storm G. and Hennink W. E., *In situ* gelling hydrogels for pharmaceutical and biomedical applications, *International Journal of Pharmaceutics*, 2008, **355**, 1-18.
30. Ko D. Y., Shinde U. P., Yeon B*., et al.*, Recent progress of *in situ* formed gels for biomedical applications, *Progress in Polymer Science*, 2013, **38**, 672-701.
31. Nguyen Q. V., Huynh D. P., Park J. H*., et al.*, Injectable polymeric hydrogels for the delivery of therapeutic agents: A review, *European Polymer Journal*, 2015, **72**, 602-619.
32. Zhou Y., Nie W., Zhao J*., et al.*, Rapidly *in situ* forming adhesive hydrogel based on a peg-maleimide modified polypeptide through michael addition, *Journal of Materials Science: Materials in Medicine*, 2013, **24**, 2277-2286.
33. Jiang Y., Chen J., Deng C*., et al.*, Click hydrogels, microgels and nanogels: Emerging platforms for drug delivery and tissue engineering, *Biomaterials*, 2014, **35**, 4969-4985.
34. Nimmo C. M. and Shoichet M. S., Regenerative biomaterials that "click": Simple, aqueous-based protocols for hydrogel synthesis, surface immobilization, and 3d patterning, *Bioconjugate Chemistry*, 2011, **22**, 2199-2209.
35. Wu X., He C., Wu Y*., et al.*, Synergistic therapeutic effects of schiff's base cross-linked injectable hydrogels for local co-delivery of metformin and 5-fluorouracil in a mouse colon carcinoma model, *Biomaterials*, 2016, **75**, 148-162.
36. Canadell J., Goossens H. and Klumperman B., Self-healing materials based on disulfide links, *Macromolecules*, 2011, **44**, 2536-2541.
37. Du X., Zhou J., Shi J*., et al.*, Supramolecular hydrogelators and hydrogels: From soft matter to molecular biomaterials, *Chemical Reviews*, 2015, **115**, 13165-13307.
38. Kim D. Y., Kwon D. Y., Kwon J. S*., et al.*, Stimuli-responsive injectable *in situ*-forming hydrogels for regenerative medicines, *Polymer Reviews*, 2015.
39. Buwalda S. J., Vermonden T. and Hennink W. E., Hydrogels for therapeutic delivery: Current developments and future directions, *Biomacromolecules*, 2017, **18**, 316-330.
40. Siepmann J. and Siepmann F., Modeling of diffusion controlled drug delivery, *Journal of Controlled Release*, 2012, **161**, 351-362.
41. Dubose J. W., Cutshall C. and Metters A. T., Controlled release of tethered molecules via engineered hydrogel degradation: Model development and validation, *Journal of Biomedical Materials Research Part A*, 2005, **74**, 104-116.
42. Roy D., Cambre J. N. and Sumerlin B. S., Future perspectives and recent advances in stimuli-responsive materials, *Progress in Polymer Science*, 2010, **35**, 278-301.
43. Wang N. X. and Von Recum H. A., Affinity-based drug delivery, *Macromolecular Bioscience*, 2011, **11**, 321-332.

44. Zhou J. and Ritter H., Cyclodextrin functionalized polymers as drug delivery systems, *Polymer Chemistry*, 2010, **1**, 1552-1559.
45. Peng K., Cui C., Tomatsu I.*, et al.*, Cyclodextrin/dextran based drug carriers for a controlled release of hydrophobic drugs in zebrafish embryos, *Soft Matter*, 2010, **6**, 3778-3783.
46. Peng K., Tomatsu I., Korobko A. V.*, et al.*, Cyclodextrin-dextran based *in situ* hydrogel formation: A carrier for hydrophobic drugs, *Soft Matter*, 2010, **6**, 85-87.
47. Liu C., Zhang Z., Liu X.*, et al.*, Gelatin-based hydrogels with [small beta]-cyclodextrin as a dual functional component for enhanced drug loading and controlled release, *RSC Advances*, **3**, 25041-25049.
48. Cai T., Yang W. J., Zhang Z.*, et al.*, Preparation of stimuli-responsive hydrogel networks with threaded [small beta]-cyclodextrin end-capped chains via combination of controlled radical polymerization and click chemistry, *Soft Matter*, **8**, 5612-5620.
49. Kratz F., Albumin as a drug carrier: Design of prodrugs, drug conjugates and nanoparticles, *Journal of Controlled Release*, 2008, **132**, 171-183.
50. Cui M., Naczynski D. J., Zevon M.*, et al.*, Multifunctional albumin nanoparticles as combination drug carriers for intra-tumoral chemotherapy, *Advanced Healthcare Materials*, 2013, n/a-n/a.
51. Wu Y., Ihme S., Feuring-Buske M.*, et al.*, A core-shell albumin copolymer nanotransporter for high capacity loading and two-step release of doxorubicin with enhanced anti-leukemia activity, *Advanced Healthcare Materials*, 2012, n/a-n/a.
52. Tada D., Tanabe T., Tachibana A.*, et al.*, Drug release from hydrogel containing albumin as crosslinker, *Journal of Bioscience and Bioengineering*, 2005, **100**, 551-555.
53. Nie T., Akins R. E., Jr. and Kiick K. L., Production of heparin-containing hydrogels for modulating cell responses, *Acta Biomaterialia*, 2009, **5**, 865-875.
54. Baldwin A. D., Robinson K. G., Militar J. L.*, et al.*, *In situ* crosslinkable heparin-containing poly(ethylene glycol) hydrogels for sustained anticoagulant release, *Journal of Biomedical Materials Research Part A*, **100A**, 2106-2118.
55. Kiick K. L., Peptide- and protein-mediated assembly of heparinized hydrogels, *Soft Matter*, 2008, **4**, 29-37.
56. Byrne M. E., Park K. and Peppas N. A., Molecular imprinting within hydrogels, *Advanced Drug Delivery Reviews*, 2002, **54**, 149-161.
57. Chen L., Xu S. and Li J., Recent advances in molecular imprinting technology: Current status, challenges and highlighted applications, *Chemical Society Reviews*, 2011, **40**, 2922-2942.
58. Baldwin A. D. and Kiick K. L., Polysaccharide-modified synthetic polymeric biomaterials, *Biopolymers*, 2010, **94**, 128-140.
59. Zelzer M., Todd S. J., Hirst A. R.*, et al.*, Enzyme responsive materials: Design strategies and future developments, *Biomaterials Science*, 2013, **1**, 11-39.
60. Hennink W. E., Talsma H., Borchert J. C. H.*, et al.*, Controlled release of proteins from dextran hydrogels, *Journal of Controlled Release*, 1996, **39**, 47-55.
61. Hennink W. E., Franssen O., Van Dijkwolthuis W. N. E.*, et al.*, Dextran hydrogels for the controlled release of proteins, *Journal of Controlled Release*, 1997, **48**, 107-114.
62. Van Dijkwolthuis W. N. E., Hoogeboom J. A. M., Van Steenbergen M. J.*, et al.*, Degradation and release behavior of dextran-based hydrogels, *Macromolecules*, 1997, **30**, 4639-4645.
63. Liu Y. and Chanpark M. B., A biomimetic hydrogel based on methacrylated dextran-graft-lysine and gelatin for 3d smooth muscle cell culture, *Biomaterials*, 2010, **31**, 1158-1170.
64. Hiemstra C., Der Aa L. J. V., Zhong Z.*, et al.*, Rapidly *in situ*-forming degradable hydrogels from dextran thiols through michael addition, *Biomacromolecules*, 2007, **8**, 1548-1556.
65. Wei Z., Yang J. H., Du X. J.*, et al.*, Dextran-based self-healing hydrogels formed by reversible diels-alder

reaction under physiological conditions, *Macromolecular Rapid Communications*, 2013, **34**, 1464-1470.

66. Huh K. M., Ooya T., Lee W. K*., et al.*, Supramolecular-structured hydrogels showing a reversible phase transition by inclusion complexation between poly(ethylene glycol) grafted dextran and α-cyclodextrin, *Macromolecules*, 2001, **34**, 8657-8662.
67. De Jong S. J., Van Eerdenbrugh B., Van Nostrum C. F*., et al.*, Physically crosslinked dextran hydrogels by stereocomplex formation of lactic acid oligomers: Degradation and protein release behavior, *Journal of Controlled Release*, 2001, **71**, 261-275.
68. Heller D. A., Levi Y., Pelet J. M*., et al.*, Modular 'click-in-emulsion' bone-targeted nanogels, *Advanced Materials*, 2013, **25**, 1449-1454.
69. De Geest B. G., Van Camp W., Du Prez F. E*., et al.*, Biodegradable microcapsules designed via 'click' chemistry, *Chemical Communications*, 2008, 190-192.
70. Ghugare S. V., Chiessi E., Cerroni B*., et al.*, Biodegradable dextran based microgels: A study on network associated water diffusion and enzymatic degradation, *Soft Matter*, 2012, **8**, 2494-2502.
71. Drogoz A., David L., Rochas C*., et al.*, Polyelectrolyte complexes from polysaccharides : Formation and stoichiometry monitoring, *Langmuir*, 2007, **23**, 10950-10958.
72. Balabushevich N. G., Sukhorukov G. B. and Larionova N. I., Polyelectrolyte multilayer microspheres as carriers for bienzyme system: Preparation and characterization, *Macromolecular Rapid Communications*, 2005, **26**, 1168-1172.
73. Jo J., Nagane K., Yamamoto M*., et al.*, Effect of amine type on the expression of plasmid DNA by cationized dextran, *Journal of Biomaterials Science-polymer Edition*, 2010, **21**, 225-236.
74. Parliament E., Directive 2010/63/eu of the european parliament and of the council of 22 september 2010 on the protection of animals used for scientific purposes, 2010, 34-35.
75. Berghmans S., Butler P., Goldsmith P*., et al.*, Zebrafish based assays for the assessment of cardiac, visual and gut function — potential safety screens for early drug discovery, *Journal of Pharmacological and Toxicological Methods*, 2008, **58**, 59-68.
76. Selderslaghs I. W. T., Hooyberghs J., Blust R*., et al.*, Assessment of the developmental neurotoxicity of compounds by measuring locomotor activity in zebrafish embryos and larvae, *Neurotoxicology and Teratology*, 2013, **37**, 44-56.
77. Menger F. M. and Angelova M. I., Giant vesicles: Imitating the cytological processes of cell membranes, *Accounts of chemical research*, 1998, **31**, 789-797.
78. Walde P., Cosentino K., Engel H*., et al.*, Giant vesicles: Preparations and applications, *ChemBioChem*, 2010, **11**, 848-865.
79. Fenz S. F. and Sengupta K., Giant vesicles as cell models, *Integrative Biology*, 2012, **4**, 982-995.
80. Horger K. S., Estes D. J., Capone R*., et al.*, Films of agarose enable rapid formation of giant liposomes in solutions of physiologic ionic strength, *Journal of the American Chemical Society*, 2009, **131**, 1810-1819.
81. Lupas A., Van Dyke M. and Stock J., Predicting coiled coils from protein sequences, *Science*, 1991, **252**, 1162-1164.
82. Burkhard P., Stetefeld J. and Strelkov S. V., Coiled coils: A highly versatile protein folding motif, *Trends in cell biology*, 2001, **11**, 82-88.

CHAPTER 2

THIOLATED HUMAN SERUM ALBUMIN CROSSLINKED DEXTRAN HYDROGEL AS A MACROSCALE DELIVERY SYSTEM

Hydrogels play an important role in macroscale delivery systems by enabling the transport of cells and molecules. Here we present a facile and benign method to prepare a dextran-based hydrogel (Dex-sHSA) using human serum albumin (HSA) as a simultaneous drug carrier and covalent crosslinker. Drug binding affinity of the albumin protein was conserved in the thiolation step using 2-iminothiolane and subsequently, in the *in situ* gelation step. Oscillation rheometry studies confirmed the formation of a three-dimensional viscoelastic network upon reaction of dextran and the HSA protein. The mechanical properties of Dex-sHSA hydrogel can be tuned by the protein concentration, and the degree of thiolation of sHSA. Sustained release of hydrophobic drugs, such as ibuprofen, paclitaxel and dexamethasone, from the Dex-sHSA network was shown over one week. Hence, this albumin-based dextran hydrogel system demonstrates its potential as a macroscale delivery system of hydrophobic therapeutics for a wide range of biomedical applications.

Part of this chapter was published in *Soft Matter*, **2014**, 10 (27), 4869-4874.

INTRODUCTION

Hydrogels are composed of crosslinked hydrophilic polymer networks, resulting in porous, macroscopic materials of high water content. Their unique physicochemical properties enable them to perform as macroscale delivery systems of bioactive agents ranging from cells to molecules.[1, 2] Within such systems, methods to gain spatiotemporal control over release of therapeutic payloads have involved diffusion,[3-7] swelling,[8-10] degradation,[11-13] light[14-19] or drug-carrier affinity interactions.[20] More specifically, the latter mechanism facilitates controlled release through the strong and reversible association of the drug molecules using non-covalent interactions such as hydrogen bonding, ionic, van der Waals, and hydrophobic interactions within the macroscale material scaffold. In the context of lipophilic drug delivery, the problem of encapsulating a lipophilic drug within a water-rich environment is resolved through the inclusion of hydrophobic side chains,[21, 22] hydrophobic drug carriers,[23] such as cyclodextrin,[24-29] within the polymer or using a molecular imprinting approach[30, 31] to prepare the polymeric scaffold. Since it is estimated that 40% of new active chemical entities discovered by pharmaceutical companies are poorly water soluble (aqueous solubility less than 10 μM),[32] macroscale drug delivery systems capable of transporting hydrophobic therapeutics are highly relevant.

Inspired by nature, human serum albumin (HSA) is emerging as an attractive drug carrier in biomedical materials.[33] HSA is the most abundant plasma protein in human (35-50 g L^{-1}) with a molecular weight of 66.5 kDa and has been shown to be biocompatible, biodegradable, non-immunogenic and non-toxic through its *in vivo* metabolism by proteases into innocuous degradation products. Naturally, HSA acts as a transport vehicle in the blood for a variety of molecules, ranging from metal ions, fatty acids, amino acids to numerous drug compounds. Furthermore, HSA has 6 potential binding sites including two major hydrophobic cavities[34] resulting in numerous possibilities for specific non-covalent interactions with drug compounds. Thus far, various approaches have been explored to develop albumin-based hydrogels for drug delivery, involving albumin crosslinking by coupling agents,[35-37] free radical polymerization,[38] UV[39, 40] or γ-ray irradiation.[41] Despite successful implementation of albumin in these drug delivery systems, the biocompatibility of the reported gelation procedures and their effect on the albumin protein remains unclear.

We here report, a facile method to simultaneously use HSA as a crosslinker and drug carrier within a dextran polymeric hydrogel system (Figure 1). Dextran is a highly water-soluble and biocompatible natural polymer. Native HSA was modified with thiol groups at lysine residues of the protein under physiological conditions. Finally, a covalently crosslinked hydrogel network was prepared using a Michael addition reaction between maleimide functionalized dextran (Dex-Mal)

and thiolated albumin (sHSA) in aqueous solution. The conformation of albumin was observed to be retained in circular dichroism (CD) experiments after thiolation and conjugation steps. Oscillatory rheometry confirmed the formation of Dex-sHSA viscoelastic network and revealed that the mechanical properties can be tuned by varying the degrees of thiolation of sHSA and its concentration relative to Dex-Mal. *In vitro* drug release profiles were evaluated with ibuprofen, paclitaxel and dexamethasone demonstrating sustained release over one week.

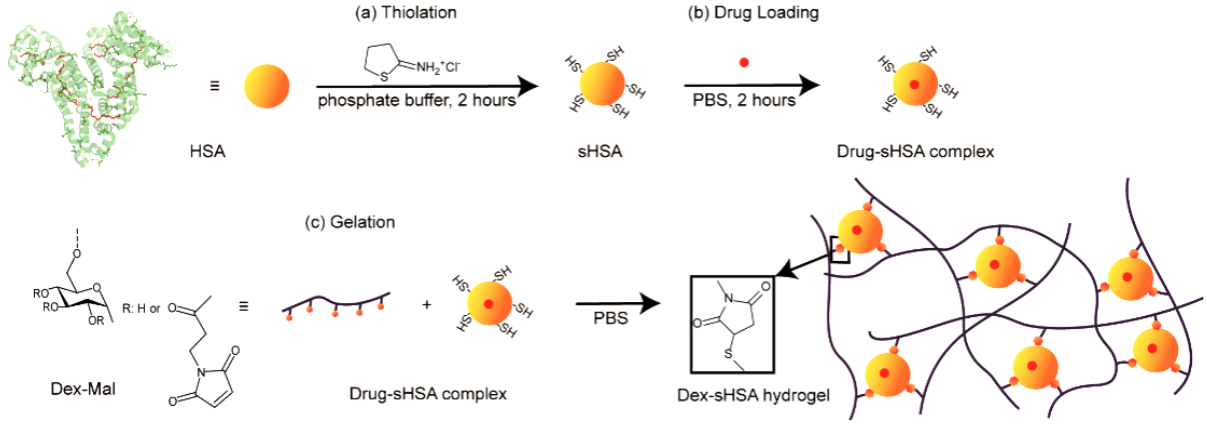

Figure 1. *Preparation of the Dex-sHSA macroscale delivery system. (a) HSA thiolation. (b) Drug loading. (c) Gelation via maleimide-thiol Michael addition.*

RESULTS AND DISCUSSION

SYNTHESIS OF SHSA

The native HSA protein contains 35 cysteine residues, one free thiol (Cys-34) and 17 disulfide bridges. The disulfide double loops of HSA play an important role in the formation of the two main hydrophobic cavities within the protein, that can be used for ligand binding.[34] Since the goal was to use sHSA as a simultaneous crosslinker and drug carrier, a gentle thiolation agent that helps to retain the native conformation and binding capacity of albumin was required. To this end, Traut's reagent, 2-IT, was selected due to its inherent water-solubility and ability to react with primary amines quantitatively in the pH range (7-10) of biological solutions. In comparison to reducing reagents such as dithiothreitol (DTT), 2-mercaptoethanol and tris(2-carboxyethyl)phosphine (TCEP) 2-IT retains intramolecular disulfide bridges and lysine residues' charge upon thiolation, thus aiding protein's stability and solubility in water.[42, 43] Using Ellman's test prior to thiolation with the native HSA, 0.24 free thiol groups per protein were detected (Table 1), indicating a majority of Cys-34 residues of the obtained native HSA was oxided. It was found that commercially available HSA contained a significant amount of oxidized Cys-34 and the

amount of oxidized Cys-34 increased with the storage time even being stored at -80°C.[44] This value increased to 3.16 free thiol groups per protein when thiolated with 20-fold of 2-IT. As shown in Table 1, the degree of thiolation (DT) can be easily varied by the molar ratio between HSA and 2-IT, thus providing a handle to control the mechanical properties of the final Dex-sHSA hydrogel (*vide infra*).

Table 1. *Controlling the degree of thiolation of sHSA by tuning the molar ratio between HSA and 2-IT.*

2-IT/HSA	DT
0	0.24
5	0.86
10	1.70
15	2.54
20	3.16

CONFORMATION OF HSA, SHSA, AND DEX-SHSA

CD spectroscopy is a convenient technique to study the structure of proteins in aqueous solution.[45] More specifically, absorption signatures in the far-UV region (below 240 nm) provide insight into protein's secondary structure while absorption in the near-UV region (260-320 nm) is often correlated with protein's tertiary structure. Hence, to investigate the effects of the thiolation by 2-IT and the conjugation of the dextran polymer on the conformation of HSA, CD spectra of a series of samples containing native HSA were collected.

A comparison of CD spectra of HSA and sHSA suggests that albumin's secondary and tertiary structure is largely retained post-thiolation by 2-IT (Figure 2). Generally, the CD spectrum of native HSA in the far-UV has two major minima of a similar ratio around 208 and 222 nm arising from the degree of protein α-helical character. The mean residue molar ellipticity $[\theta]$ of thiolated sHSA at both 222 and 208 nm was found to decrease post-thiolation. relative to the native form by 13%, thus indicating a slight loss of α-helicity. Additionally, the near-UV CD spectrum shows a subtle decrease in the intensity of $[\theta]$ for the thiolated form. This decrease may be correlated with structural rearrangements occurring nearby HSA's disulfide bridges and tryptophan residues.[46, 47] Subsequently, we examined the CD signature of the HSA protein upon reacting an equivalent molar ratio of maleimide functionalized dextran polymer and thiolated sHSA. To prevent gelation from occurring during conjugate formation in the CD cuvette, the concentration of sHSA was kept at 0.5 mg mL^{-1}. The CD spectrum of HSA recorded after formation of the Dex-sHSA conjugate is nearly identical to the far-UV CD curve of sHSA and is suggestive of α-helical character retention.

More specifically, in the near-UV region, the intensity of *[θ]* increased slightly after conjugation, on par with the native protein. A similar result was previously reported by Antonov,[48] whom suggested that hydrogen bond formation between the hydroxyl groups of dextran with the tryptophan residues located on bovine serum albumin leads to the observed increase in CD signal. Gratifyingly, a negligible effect on HSA conformation is observed upon reaction with 2-IT and subsequently, with the dextran polymer by CD spectroscopy.

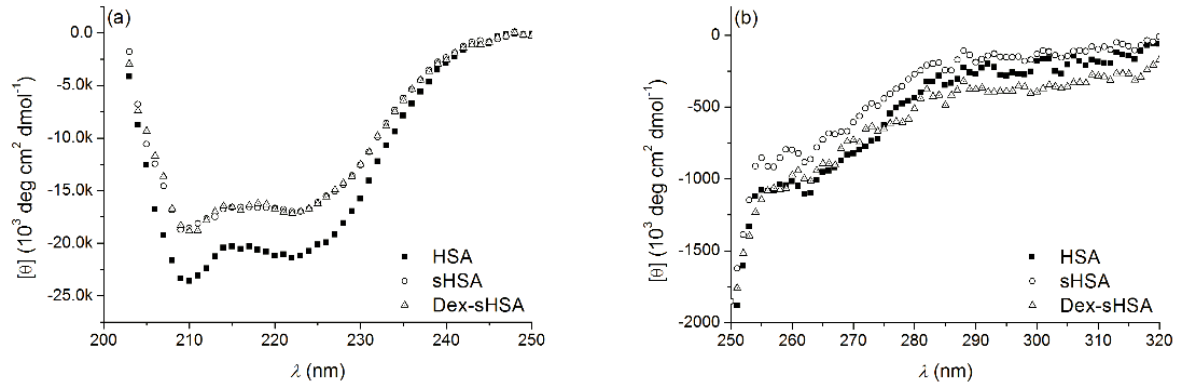

Figure 2. *Far-UV CD (a) and near-UV CD (b) spectra of HSA, sHSA and Dex-sHSA (1:1 maleimide:thiol) in sodium phosphate buffer (50 mM, pH 7).*

FORMATION OF DEX-SHSA HYDROGELS

Dex-sHSA hydrogels were formed *via* maleimide-thiol Michael addition, a rapid, widely used click reaction in biological applications. Since this reaction does not require any initiator, catalyst or crosslinking agent, cell viability can be retained after *in situ* hydrogel formation.[2, 49]

The gelation process of Dex-sHSA hydrogels was monitored by an oscillatory time sweep. After loading and mixing of the Dex-Mal and sHSA solutions on the rheometer plate, the hydrogel was formed on the order of seconds (Figure 3a). Values of storage modulus (*G*') were observed above the loss modulus (*G*") from the start of the experiment due to the rapid gelation of the sample. Hence, the cross-over point of *G*' and *G*" (generally considered as the gel point) could not be observed. In less than half an hour, *G*' reached a plateau indicating that the bulk of the gelation process occurred. Moreover, the gelation time was found to be dependent on the initial concentrations of Dex-Mal and sHSA. In comparison with the 4 wt% Dex-sHSA hydrogel, 6 wt% samples were found undergo a more rapid gelation process, resulting in a greater storage modulus on the initial reading.

The resulting hydrogels were further examined by amplitude and angular frequency sweep measurements. Amplitude sweep measurements (Figure 3b) provided information regarding the

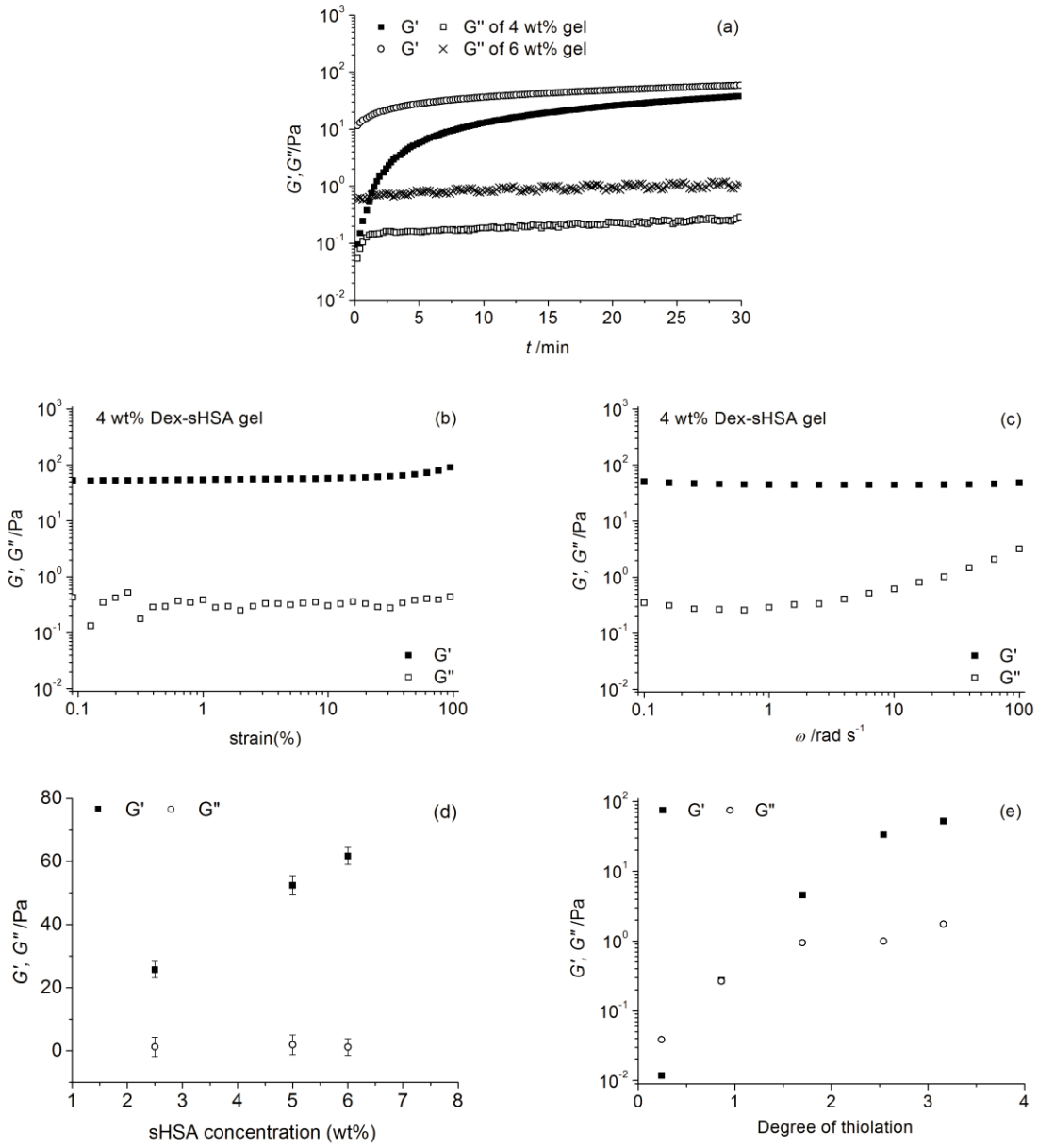

Figure 3. *Oscillatory rheometry of Dex-sHSA hydrogels at 37 °C. (a) Time sweep of 4 wt% and 6 wt% hydrogels at 1 rad s^{-1} and 5% strain. (b) Amplitude sweep from 0.5% to 100% at 1 rad s^{-1}. (c) Angular frequency sweep from 100 rad s^{-1} to 0.1 rad s^{-1} and 5% strain. Effect of (d) the relative concentration of sHSA (DT=3.16) to Dex-Mal, and (e) the degree of thiolation of sHSA on the storage and loss modulus (G' and G") of 5 wt% Dex-sHSA hydrogels.*

linear viscoelastic region of the Dex-sHSA hydrogel, which was found to be in the range of 0.1% to 100%. Angular frequency sweep measurements (Figure 3c) showed that *G'* was at least an order of magnitude greater than G" over the range of 0.1-100 rad s^{-1}; in agreement with the formation of a three-dimensional crosslinked network.

Since sHSA acts as a crosslinker in the dextran polymeric network, both the relative concentrations

and the degrees of thiolation (DT) of sHSA can influence the mechanical properties of Dex-sHSA hydrogels. For the former method, the concentration of Dex-Mal was held constant while the concentration of sHSA was varied corresponding to the molar ratio of between thiols and maleimide. As shown in Figure 3d, the storage modulus (*G*') of Dex-sHSA gels increased from 25 Pa to 52 Pa when sHSA concentration doubled from 2.5 wt% to 5 wt%. By further increasing the concentration to 6 wt%, *G*' of the gels went up to 62 Pa. In the latter method, increasing degrees of thiolation of the sHSA protein also yielded a concomitant increase in the mechanical properties of the resulting Dex-sHSA conjugates.

In Figure 3e, at low DT, sHSA can be covalently ligated to Dex-Mal, but a limited number of thiol groups on the albumin surface prevents the formation of hydrogels. For these samples, *G*" was greater than *G*' in all oscillation measurements exhibiting predominant viscous-behavior. When the DT increased to 1.7 and over, *G*' was found to be greater than *G*" in angular frequency sweep measurements and a viscoelastic material was formed. Hence, both methods, either increasing protein concentration or DT of the protein, provide a facile handle to tune mechanical properties of the macroscale delivery scaffold.

IN VITRO DRUG RELEASE

Drug release kinetics from HSA binding pockets within the Dex-sHSA hydrogels were evaluated using ibuprofen (IBU), paclitaxel (PTX) and dexamethasone (DXM). IBU is a typical non-steroidal anti-inflammatory drug. PTX is an antimicrotubule chemotherapeutic agent currently used in the treatment of solid tumour malignancies. Both IBU and PTX have been shown to be highly bound to plasma proteins (above 95%).[50, 51] DXM is a synthetic corticosteroid widely used as anti-inflammatory and immunosuppressant in clinical treatments, which is moderately bound to plasma proteins (70-80% depending on the test procedure).[52] Despite the lipophilic and poor water-soluble character of the three drugs tested (See supporting information Table S1), the drugs were co-dissolved with the HSA drug carrier to form water-soluble drug-HSA complexes and reacted with the hydrogel material. High drug loading efficiencies of IBU, PTX and DXM within the Dex-sHSA material were obtained (91.3%, 87.7% and 92.1%, respectively). By this method, organic solvents such as DMSO become unnecessary for the dispersion of various therapeutics, and further ligation to the hydrogel scaffold enables their prolonged delivery.

In vitro drug release of Dex-sHSA hydrogels were performed under physiological conditions (PBS, pH 7.4) at 37 °C. As shown in Figure 4, the release of all three drugs from the hydrogels occurred in two stages: a fast release in the initial 10 hours, followed by a second stage of slower and sustained release up to 140 hours. In the first stage, hydrophobic drug release was driven by diffusion and swelling (See supporting information, Figure S2) of the hydrogel matrix. In the second stage, the erosion of the hydrogel plays an important role in release kinetics. The release

curve of DXM exhibited a faster release rate than IBU and PTX, which may arise from differences in hydrophobic character and binding interactions with HSA. However, it is anticipated that these release profiles will change when these networks are presented with proteases due to the enzymatically sensitive HSA crosslinks. Overall, this assay shows that Dex-sHSA hydrogels can be easily loaded with hydrophobic therapeutics and show sustained release.

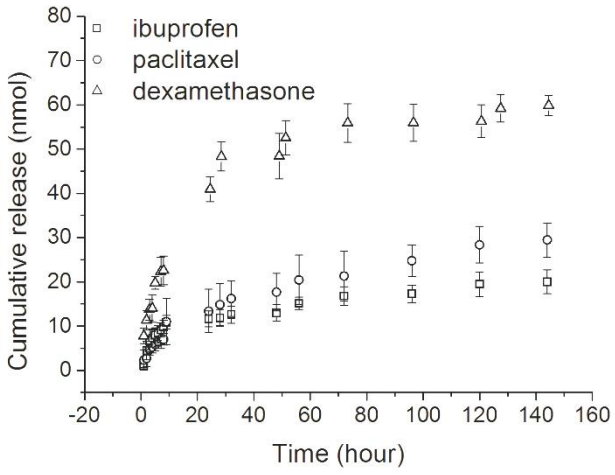

Figure 4. *In vitro drug release profiles of IBU, PTX and DXM from Dex-sHSA hydrogels (4.5 wt%, DT=3.16) in PBS (150 mM, pH 7.4) at 37 °C.*

CONCLUSION

In this work, we have demonstrated a facile and benign method to simultaneously use HSA as a drug carrier and hydrogel crosslinker in a macroscale drug delivery system. Thiol groups were introduced to HSA by a mild thiolation agent 2-IT, which assisted in the preservation of the native protein conformation as observed by CD spectroscopy. Mixing of sHSA and Dex-Mal resulted in rapid *in situ* gelation with the potential to tune mechanical properties by modulating protein concentration and the degrees of thiolation of sHSA. Moreover, the incorporation of HSA into these networks provided access to sustained delivery of hydrophobic therapeutics on the order of one week. This hydrogel based macroscale delivery system combines the advantage of the versatile drug-binding capability of HSA and the biocompatible, highly hydrophilic nature of dextran polymers. Beyond therapeutic delivery applications in an *in vivo* context, such scaffolds can also be candidates for high throughput screening of therapeutics *in vitro* in a 3D cell culture setting.

EXPERIMENTAL

MATERIALS

Dextran (70 kDa), human serum albumin (HSA), N,N'-diisopropylcarbodiimide (DIC), 2-iminothiolane (2-IT), 5,5'-dithiobis(2-nitrobenzoic acid) (DTNB), dimethyl sulfoxide (DMSO), ethylenediaminetetraacetic acid (EDTA), ibuprofen (IBU), paclitaxel (PTX) and dexamethasone (DXM) were purchased from Sigma-Aldrich. Dextran was dried in a vacuum oven (30 °C) and DMSO was dried over 4Å molecular sieves before use. 3-maleimidopropionic acid and 4-(dimethylamino)pyridinium 4-toluenesulfonate (DPTS) were synthesized as previously reported.[53,54] Dialysis membranes (MWCO 3,500-5,000 Da) were obtained from Spectrum Laboratories, Inc.

SYNTHESIS OF DEX-MAL

Dextran (1 g, 6.17 mmol), 3-maleimidopropionic acid (417 mg, 2.47 mmol), and DPTS (115.7 mg, 0.247 mmol) were dissolved in DMSO (33 mL) followed by the addition of DIC (580 μL, 3.7 mmol). After stirring overnight at room temperature, N, N'-dialkylurea was removed by filtration and the crude product was obtained by precipitation in cold isopropanol. The precipitate was dialyzed against Milli-Q water using a 3500-5000 MWCO cut-off membrane and subsequently lyophilized. ^{1}H NMR (400 MHz, D_2O): δ 3.3-4.0 (m, dextran glucopyranosyl ring protons), 4.9 (s, dextran anomeric proton), 6.9 (s, maleimide).

The degree of substitution of the dextran polymer (DS[Mal]) is defined as the number of maleimide groups per 100 glucopyranose residues. The DS[Mal] is calculated using the ratio: (100x)/(2y), in which x is the integral of the maleimide protons (δ 6.9) and y is the integral of the anomeric proton of dextran (δ 4.9) from the ^{1}H NMR spectra measured by a Bruker AV-400 spectrometer.[55] The DS[Mal] of the dextran polymer (Dex-Mal) synthesized in this work was 4.6.

SYNTHESIS OF THE THIOLATED HUMAN SERUM ALBUMIN (SHSA)

HSA was dissolved in 50 mM sodium phosphate buffer (pH 8, including 5 mM EDTA) and stirred gently at 0 °C on ice. Subsequently, an aqueous solution of 2-IT (20 mg mL^{-1}) was added drop-wise to the HSA solution. After 2 hours, the mixture was brought back to room temperature. The product was first dialyzed against 10 mM HEPES buffer (pH 7) three times over 24 hours and then, against Milli-Q water three times over 2 days at 4 °C. Finally, sHSA was lyophilized and stored at -20 °C.

The degrees of thiolation (DT) of sHSA were quantified by the Ellman's test.[56, 57] Briefly, 100 μL 2 mM DTNB, 200 μL 10 mg mL^{-1} sHSA and 700 μL 0.1 M sodium phosphate buffer (pH 8) were

mixed and incubated for one hour at room temperature. During this reaction, the formation of the 2-nitro-5-thiobenzoate anion (TNB^{2-}) resulted in an intense yellow colour with an absorbance at 412 nm by UV-vis spectroscopy (Agilent, Cary-300). The molar extinction coefficient of TNB^{2-} at 412 nm, ε_{TNB2^-} = 14150 M^{-1} cm^{-1}, was used to calculated the concentration of free thiol groups in the tested sHSA solution. The concentration of albumin in a control group (200 μL 10 mg mL^{-1} sHSA and 800 μL 0.1 M sodium phosphate buffer) was determined with the absorbance at 279 nm by UV-vis spectroscopy ($\varepsilon_{albumin}$ = 0.531 M^{-1} cm^{-1}). The DT of sHSA was then calculated by dividing the concentration of free thiol groups by the concentration of albumin.

CIRCULAR DICHROISM (CD)

Circular dichroism spectra were obtained on a Jasco J-815 spectrometer. All spectra were collected with a scan speed of 50 nm min^{-1} and a response time of 1 second at 20 °C. Each spectrum was averaged over 5 scans. Samples of native HSA, sHSA (DT=3.2), Dex-sHSA conjugate (molar ratio of thiol to maleimide 1:1) were prepared in sodium phosphate buffer (50 mM, pH 7). Native HSA and sHSA solutions were filtered through 0.2 μm syringe filters before CD measurements. For near-UV measurements (250-330 nm), a 1 cm path length quartz cuvette was used for 0.5 mg mL^{-1} protein samples. For far-UV measurements (200-250 nm), a 0.1 cm path length quartz cuvette was applied for 0.1 mg mL^{-1} protein samples.

CD data were presented in terms of ellipticity [θ] (degrees) and converted to the mean residue molar ellipticity [θ] in deg cm^2 $dmol^{-1}$ by equation **1**, where n is the number of amino acid residues (585), l is the path length of the cuvette, and C_p is the mole fraction.

$$[\theta] = \frac{\theta(mdeg)}{C_p \times n \times l \times 10} \quad (\mathbf{1})$$

α-helix content was calculated from the value of [θ] at 222 nm[58] by equation **2**.

$$\alpha - helix\ \% = \left(\frac{[\theta] - 2430}{30300}\right) \times 100 \quad (\mathbf{2})$$

DEX-SHSA HYDROGELS

Dex-Mal and sHSA were dissolved in phosphate buffered saline (PBS, 150 mM, pH 7.4) individually and then mixed together using a pipette to prepare the hydrogel samples (1:1 molar ratio of maleimide to thiol).

An AR-G2 rheometer (TA Instruments) was used to measure the mechanical properties of Dex-sHSA hydrogels in oscillatory mode at 37 °C using the parallel plate geometry (40 mm diameter). Solutions of Dex-Mal and sHSA were loaded at 300 μL of each component onto the bottom plate and the geometry was lowered to a gap of 0.40 mm for all experiments. Time sweep measurements

were performed to follow gel curing at 1 rad s^{-1} with 5% strain. The linear viscoelastic regime was determined using an amplitude sweep measurement at 1 rad s^{-1} from 0.1% to 100% strain. Frequency sweep measurements were performed from 100 to 0.1 rad s^{-1} with 5% strain in the linear viscoelastic regime.

IN VITRO DRUG RELEASE

Lipophilic drugs (IBU, PTX or DXM) and sHSA were co-dissolved in PBS (150 mM, pH 7.4, 0.02% NaN_3) and incubated for 2 hours at 37 °C prior to gelation. The molar ratio of sHSA and drug was kept at 1:1 in all samples. The drug-sHSA solution was subsequently crosslinked with the Dex-Mal polymer solution to form the drug-loaded hydrogels for *in vitro* drug release.

To examine the drug loading efficiency, 1 mL 0.25% trypsin solution (25 mM HEPES buffer, pH 7) was added on top of 200 μL drug loaded Dex-sHSA gel (4.5 wt%) and incubated at 37 °C. 2 mL acetonitrile was added to the mixture and the precipitates were removed by ultracentrifuge at 13 000 rpm for 10 minutes. The amount of drug was subsequently quantified by reversed-phase high performance liquid chromatography (RP-HPLC) analysis using two LC-8A pumps, SPD-10AVP UV-VIS and ELSD-LTII detectors from Shimadzu. The separation was performed on a Gemini C18 column at a flow rate of 1 mL min^{-1} with a linear gradient from 90% B to 10% B, where A was acetonitrile with 0.1 vol% TFA and B was H_2O with 0.1 vol% TFA. The eluate was monitored at both 220 and 254 nm. The drug loading efficiency was calculated from the amount of drug recovered from the gel divided by the amount of drug loaded expressed in percent.

For *in vitro* drug release study, the drug loaded Dex-sHSA gel was immersed in PBS at 37 °C. At predetermined time intervals, the supernatant buffer solution was collected and replaced with fresh PBS. The collected buffer solutions at each time point were analysed by RP-HPLC. All drug release experiments were performed in triplicate.

REFERENCES

1. Kearney C. J. and Mooney D. J., Macroscale delivery systems for molecular and cellular payloads, *Nature Materials*, 2013, **12**, 1004-1017.
2. Kharkar P. M., Kiick K. L. and Kloxin A. M., Designing degradable hydrogels for orthogonal control of cell microenvironments, *Chem Soc Rev*, 2013, **42**, 7335-7372.
3. Uhrich K. E., Cannizzaro S. M., Langer R. S.*, et al.*, Polymeric systems for controlled drug release, *Chem Rev*, 1999, **99**, 3181-3198.
4. Censi R., Vermonden T., Deschout H.*, et al.*, Photopolymerized thermosensitive poly(hpmalactate)-peg-based hydrogels: Effect of network design on mechanical properties, degradation, and release behavior, *Biomacromolecules*, 2010, **11**, 2143-2151.
5. Pescosolido L., Feruglio L., Farra R.*, et al.*, Mesh size distribution determination of interpenetrating polymer network hydrogels, *Soft Matter*, 2012, **8**, 7708-7715.
6. Dhanasingh A. and Groll J., Polysaccharide based covalently linked multi-membrane hydrogels, *Soft Matter*, 2012, **8**, 1643-1647.
7. Zustiak S. P., Boukari H. and Leach J. B., Solute diffusion and interactions in cross-linked poly(ethylene glycol) hydrogels studied by fluorescence correlation spectroscopy, *Soft Matter*, 2010, **6**, 3609-3618.
8. Lin C. C. and Metters A. T., Hydrogels in controlled release formulations: Network design and mathematical modeling, *Adv Drug Deliver Rev*, 2006, **58**, 1379-1408.
9. Moghadam M. N., Kolesov V., Vogel A.*, et al.*, Controlled release from a mechanically-stimulated thermosensitive self-heating composite hydrogel, *Biomaterials*, 2014, **35**, 450-455.
10. Schillemans J. P., Hennink W. E. and van Nostrum C. F., The effect of network charge on the immobilization and release of proteins from chemically crosslinked dextran hydrogels, *Eur. J. Pharm. Biopharm.*, 2010, **76**, 329-335.
11. Kiick K. L., Peptide- and protein-mediated assembly of heparinized hydrogels, *Soft Matter*, 2008, **4**, 29-37.
12. Binauld S. and Stenzel M. H., Acid-degradable polymers for drug delivery: A decade of innovation, *Chem Commun*, 2013, **49**, 2082-2102.
13. Yamaguchi N. and Kiick K. L., Polysaccharide-poly(ethylene glycol) star copolymer as a scaffold for the production of bioactive hydrogels, *Biomacromolecules*, 2005, **6**, 1921-1930.
14. Fairbanks B. D., Singh S. P., Bowman C. N.*, et al.*, Photodegradable, photoadaptable hydrogels via radical-mediated disulfide fragmentation reaction, *Macromolecules*, 2011, **44**, 2444-2450.
15. Kloxin A. M., Tibbitt M. W. and Anseth K. S., Synthesis of photodegradable hydrogels as dynamically tunable cell culture platforms, *Nature Protocols*, 2010, **5**, 1867-1887.
16. Tibbitt M. W., Kloxin A. M., Sawicki L. A.*, et al.*, Mechanical properties and degradation of chain and step-polymerized photodegradable hydrogels, *Macromolecules*, 2013, **46**, 2785-2792.
17. Peng K., Tomatsu I. and Kros A., Light controlled protein release from a supramolecular hydrogel, *Chemical Communications*, 2010, **46**, 4094-4096.
18. Peng K., Tomatsu I., van den Broek B.*, et al.*, Dextran based photodegradable hydrogels formed via a michael addition, *Soft Matter*, 2011, **7**, 4881-4887.
19. Tomatsu I., Peng K. and Kros A., Photoresponsive hydrogels for biomedical applications, *Advanced Drug Delivery Reviews*, 2011, **63**, 1257-1266.
20. Wang N. X. and von Recum H. A., Affinity-based drug delivery, *Macromolecular Bioscience*, 2011, **11**, 321-332.
21. Mullarney M. P., Seery T. A. P. and Weiss R. A., Drug diffusion in hydrophobically modified n,n-dimethylacrylamide hydrogels, *Polymer*, 2006, **47**, 3845-3855.

22. Liu Y. Y., Shao Y. H. and Lu J., Preparation, properties and controlled release behaviors of ph-induced thermosensitive amphiphilic gels, *Biomaterials*, 2006, **27**, 4016-4024.
23. Hoare T. R. and Kohane D. S., Hydrogels in drug delivery: Progress and challenges, *Polymer*, 2008, **49**, 1993-2007.
24. Thatiparti T. R., Shoffstall A. J. and von Recum H. A., Cyclodextrin-based device coatings for affinity-based release of antibiotics, *Biomaterials*, 2010, **31**, 2335-2347.
25. Zhou J. and Ritter H., Cyclodextrin functionalized polymers as drug delivery systems, *Polymer Chemistry*, 2010, **1**, 1552-1559.
26. Peng K., Cui C., Tomatsu I.*, et al.*, Cyclodextrin/dextran based drug carriers for a controlled release of hydrophobic drugs in zebrafish embryos, *Soft Matter*, 2010, **6**, 3778-3783.
27. Peng K., Tomatsu I., Korobko A. V.*, et al.*, Cyclodextrin-dextran based *in situ* hydrogel formation: A carrier for hydrophobic drugs, *Soft Matter*, 2010, **6**, 85-87.
28. Liu C., Zhang Z., Liu X.*, et al.*, Gelatin-based hydrogels with [small beta]-cyclodextrin as a dual functional component for enhanced drug loading and controlled release, *RSC Advances*, **3**, 25041-25049.
29. Cai T., Yang W. J., Zhang Z.*, et al.*, Preparation of stimuli-responsive hydrogel networks with threaded [small beta]-cyclodextrin end-capped chains via combination of controlled radical polymerization and click chemistry, *Soft Matter*, **8**, 5612-5620.
30. Singh B., Chauhan N. and Sharma V., Design of molecular imprinted hydrogels for controlled release of cisplatin: Evaluation of network density of hydrogels, *Industrial & Engineering Chemistry Research*, 2011, **50**, 13742-13751.
31. Salian V. D. and Byrne M. E., Controlled drug release from weakly crosslinked molecularly imprinted networks: The benefit of living radical polymerization, *Macromolecular Chemistry and Physics*, 2013, **214**, 2355-2366.
32. Heimbach T., Fleisher D. and Kaddoumi A., in *Prodrugs*, eds. V. Stella, R. Borchardt, M. Hageman, R. Oliyai, H. Maag and J. Tilley, Springer New York, 2007, vol. V, pp. 157-215.
33. Kratz F., Albumin as a drug carrier: Design of prodrugs, drug conjugates and nanoparticles, *Journal of Controlled Release*, 2008, **132**, 171-183.
34. He X. M. and Carter D. C., Atomic-structure and chemistry of human serum-albumin, *Nature*, 1992, **358**, 209-215.
35. Hirose M., Tachibana A. and Tanabe T., Recombinant human serum albumin hydrogel as a novel drug delivery vehicle, *Materials Science & Engineering C-Materials for Biological Applications*, 2010, **30**, 664-669.
36. Kakinoki S., Taguchi T., Saito H.*, et al.*, Injectable *in situ* forming drug delivery system for cancer chemotherapy using a novel tissue adhesive: Characterization and *in vitro* evaluation, *European Journal of Pharmaceutics and Biopharmaceutics*, 2007, **66**, 383-390.
37. Tada D., Tanabe T., Tachibana A.*, et al.*, Albumin-crosslinked alginate hydrogels as sustained drug release carrier, *Materials Science & Engineering C-Biomimetic and Supramolecular Systems*, 2007, **27**, 870-874.
38. Tada D., Tanabe T., Tachibana A.*, et al.*, Drug release from hydrogel containing albumin as crosslinker, *Journal of Bioscience and Bioengineering*, 2005, **100**, 551-555.
39. Oss-Ronen L. and Seliktar D., Photopolymerizable hydrogels made from polymer-conjugated albumin for affinity-based drug delivery, *Advanced Engineering Materials*, 2010, **12**, B45-B52.
40. Oss-Ronen L. and Seliktar D., Polymer-conjugated albumin and fibrinogen composite hydrogels as cell scaffolds designed for affinity-based drug delivery, *Acta Biomaterialia*, 2011, **7**, 163-170.
41. El-Sherif H., El-Masry M. and Abou Taleb M. F., Ph-sensitive hydrogels based on bovine serum albumin for anticancer drug delivery, *Journal of Applied Polymer Science*, 2010, **115**, 2050-2059.

42. Manjappa A. S., Chaudhari K. R., Venkataraju M. P.*, et al.*, Antibody derivatization and conjugation strategies: Application in preparation of stealth immunoliposome to target chemotherapeutics to tumor, *Journal of Controlled Release*, 2011, **150**, 2-22.
43. Weber C., Reiss S. and Langer K., Preparation of surface modified protein nanoparticles by introduction of sulfhydryl groups, *Int J Pharm*, 2000, **211**, 67-78.
44. Funk W. E., Li H., Iavarone A. T.*, et al.*, Enrichment of cysteinyl adducts of human serum albumin, *Anal Biochem*, 2010, **400**, 61-68.
45. Kelly S. M., Jess T. J. and Price N. C., How to study proteins by circular dichroism, *Bba-Proteins Proteom*, 2005, **1751**, 119-139.
46. Dockal M., Carter D. C. and Ruker F., The three recombinant domains of human serum albumin - structural characterization and ligand binding properties, *Journal of Biological Chemistry*, 1999, **274**, 29303-29310.
47. Dockal M., Carter D. C. and Ruker F., Conformational transitions of the three recombinant domains of human serum albumin depending on ph, *Journal of Biological Chemistry*, 2000, **275**, 3042-3050.
48. Antonov Y. A. and Wolf B. A., Calorimetric and structural investigation of the interaction between bovine serum albumin and high molecular weight dextran in water, *Biomacromolecules*, 2005, **6**, 2980-2989.
49. Nair D. P., Podgórski M., Chatani S.*, et al.*, The thiol-michael addition click reaction: A powerful and widely used tool in materials chemistry, *Chemistry of Materials*, 2013.
50. Valko K., Nunhuck S., Bevan C.*, et al.*, Fast gradient hplc method to determine compounds binding to human serum albumin. Relationships with octanol/water and immobilized artificial membrane lipophilicity, *J Pharm Sci-Us*, 2003, **92**, 2236-2248.
51. Singla A. K., Garg A. and Aggarwal D., Paclitaxel and its formulations, *Int J Pharm*, 2002, **235**, 179-192.
52. Waters N. J., Jones R., Williams G.*, et al.*, Validation of a rapid equilibrium dialysis approach for the measurement of plasma protein binding, *J Pharm Sci-Us*, 2008, **97**, 4586-4595.
53. de Figueiredo R. M., Oczipka P., Frohlich R.*, et al.*, Synthesis of 4-maleimidobutyric acid and related maleimides, *Synthesis-Stuttgart*, 2008, 1316-1318.
54. Moore J. S. and Stupp S. I., Room-temperature polyesterification, *Macromolecules*, 1990, **23**, 65-70.
55. Vandijkwolthuis W. N. E., Franssen O., Talsma H.*, et al.*, Synthesis, characterization, and polymerization of glycidyl methacrylate derivatized dextran, *Macromolecules*, 1995, **28**, 6317-6322.
56. Habeeb A. F. S. A., [37] reaction of protein sulfhydryl groups with ellman's reagent, *Methods in Enzymology*, 1972, **25**, 457-464.
57. Ellman G. L., Tissue sulfhydryl groups, *Archives of Biochemistry and Biophysics*, 1959, **82**, 70-77.
58. Ahmad B., Parveen S. and Khan R. H., Effect of albumin conformation on the binding of ciprofloxacin to human serum albumin: A novel approach directly assigning binding site, *Biomacromolecules*, 2006, **7**, 1350-1356.

SUPPORTING INFORMATION

^{1}H NMR SPECTRA

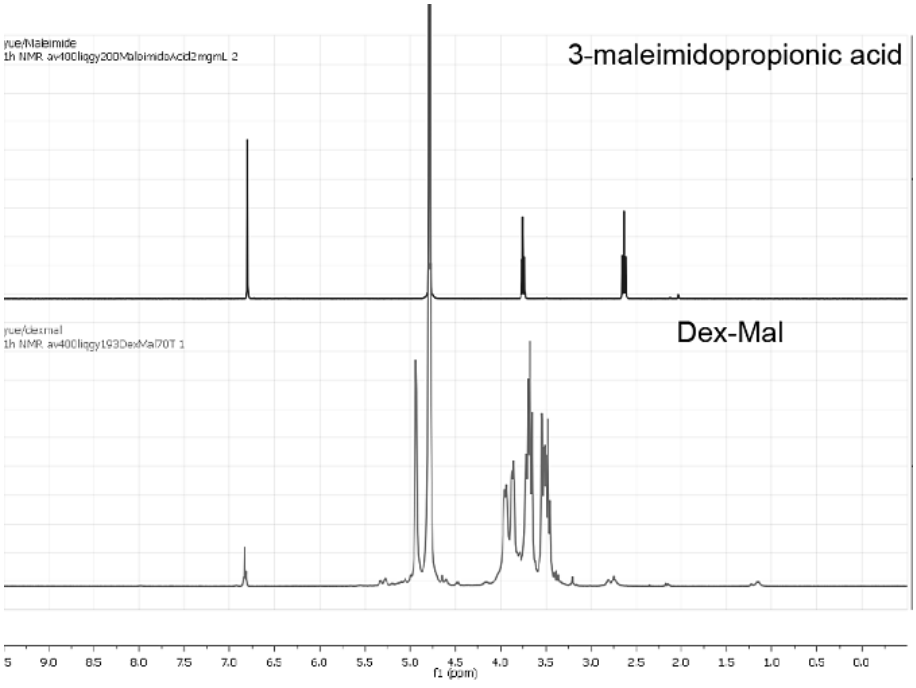

Figure S1. *^{1}H NMR (D_2O) spectra of 3-maleimidopropionic acid and Dex-Mal.*

SWELLING PROPERTIES OF DEX-SHSA HYDROGEL

A Dex-sHSA hydrogel sample (4.5 wt%) was immersed in 150 mM phosphate buffered saline (PBS, pH 7.4, 0.02% sodium azide) at 37 °C. At predetermined time intervals, the entire buffer weight was weighed and fresh buffer was refilled afterwards. The normalized hydrogel weight (NW_h) was calculated by the following equation:

$$NW_h = \frac{W_t}{W_0}$$

Where W_t is the hydrated mass at time t and W_0 the initial mass of the hydrogel after gelation.

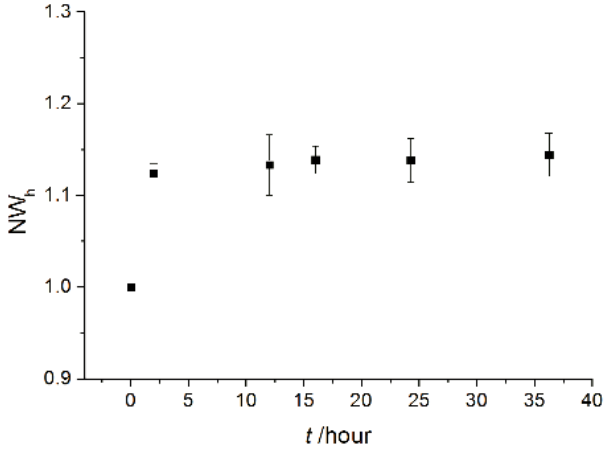

Figure S2. *Swelling properties of Dex-sHSA hydrogels.*

IN VITRO DRUG RELEASE

Table S1. *Physicochemical properties of applied drugs.*

Drugs	M_w	Water solubility (25 °C)*	logP*
ibuprofen	206.28	21 mg/L	3.97
paclitaxel	853.91	insoluble	3
dexamethasone	392.46	89 mg/L	1.83

(* Data obtained from the DrugBank Database: www.drugbank.ca)

In order to quantify the amount of drugs released from the Dex-sHSA gels, calibration curves between drug's concentration and its peak intensity from RP-HPLC analysis were determined prior to the *in vitro* drug release study.

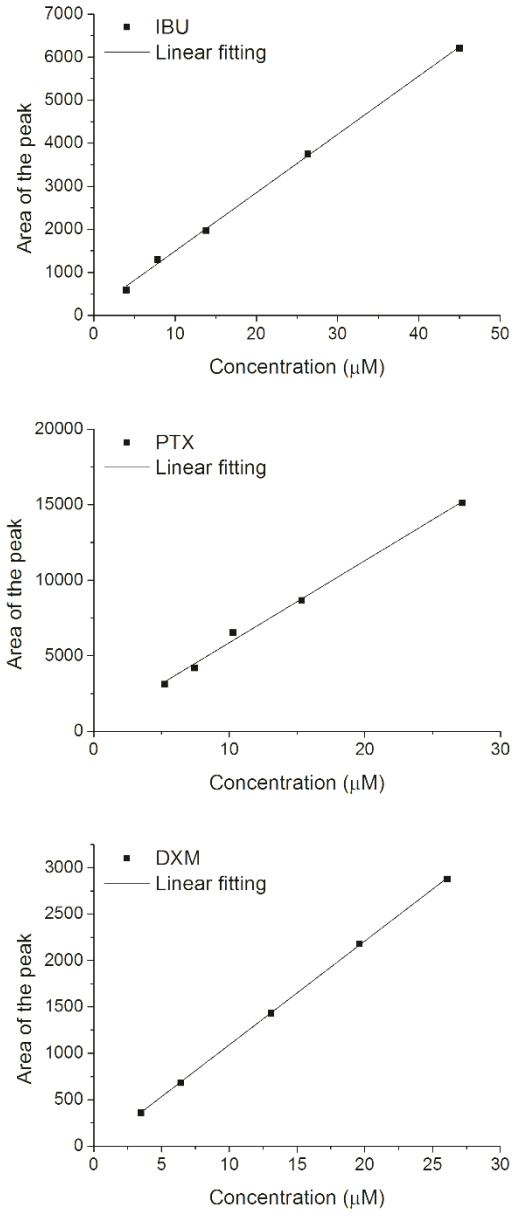

Figure S3. *Calibration curves of IBU, PTX and DXM by RP-HPLC for quantification of the released drug.*

CHAPTER 3

DUAL-CROSSLINKED HUMAN SERUM ALBUMIN-POLYMER HYDROGELS FOR AFFINITY-BASED DRUG DELIVERY

A dual-crosslinked *in situ* gelling drug delivery scaffold based on dextran, thiolated serum albumin and poly(ethylene glycol) is presented. Dextran-vinyl sulfone conjugates with varied molecular weight and degrees of substitution were synthesized by controlling the reaction time and temperature with divinyl sulfone. Dextran-human serum albumin hydrogels were prepared using a thiol-vinyl sulfone Michael addition reaction with thiolated albumin as the crosslinker. Poly(ethylene glycol) dithiol was added as a third component to the crosslinked dextran-human serum albumin hydrogel to facilitate additional crosslinking; simultaneously reducing the gelation time and increasing the tunability of the physicochemical properties of the Dex-sHSA-PEG network. The onset of gelation of the modular three-component dual-crosslinked hydrogel network ranged from 45 minutes to 1.5 hours depending on both gel constituent concentrations and the gelation temperature (25 °C or 37 °C). All gels remained stable for over a 25-day period under physiological conditions. *In vitro* drug release assays showed that dual-crosslinked Dex-sHSA-PEG hydrogels can deliver Doxorubicin in a sustained manner over 7 days. Finally, an MTT assay showed the biocompatible nature of the Dex-sHSA-PEG hydrogels and capacity to deliver Doxorubicin successfully to MCF-7 breast cancer cells.

Part of this chapter was published in *Macromolecular Materials and Engineering* **2017**, 302 (10), 1700243.

INTRODUCTION

Macroscale drug delivery systems have garnered much attention in pharmaceutical research because of their potential to exert control over drug release spatiotemporally.[1, 2] Rather than conventional oral or intravenous drug administrations, novel macroscale drug delivery systems are usually implanted at a site of need for use in long-term or drug delivery. By releasing therapeutics locally at a desired site, side effects and toxicity can be diminished due to lower dosing quantities. Typical drug release mechanisms applied in drug delivery systems include diffusion-controlled drug release,[3] degradation-controlled drug release[4] and stimuli-triggered drug release,[5] each with its own inherent advantages and disadvantages in a therapeutic setting.

Affinity-based drug release systems have emerged to be an attractive platform for their delivery due to the capacity to exploit interactions between the delivery system and the therapeutic drug using a combination of non-covalent interactions to control drug release such as hydrophobicity, hydrogen bonding, electrostatics or van der Waals forces.[6] Advantages of affinity-based drug delivery systems include improved drug loading, prolonged drug stability and sustained release. Drug-binding hosts can be introduced into the polymeric scaffolds using (macro)molecules such as cyclodextrin,[7-11] serum albumin[12-15] and heparin,[16-18] or by generation of cavities within the bulk polymer material by molecular imprinting.[19, 20] A particularly attractive carrier is the most abundant plasma protein (35-50 g L^{-1}) human serum albumin (HSA). HSA has been shown to be biocompatible, biodegradable, non-immunogenic and non-toxic, and is known to bind and transport numerous molecules in the blood circulation, such as fatty acids, bilirubin, hormones, and metal ions.[13, 21] Several therapeutic drugs have also been shown to bind various locations of the albumin protein by several non-covalent interactions with high affinity. Consequently, HSA has been exploited for use as a drug depot in a broad range of particulate carriers,[22-24] but fewer examples of its use in macroscale hydrogel systems have been reported.[12, 25-30] Until now, the synthesis of human serum albumin-based hydrogel materials involves the use of various coupling agents,[25-27] free radical polymerization,[12] UV[29, 30] and γ-ray irradiation[28] in order to facilitate gelation of HSA with varying degrees of biocompatibility. However, in order to apply these HSA-based materials in the biomedical domain, benign gelation strategies that enable control over the resultant hydrogel physicochemical properties are still very much needed.

Injectable, *in situ* gelling hydrogels are practical clinically for deploying macroscale drug delivery systems because of their potential for administration in a minimally invasive manner, reducing patient discomfort, recovery time and treatment workload.[31, 32] The thiol-Michael addition "click" reaction, involving nucleophilic thiols and electron-deficient carbon-carbon double bonds, is highly attractive to form *in situ* gelling hydrogel scaffolds because of its ability to operate selectively under

physiological conditions and with high efficiency.[33, 34] Acrylates, methacrylates, vinyl sulfones and maleimides are typical Michael acceptors ranging in reactivity towards thiols,[35] opening the door for modulating the kinetics of polymer network formation. Generally, the more electron-deficient the C=C bond, the more likely it is to engage in a Michael addition reaction. Although vinyl sulfones present relatively slower reaction kinetics as Michael acceptors with thiols in comparison to maleimides,[34, 36-38] they can form very stable thioether sulfone bonds under mild reaction conditions.[39-47] Moreover, the resulting thioether sulfone bonds are more resistant to hydrolytic degradation over succinimide thioether bonds,[48] which can even undergo competitive exchange with excess thiols or disulfides present in solution.[49]

Previously, we reported a covalently crosslinked dextran hydrogel system[50] that is rapidly formed by a thiol-maleimide Michael addition reaction between the thiol groups of thiolated human serum albumin (sHSA) and maleimide groups of a maleimide-modified dextran (Dex(Mal)). The dextran polymer was selected for its biocompatible character. In this Dex(Mal)-sHSA hydrogel system, sHSA acts as both crosslinker and drug carrier facilitating the sustained release of several drug molecules. However, an issue that limits their broad application is that they were found to degrade after one week at 37 °C in phosphate buffer. This result can be either due to the hydrolysis of the ester bonds connecting the reactive maleimide group to dextran, or the back reaction of the succinimide thioether in presence of excess thiols.[49] To increase the stability of Dex-sHSA hydrogels for long-term release applications, we simultaneously replaced the ester linkage and the succinimide thioether by reacting dextran with divinyl sulfone to provide an ether-linked reactive group for Michael addition. The hydrogel physicochemical properties were tuned by modifying the degrees of substitution of the Dex(VS) polymer. Moreover, the addition of poly(ethylene glycol) dithiol (PEG), a biocompatible and FDA approved polymer, to the Dex-sHSA hydrogel as a second crosslinker was explored, while maintaining the sHSA concentration constant, to increase gelation kinetics while simultaneously modifying mechanical stiffness under physiological conditions. Finally, the capacity of the improved and biocompatible dual-crosslinked Dex-sHSA-PEG hydrogel to deliver a therapeutic payload in a sustained manner was tested using Doxorubicin *in vitro* and in the presence of MCF-7 breast cancer cells (Figure 1).

RESULTS AND DISCUSSION

SYNTHESIS OF DEXTRAN-VINYL SULFONE CONJUGATES

The vinyl sulfone substituted dextran polymer was prepared according to the method outlined by Yu *et al.*[51] because of its potential for zero-length conjugation and synthetic facility in contrast to earlier approaches for polysaccharides.[52, 53] In their approach, dextran polymers were dissolved in

various concentrations of sodium hydroxide (NaOH) solutions (*e.g.* 0.01 M, 0.1 M, 0.2 M, etc.) to generate alkoxides, followed by their reaction with divinyl sulfone (DVS) to form stable ether linkages on the order of minutes. The degree of substitution was modulated as a function of pH, ratio of DVS to OH, and reaction time. The most optimal reaction conditions, enabling control over the reaction rate and product formation, were found when applying 0.1 M NaOH solution (pH = 13) and using a DVS to –OH molar ratio of 1.25 equivalents. We therefore applied these conditions to prepare vinyl sulfone-substituted dextran polymers of various molecular weights (M_n = 20, 70, 150, and 250 kDa) (Table 1) and we examined the reaction time and temperature to control the degree of substitution.

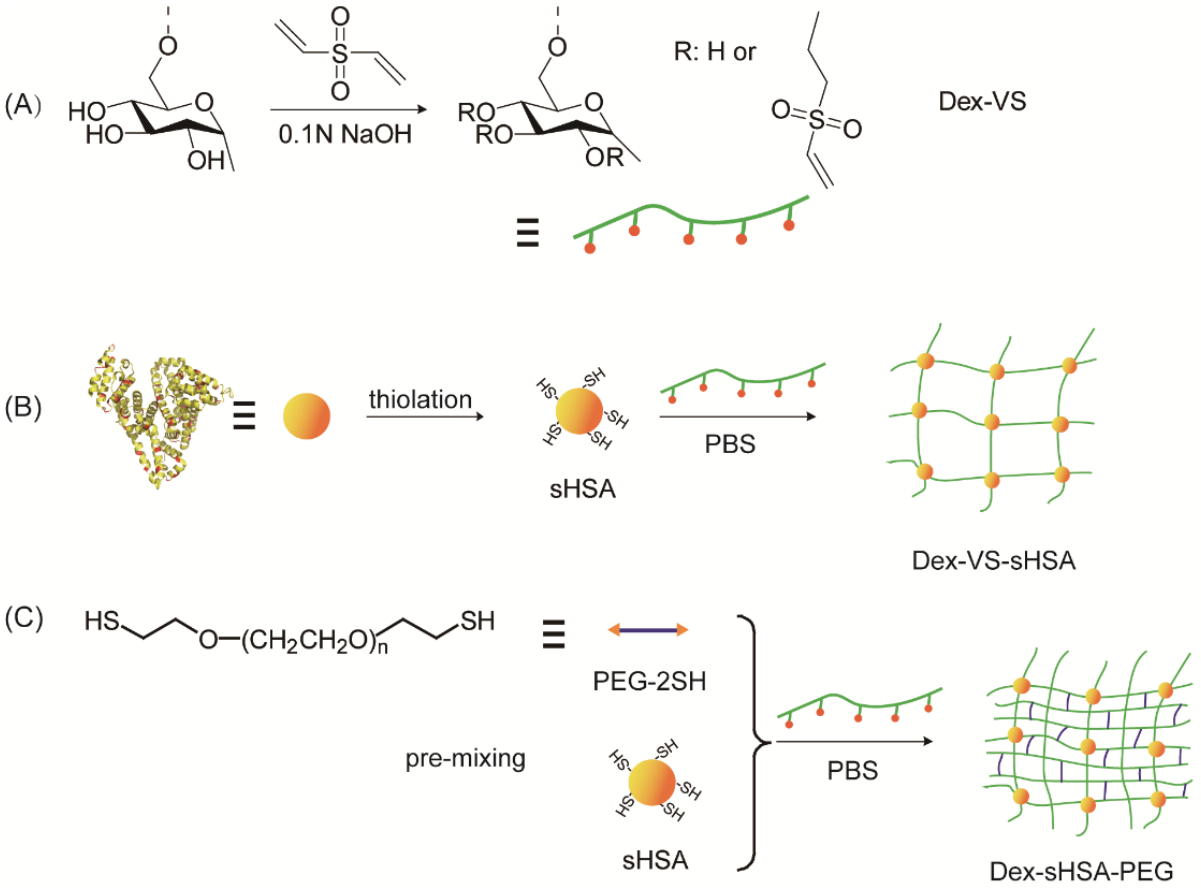

Figure 1. *Schematic representation of the polymers, proteins and resulting hydrogels in this study: (A) Dex(VS), (B) Dex(VS)-sHSA hydrogels, and (C) Dex(VS)-sHSA-PEG hydrogels.*

We first examined the effect of reaction time of reacting divinyl sulfones on the dextran polymers (M_n = 20 and 70 kDa) at room temperature for 5 minutes as previously described.[51] Precipitation occurred for both dextran polymers (M_n = 20 and 70 kDa) before the reaction was halted, suggesting a high degree of substitution of vinyl sulfone and putative crosslinking of the dextran polymers. The precipitated Dex20k(VS) and Dex70k(VS) were examined by ^{1}H NMR spectra in

deuterated DMSO. The degree of substitution of both dextran polymers (M_n = 20 and 70 kDa) were higher than 80 indicating that at least one vinyl sulfone group can be found per anhydroglucose unit of the dextran polymer. Because soluble polymers are required to facilitate *in situ* crosslinking to form hydrogels, we decreased the reaction time to reduce the degree of substitution of the substituted Dex(VS) polymer. In the case of functionalizing of a dextran polymer with a molecular weight of 20 kDa in 0.1 M NaOH solution at room temperature, when the reaction time was reduced to 2, 1 and 0.5 minutes the degree of substitution of obtained Dex20k(VS) conjugates were 31.4, 17.5 and 8.4 % respectively (Table 1). These results show that the reaction time correlates positively with the degree of substitution of Dex(VS), but the relatively rapid reaction time can make the degree of substitution difficult to control.

Table 1. *Influence of the reaction time and temperature on the degree of substitution of dextran polymers with vinyl sulfone.*

	Reaction time [min]	Reaction temperature [°C]	Degree of substitution [%]
Dex20k	5	RT	86
Dex20k	2	RT	31
Dex20k	1	RT	17
Dex20k	0.5	RT	8
Dex70k	5	RT	83
Dex20k	1	0	5
Dex70k	2	0	6
Dex70k	1	0	4
Dex150k	1	0	3
Dex250k	1	0	3

To further control the functionalization of the dextran polymer, we turned to using the reaction temperature to modulate the reaction kinetics. We decreased the reaction temperature to 0 °C while retaining the other reaction conditions including the stoichiometry of the reagents. In the case of dextran (M_n = 20 kDa) with a reaction time of one minute, the degree of substitution was successfully decreased from 17.5 to 5.3 % when the reaction temperature was lowered from room temperature to 0 °C (Table 1) demonstrating increased control over the reaction. This positive result with Dex20k(VS) encouraged us to use both reaction time and temperature to control the

degree of substitution for a broader range of dextran polymers from 20 – 250 kDa. Dextrans with higher molecular weights such as 70, 150 and 250 kDa, showed decreased degrees of substitution in comparison to the 20 kDa polymer. Most likely, the accessibility of the generated alkoxide ions on dextran are sterically hindered by the increased polymer length precluding reaction with the electrophilic double bonds of DVS. Additionally, the solubility of the substituted Dex150k(VS3) and Dex250k(VS3) conjugates was limited. At a concentration of 2 w/v%, neither of the Dex150k(VS3) and Dex250k(VS3) resulted in clear solutions when dissolved in water, while the corresponding unfunctionalized dextran polymers are soluble in water at 2 w/v% (Table 1). Since the vinyl sulfone substituents can increase the hydrophobic character of the dextran polymer affecting its water solubility, both the degree of substitution and the molecular weight of the dextran polymer become important factors to take into consideration for their applications in *in situ* forming hydrogels.

HYDROGEL FORMATION AND MICROSTRUCTURE

The variably substituted Dex(VS) polymers were then evaluated for their capacity to form affinity-based hydrogels by the Michael addition click reaction with the thiolated human serum albumin protein (sHSA). sHSA, prepared with 2-iminothiolane (2-IT) prior to dextran conjugation, was used simultaneously as a therapeutic depot and crosslinker. All hydrogels were prepared by mixing an equimolar ratio of thiols on the sHSA protein to vinyl sulfone groups on the dextran polymer in phosphate buffered saline at pH 7.4 at room temperature. The concentration of sHSA was kept at 5 % (w/v) in resulting hydrogels as previously observed in our Dex(Mal)-sHSA hydrogel systems.[50] Consequently, the amount of Dex(VS) polymer used to prepare Dex(VS)-sHSA hydrogels was varied accordingly to maintain an equimolar ratio with the number of thiol groups on sHSA.

The vial tilting method was used to evaluate the gelation time of the Dex(VS)-sHSA hydrogels at room temperature. The effect of Dex(VS) polymer chain length on the gelation time of Dex(VS)-sHSA hydrogel samples was also evaluated with Dex20k(VS5), Dex70k(VS4), and Dex150k(VS3) by controlling the molar concentration of functional groups (-VS and -SH) at a fixed concentration of 4 mM (Figure 2). Hydrogels were formed under all conditions tested. An increased gelation time for the higher molecular weight polymer was found, which may be due to the reduced accessibility of vinyl sulfone groups resulting in a decreased rate of thiol-Michael addition with the sHSA.

To increase the applicability of this affinity-based hydrogel system for drug delivery, we sought to further tune the rate of hydrogel formation by increasing the concentration of functional groups, and thus crosslinks within the network. Since the amount of sHSA in the hydrogel was kept on par with the concentration reported in plasma, 35-50 g/L, an additional synthetic polymer was required to strengthen the network by crosslinking. For this purpose, poly(ethylene glycol) dithiol (PEG,

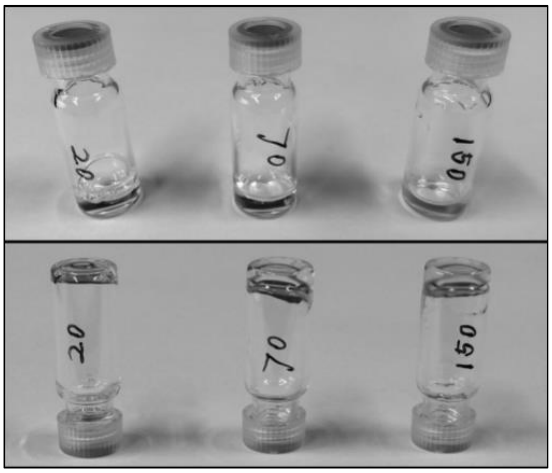

Figure 2. *Gel inversion tests of Dex(VS)-sHSA hydrogels prepared from 5.6 w/v% Dex20k(VS5)-sHSA (left), 5.9 w/v% Dex70k(VS4)-sHSA (middle), 6 w/v% Dex150k(VS3)-sHSA (right) at room temperature, showing the gelation mixtures (top) and their resulting hydrogels (bottom).*

M_n = 3400) was selected to be added to the dextran-sHSA network to provide polymeric bulk and an increased number of crosslinks. PEG was first mixed sHSA (5 w/v%) prior to addition of the corresponding Dex(VS) solution. The dual-crosslinked Dex70k(VS6)-sHSA-PEG hydrogels were prepared at various polymeric crosslinker concentrations (7.5, 10, 11.5 and 13 w/v%) keeping the concertation of sHSA constant and only linearly increasing the concentrations of Dex70(VS6) and PEG (the exact molar ratios of all polymer concentrations are presented in Table 2 at room temperature. All Dex70k(VS6)-sHSA-PEG samples turned from sols to gels upon inversion in 6 hours (Figure 3A). Faster gelation rates were achieved in presence of PEG upon maintaining the final concentration of sHSA at 5 w/v%. By such an approach, the gelation time of the Dex(VS)-sHSA-PEG hydrogels can be tuned without modifying the sHSA concentration, providing the flexibility to independently vary the amount of crosslinks and drug binding sites.

Whereas the dual-crosslinked Dex70k(VS6)-sHSA-PEG hydrogels showed faster gelation kinetics over Dex70k(VS6)-sHSA gels by vial inversion tests, we additionally quantified their onset of gelation and mechanical properties by oscillatory rheology. An amplitude sweep was conducted from 0.01 to 100 % strain in order to determine the linear viscoelastic regime of a 10 w/v% Dex70k(VS6)-sHSA-PEG hydrogel (Figure 3C). The gelation process was followed by growth of the storage modulus (*G*') of the freshly mixed polymer solutions of Dex(VS) and PEG and sHSA with respect to time (Figure 3B) at 25 ºC. As shown in Figure 2b, *G*' started to increase dramatically after 45 minutes and reached a plateau after two and a half hours at 2900 Pa for the 13 w/v% Dex70k(VS6)-sHSA-PEG hydrogel sample at 25 ºC. For 10 and 11.5 w/v% Dex70k(VS6)-sHSA-PEG hydrogel samples took a longer time to reach a plateau during measurement, and the absolute value of *G*' decreased significantly with crosslinking density. In the 7.5 w/v% Dex70k(VS6)-sHSA-

PEG hydrogel sample, the time for gelation to occur was greater than 3 hours and drying of the sample was found to be significant during the oscillatory rheology experiment and is therefore not represented here. Once the rate of gelation and storage moduli were examined for all samples, the mechanical properties of the Dex(VS)-sHSA-PEG hydrogels were further probed by angular frequency sweeps. Frequency sweep measurements showed the formation of a viscoelastic network with *G*' being greater than *G*" by two orders of magnitude from 0.1 to 12.56 rad/s (Figure 3D). Interestingly, gelation kinetics could be increased by elevating the reaction temperature from 25 °C to 37 °C, resulting in both faster gelation (from 1.5 hours to 45 minutes, respectively) and increased mechanical properties of the hydrogels (from 180 Pa to 716 Pa) (Figure 3E) for the 5 w/v% sample. Furthermore, it is anticipated that the gelation kinetics can be further increased by raising their concentration or their degree of functionalization opening the door for their use as practical and tunable hydrogel scaffolds in the biomedical domain. Cryo-scanning electron microscopy (cryo-SEM) images of 7.5 w/v% Dex70k(VS6)-sHSA-PEG hydrogels support the measured rheology data depicting a continuous and porous hydrogel microstructure consistent with other covalent hydrogel systems with pore diameters in the range of 2 - 10 μm (Figure 4).

The effect of sHSA on the gelation behavior of the dual-crosslinked Dex(VS)-sHSA-PEG hydrogels was then examined by comparing time sweep measurements of hydrogels with and without sHSA on hydrogel formation. The rheological properties of 10 w/v% Dex70k(VS6)-

Table 2. *Compositions of various Dex(VS)-sHSA and Dex(VS)-sHSA-PEG hydrogels.*

	Polymer concentration [w/v%]	-VS on Dex [mM]	-SH on HSA [mM]	-SH on PEG [mM]
Dex20k(VS5)-sHSA	5.6	4	4	-
Dex70k(VS4)-sHSA	5.9	4	4	-
Dex150k(VS3)-sHSA	6	4	4	-
Dex70k(VS6)-sHSA	5.4	4	4	-
Dex70k(VS6)-sHSA-PEG	7.5	8	4	4
Dex70k(VS6)-sHSA-PEG	10	15	4	11
Dex70k(VS6)-sHSA-PEG	11.5	20	4	16
Dex70k(VS6)-sHSA-PEG	13	25	4	21
Dex70k(VS6)-PEG	5	15	-	15

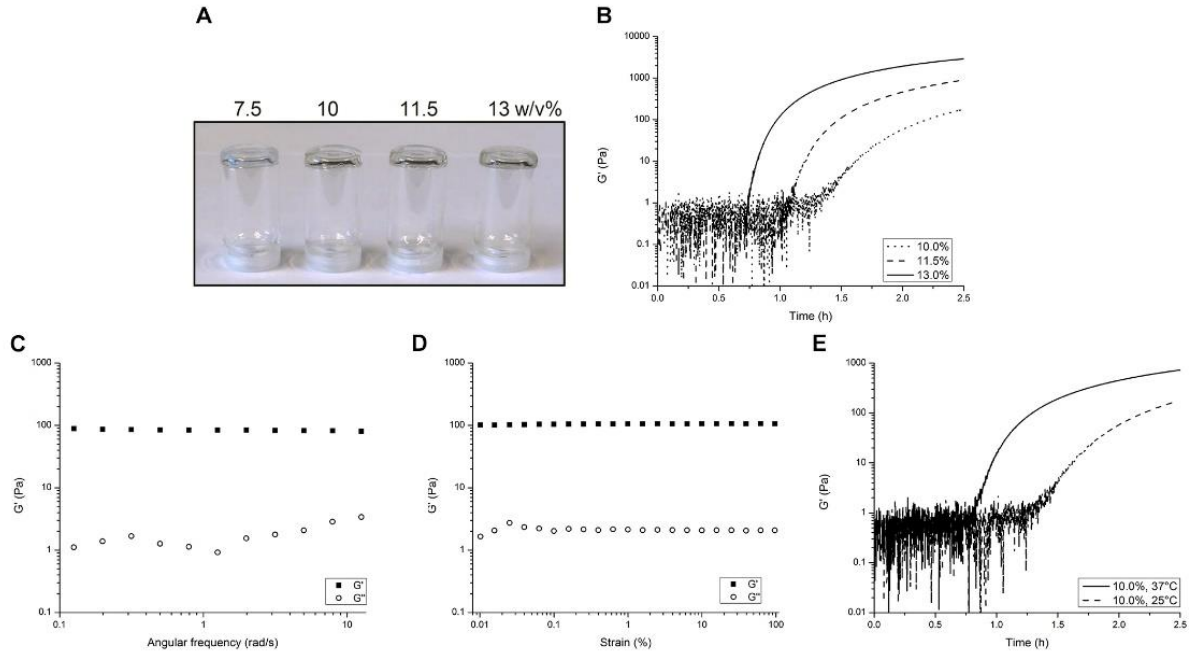

Figure 3. *(A) Gel inversion of 7.5, 10, 11.5 and 13 w/v% Dex70k(VS6)-sHSA-PEG hydrogels. Oscillatory rheology measurements of Dex70k(VS6)-sHSA-PEG hydrogels at 25 °C (25 mm plate-plate geometry); (B) time sweep measurement of 10, 11.5 and 13 w/v% Dex70k(VS6)-sHSA-PEG hydrogels at 6.28 rad/s with 0.05 % strain at 25 ºC; (C) amplitude sweep measurement of 10 w/v% Dex70k(VS6)-sHSA-PEG hydrogels from 0.1 to 12.56 rad/s with 0.05 % strain at 25 ºC; (D) angular frequency sweep measurement of 10 w/v% Dex70k(VS6)-sHSA-PEG hydrogels from 0.01 to 100 % strain at 6.28 rad/s at 25 ºC; (E) comparison of gelation of 10 w/v% Dex70k(VS6)-sHSA-PEG hydrogels at 25 °C and 37 °C.*

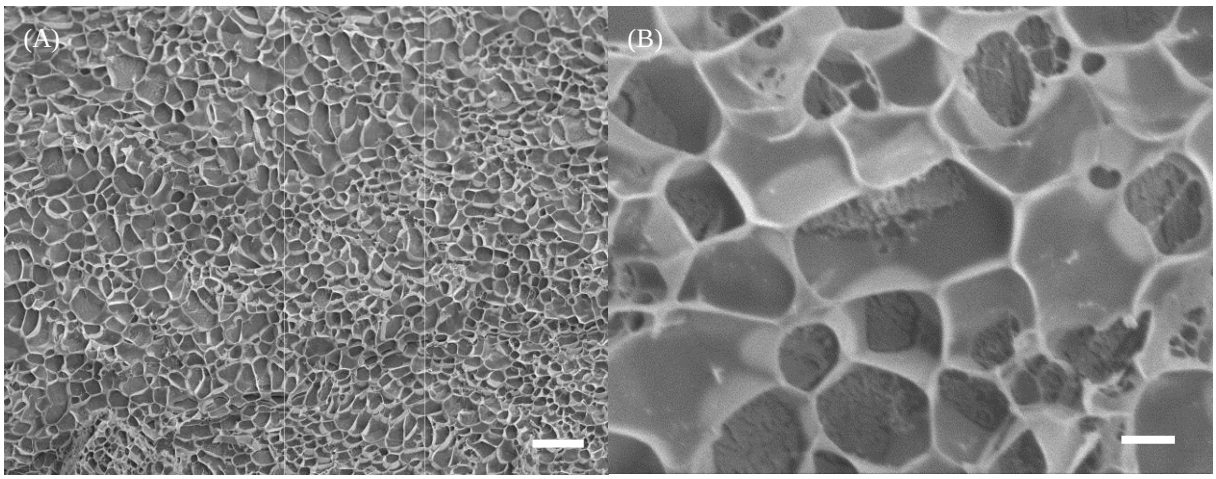

Figure 4. *Cryo-SEM images of 8 mM Dex70k-VS6-sHSA-PEG hydrogel prepared in phosphate buffer saline (pH=7.4). Scale bars: (A) 10 μm; (B) 1 μm.*

sHSA-PEG showed both slower gelation kinetics and lower mechanical stiffness and 5 w/v% Dex70k(VS6)-PEG hydrogels were compared, in which for the latter sample to maintain an equimolar ratio of thiol and vinyl sulfone groups the molar equivalents of sHSA were replaced by additional PEG (Table 2). Interestingly, the Dex70k(VS6)-sHSA-PEG hydrogels after 2.5 hours than the Dex70k(VS6)-PEG hydrogels (Figure S2). Most likely, the higher molecular weight and more compact conformation of albumin reduce the accessibility of thiol groups of sHSA to Dex(VS) polymers resulting in slower reaction and gelation kinetics of Dex(VS)-sHSA-PEG hydrogels relative to the Dex-PEG hydrogels and overall lower mechanical properties. However, our previous work using Dex-sHSA hydrogels does show that sHSA can act as a crosslinker so the sHSA has a combined role in both to some extent contributing to crosslinking within the hydrophilic Dex-sHSA-PEG network in addition to its envisioned role as a drug carrier, albeit at the cost of network stiffness compared to native Dex-PEG hydrogels.

HYDROGEL SWELLING AND DEGRADATION

Equilibrium swelling measurements were performed to evaluate hydrogel network swelling and stability.[54] Previously, we demonstrated that Dex(Mal)-sHSA gels (5 w/v%), prepared from sHSA and a maleimide-functionalized by an ester bond to dextran (Dex(Mal)), were observed to maintain their integrity in PBS for more than three weeks at room temperature in swelling experiments. However, on performing the same experiment at 37 °C complete degradation of the Dex(Mal)-sHSA gels was observed in one week. Consequently, we sought to increase the stability of the hydrogel network under physiological conditions by changing the ester-linked maleimides to vinyl sulfone groups in the Michael addition reaction.

Hydrogels composed of Dex70k(VS6)-sHSA-PEG (10, 11.5, and 13 w/v%) and Dex70k(VS6)-sHSA (5.9 w/v%) were probed every day at 37 °C for a total of 24 days with all hydrogels being stable over the measuring period (Figure 5A). Both the Dex70k(VS6)-sHSA-PEG and Dex70k(VS6)-sHSA hydrogels displayed slight swelling in the first 48 hours and a subsequent decrease over the remaining time period. This decrease in swelling is consistent with the diffusion of unreacted polymer or protein components from the network; consistent with other covalent polymer hydrogel systems.[55] After 3 to 4 days, the swelling ratio eventually became constant reaching equilibrium. The Dex70k(VS6)-sHSA-PEG hydrogels showed a lower degree of swelling compared to the Dex70k(VS6)-sHSA hydrogels, which is on par with a polymer network that possesses a higher crosslinking degree due to the added poly(ethylene glycol).

The release of albumin from the hydrogel network during the swelling process was quantified over time to better understand the extent of sHSA coupling and to evaluate the effect of PEG addition to the hydrogel network. Hydrogels consisting of thiolated (sHSA) and native (HSA) albumin were compared for their release. In all cases the amount of albumin loaded was kept constant at 5 w/v%.

The native albumin protein, lacking additional free thiol groups and unable to act as a crosslinker, was physically encapsulated to form a 10 w/v% Dex70k(VS6)-PEG hydrogel, and its release was compared to hydrogels containing thiolated albumin, 5.4 w/v% Dex70k(VS6)-sHSA, 7.5, 10, 11.5 and 13 w/v% Dex70k(VS6)-sHSA-PEG hydrogels. After 48 hours, nearly 80 % of the loaded native albumin was released from 10 w/v% Dex70k(VS6)-PEG hydrogel network (Figure 5B, presented as star symbols). On the other hand, 35 % of sHSA was released from the 5.4 w/v% Dex70k(VS6)-sHSA hydrogels to the surrounding buffer solutions after 48-hour incubation (Figure 5B, presented in cross symbols). This result demonstrates that a fraction of the added sHSA protein remains unconjugated to the Dex(VS) polymer despite having reactive groups and that crosslinking retards its diffusion from the network. All 10, 11.5 and 13 w/v% Dex70k(VS6)-sHSA-PEG hydrogels (Figure 5B, presented in square, circle and triangle symbols respectively), retained the thiolated albumin protein to an even greater extent with less than 20 w/v% of sHSA being released up to 6 days, putatively due to the increased crosslinking of the network from the addition of the PEG.

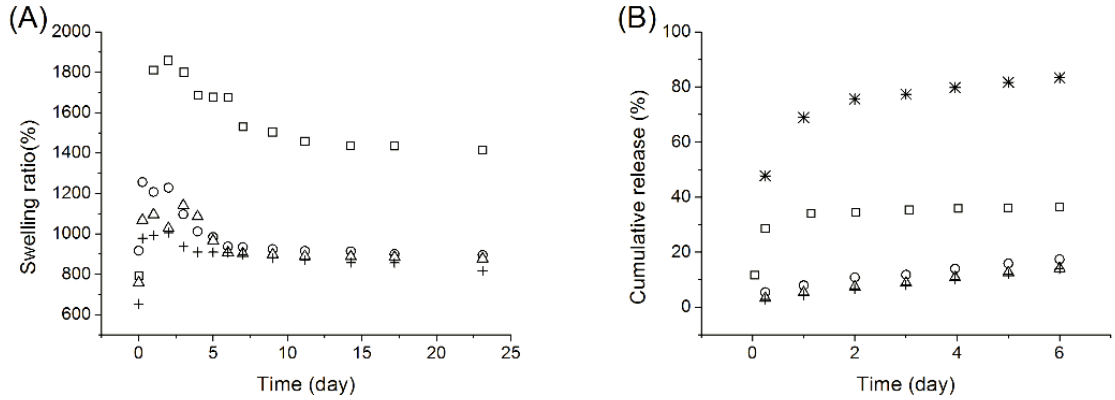

Figure 5. *(A) Equilibrium swelling study of 10 (○), 11.5 (⊿) and 13 (+) wt% Dex70k(VS6)-sHSA-PEG and 5.9 w/v% Dex70k(VS6)-sHSA (□) hydrogels at 37 °C over 24 days. (B) Albumin release studies from 10 (○), 11.5 (⊿) and 13 (+) w/v% Dex70k(VS6)-sHSA-PEG, and 5.9 w/v% Dex70k(VS6)-sHSA (□) hydrogels with thiolated sHSA and 5 w/v% Dex70k(VS6)-PEG (✳) hydrogel with native HSA, respectively.*

In comparison to the earlier reported Dex(Mal)-sHSA hydrogels, the Dex(VS)-sHSA and dual-crosslinked Dex(VS)-sHSA-PEG hydrogels with the new thioether linkages showed increased stability for use under physiological conditions at 37 ºC. Moreover, the addition of PEG as a crosslinker can modulate the gelation time, mechanical stiffness and the equilibrium swelling of the network providing access to a highly tuneable platform for drug delivery.

DRUG DELIVERY FROM DEX(VS)-SHSA-PEG HYDROGELS

Once the physicochemical properties of the dual-crosslinked Dex(VS)-sHSA-PEG hydrogel

network were examined, we then sought to evaluate its potential as an affinity-based drug scaffold by using the bound sHSA to bind a chemotherapeutic drug Doxorubicin (DOX). DOX is well-known to intercalate within the DNA base pairs and to interact with DNA-associated proteins, such as topoisomerase enzymes I and II, to produce cytotoxic effects through DNA damage.[56] Because of the notorious cardiotoxicity of DOX, delivery systems that enable its sustained release are of interest in the medical field. Slow release of DOX from the network is anticipated due to the known binding of DOX to HSA (K_d= 1.1*10^4 L mol^{-1}).[57] As a first approach, an *in vitro* release DOX release assay was performed by incubation of 0.5 mg/mL DOX with sHSA to facilitate its encapsulation prior to crosslinking with PEG to form the 10 w/v% Dex70k(VS6)-sHSA-PEG hydrogel at 25 °C to benchmark the release properties of the hydrogel, resulting in a sustained release over 7 days. Subsequently, two different concentrations (0.5 and 1.0 mg/mL) were probed at 37 °C to better understand the kinetics of DOX release from the network under physiological conditions. The continuous release of DOX was observed over 7 days where 1.0 mg/mL DOX loaded gels expectedly released the therapeutic cargo faster than their 0.5 mg/mL loaded counterparts (Figure 6). Interestingly, the hydrogels prepared at 37 °C showed decreased release kinetics most likely due to the formation of more crosslinked materials as observed by oscillatory rheology.

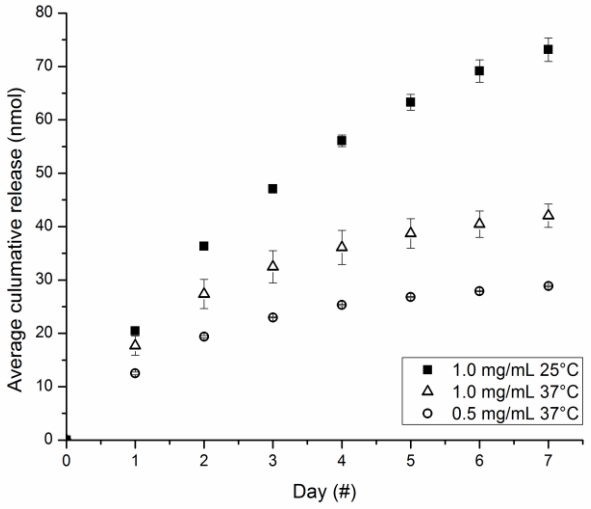

Figure 6. *In vitro drug release profile of Doxorubicin (0.5 and 1.0 mg/mL) from 10 w/v% Dex70k(VS6)-sHSA-PEG hydrogels at 25 °C and 37 °C measured over 7 days.*

Overall, the albumin drug carrier can effectively aid in the solubility and binding of the drug in the hydrogel while reducing its diffusivity and retarding its release as a function of DOX concentration. Therefore, Dex(VS)-sHSA-PEG hydrogels demonstrate their potential for use as materials for sustained drug delivery under physiological conditions.

Subsequently, the toxicity of the Dex(VS)-sHSA-PEG hydrogel network and its capacity to deliver therapeutics to MCF-7 breast cancer cells was probed (Figure 7). Native hydrogels, DOX-loaded hydrogels (0.5 mg/mL) and as a negative control a 1 μM DOX solution were incubated with MCF-7 cells for up to three days and cell viability was monitored using an MTT assay. The native hydrogel showed a negligible decrease (~10 %) of cell viability compared to the untreated MCF-7 cells, indicating that the material by itself shows no cytotoxic effects towards MCF-7 cells over this period. The negative control containing free DOX showed a reduction in cell viability of ~ 86% after three days. The cells incubated with DOX-loaded hydrogels showed a drastic reduction in cell viability, 80% after 3 days, demonstrating the potency of the drug against cancerous cells when released from the gel network.

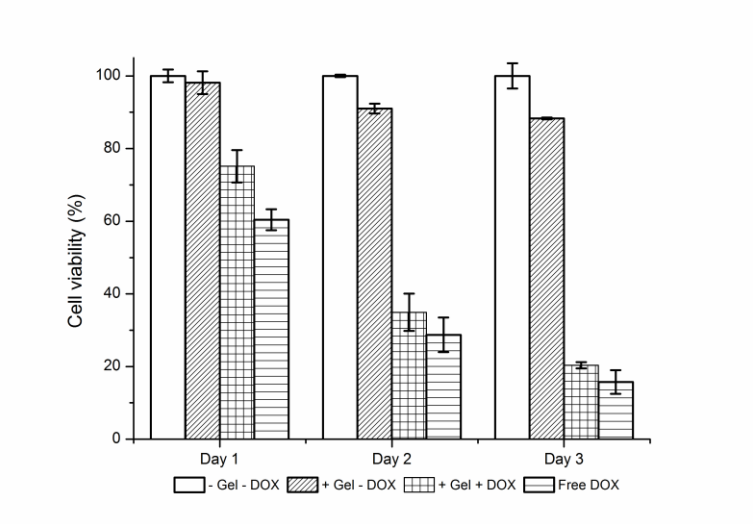

Figure 7. *In vitro MTT cytotoxicity assay on the effects of Doxorubicin drug-release from 10 w/v% Dex70k(VS6)-sHSA-PEG hydrogels on MCF-7 breast cancer cells. Conditions: untreated MCF-7 cells (white), treated with native hydrogel (diagonal stripes), treated with Doxorubicin containing hydrogel (check pattern), treated with free DOX (horizontal stripes).*

CONCLUSION

A novel and stable dual-crosslinked affinity-based drug delivery system based on dextran, human serum albumin and poly (ethylene glycol) was successfully prepared using thiol-vinyl sulfone Michael addition. Vinyl sulfone modified dextran polymers with various degrees of substitution and molecular weights were synthesized in a controllable manner by using time and decreasing the reaction temperature of the dextran reaction with divinyl sulfone. Through tethering vinyl sulfone reactive groups by an ether linkage to the dextran polymer, stable hydrogel systems were prepared that can be used at 37 ºC for several weeks. Moreover, the addition of PEG as a secondary crosslinker and modulation of the reaction temperature resulted in the formation mechanically tunable networks with a more rapid gelation time and the stable incorporation of albumin. Finally,

we validated Dex(VS)-sHSA-PEG hydrogels as a sustained drug delivery system and showed efficient doxorubicin-mediated cytotoxicity. These results highlight that by using human serum albumin as a drug carrier in such materials, a broad range of therapeutics can be loaded efficiently within them enabling their sustained release. Moreover, the biocompatible nature of all three hydrogel components and the tunability of the hydrogels with respect to their gelation times and properties open the door for their future widespread application in the biomedical domain.

EXPERIMENTAL

MATERIALS

Dextran (M_n = 70 kDa), divinyl sulfone, human serum albumin (HSA) (fatty acid free), 2-iminothiolane (2-IT), 5,5'-dithiobis(2-nitrobenzoic acid) (DTNB), sodium hydroxide, sodium azide, hydrochloric acid (37%), poly(ethylene glycol) dithiol (PEG, M_w = 3.4 kDa), dimethyl sulfoxide (DMSO), and doxorubicin hydrochloride (DOX) were obtained from Sigma-Aldrich. Dextrans (M_n = 20 kDa, 150 kDa and 250 kDa) were purchased from Pharmacosmos. Dialysis membranes (MWCO = 3.5 - 5 kDa) were obtained from Spectrum Laboratories Inc. Dextran was dried in a vacuum oven (30 °C) before use. Phosphate buffered saline stock (1x) was obtained from the Cell Observatory of Leiden University. 24-well Corning® Transwell® polyester membrane cell culture inserts plate were purchased from Sigma.

SYNTHESIS OF DEXTRAN-VINYL SULFONE CONJUGATES

Dex(VS) was synthesized according to the method reported by Yu *et al.*[51] In general, a 2 % (w/v) dextran solution (M_W = 20, 70, 150 or 250 kDa, synthesis is described for 70 kDa as an example) was prepared by dissolving dextran (1 g, 14.3 μmol) in 0.1 M NaOH (50 mL). Divinyl sulfone (DVS) (0.778 mL, 7.75 mmol) was added to a vigorously stirred dextran solution at either 0 °C or room temperature for a specific time ranging from 0.5 - 5 min. The reaction was quenched using 5 M HCl adjusting the pH to 5 and the product was dialyzed against Milli-Q water 5 times over 3 days and lyophilized. ^{1}H NMR recorded on a Bruker AV-400 (D_2O, 400 MHz): δ 3.3–4.1 (m, dextran glucosidic protons), 4.97 (s, dextran anomeric proton), 6.3-6.5 ppm (m, $-SO_2CH=CH_2$), 6.9-7.0 (m, $-SO_2CH=CH_2$). The obtained Dex(VS)-polymers were further confirmed by ^{1}H NMR and ^{1}H-^{13}C HSQC 2D spectra spectra measured by a Bruker AV-400 spectrometer (Figure S1).

The degree of substitution of the vinyl sulfone functionalized dextran polymer (Dex(VS)) is defined as the number of vinyl sulfone groups per 100 glucopyranose residues. The degree of substitution is calculated from the ^{1}H NMR spectrum of Dex(VS) using the ratio: (100x)/(2y), in which x is the integral of vinyl sulfone protons (δ 6.3-6.5) and y is the integral of the anomeric proton of dextran

(δ 4.9). Therefore, the nomenclature of the various polymers consists of the molecular weight of the dextran used (*e.g.* Dex70k(VS6))and the degree of substitution of vinyl sulfone on the particular polymer (*e.g.* Dex70k(VS6)). A complete overview of the polymers synthesized in this work is shown below in Table 1.

SYNTHESIS OF THIOLATED HUMAN SERUM ALBUMIN (SHSA)

HSA (1 g) was dissolved in 50 mM sodium phosphate buffer (45 mL, pH 8, including 5 mM EDTA) and stirred at 0 °C in ice bath. To this an aqueous solution of 2-IT (104 mg, 5.2 mL) was added in a drop-wise manner. After 2 hours, the reaction mixture was dialyzed against 10 mM HEPES buffer (pH 7) three times over 24 hours and then against Milli-Q water three times over 2 days at 4 °C. Finally, sHSA was lyophilized and stored at -20 °C.

The degree of thiolation of sHSA was quantified using an Ellman's test.[58, 59] In short, DTNB (2 mM, 100 μL) and sHSA (2 mg, 200 μL) were mixed with sodium phosphate buffer (700 μL, 0.1M pH8) and incubated at room temperature for one hour. The formation of the yellow 2-nitro-5-thiobenzoate anion (TNB^{2-}) due to the presence of free thiols was quantified using UV-Vis spectroscopy at 412 nm using the molar extinction coefficient $\varepsilon = 14150\ M^{-1}$ and used to calculate the concentration of free thiol groups on the sHSA, which was found to be 2.7.

GELATION PROTOCOL

Dex(VS)-sHSA and Dex(VS)-sHSA-PEG hydrogels were prepared from independent solutions of Dex(VS), sHSA and PEG-dithiol dissolved in phosphate buffer saline. An example of the preparation of a Dex(VS)-sHSA-PEG hydrogel is described below. The same protocol applies to Dex(VS)-sHSA hydrogels only omitting the addition PEG. Molar ratios of the various constituents of the hydrogels used in this work are listed in Table 2.

Generally, a sHSA solution (300 μL) was first mixed with a PEG solution (300 μL) at room temperature in a nitrogen atmosphere. When a clear solution was obtained, the Dex(VS) solution (300 μL) was added to the mixture at an equimolar ratio of the combined thiols to the vinyl sulfone groups and vortexed for 10 s, prior to standing at room temperature for gelation to occur.

The vial tilting method was used to evaluate the gelation of the Dex(VS)-sHSA hydrogels by gently inverting the gelation mixtures every half hour. When the sample showed a lack of flow upon tilting the vial 180° for one minute, it was regarded as a gel and the time was recorded.

OSCILLATORY RHEOLOGY

A DHR-2 rheometer (TA Instruments) was used to measure the mechanical properties of hydrogels in oscillatory mode using a parallel plate geometry (25 mm diameter) at 25 °C or 37 °C.

The axial force was kept constant at 0.1 N and a water trap was applied to prevent sample evaporation during measurement. The precursor solutions of Dex(VS), sHSA and PEG were mixed thoroughly in an Eppendorf tube (gel samples shown in Table 2) in a 300 μL volume and loaded immediately onto the lower plate of the rheometer. The upper plate was lowered until the sample filled the gap (500 μm). Time sweep measurements were performed at an angular frequency of 6.28 rad s^{-1} and 0.05 % strain. The linear viscoelastic regime (LVR) for each material was determined by an amplitude sweep measurement from 0.01 to 100 % strain at an angular frequency of 6.28 rad s^{-1}. Frequency sweep measurements were collected within the LVR from 12.56 to 0.1 rad s^{-1} with 0.05 % strain. All experiments were performed in duplicate.

SCANNING ELECTRON MICROSCOPY

The morphologies of the hydrogels in the swollen state were observed by a JEOL 6330 Cryo Field Emission Scanning Electron Microscope from the General Instrumentation Facility at Radboud University (Nijmegen, The Netherlands). 5 μL of 7.5 w/v% Dex70k(VS6)-sHSA-PEG hydrogel was taken and injected into a hollow cylindrical sample holder and immediately flash frozen in liquid nitrogen. The sample was then inserted in the cold-stage of the SEM cyro-preparation chamber and cleaved to make a horizontal fracture plane. The water was sublimated during 15 minutes and the fracture plane was coated with a thin gold-palladium layer and subsequently the sample is transferred into the SEM chamber, where it remained frozen during the imaging process.

EQUILIBRIUM SWELLING

Hydrogel samples (5.4 w/v% Dex70k(VS6)-sHSA, 10, 11.5 and 13 w/v% Dex70k(VS6)-sHSA-PEG hydrogels) were prepared in phosphate buffer saline in a glass vial at room temperature and left standing overnight to gelate. Phosphate buffer saline (pH = 7.4) supplemented by 0.02 % NaN_3 (2 mL) was added on top of the formed hydrogel at 37 °C. At specific time points, the buffer was removed from the swollen hydrogel, weighed and fresh buffer was layered on top afterwards. When the weight of swollen hydrogel reached a plateau, the equilibrium swelling ratio (ESR) was calculated using equation **1**. Where W_s is the swollen weight at equilibrium and W_d the dry weight of the hydrogel. Hydrogel samples were measured in triplicate.

$$ESR = \frac{W_s}{W_d} \qquad (\mathbf{1})$$

GEL DEGRADATION

Erosion of hydrogel samples (5.4 w/v% Dex70k(VS6)-sHSA, 10, 11.5 and 13 w/v% Dex70k(VS6)-sHSA-PEG hydrogels) over time was assayed by quantifying the amount of albumin released from the network over a period of ~ 6 days. Hydrogel samples (200 μL) were made in phosphate buffer saline in a glass vial at room temperature and left to stand overnight. The hydrogels were layered

with phosphate buffer saline (containing 0.02% NaN_3, pH = 7.4, 2 mL) and placed in an incubator at 37 °C. The buffer solution was removed after 24 hours for analysis and replenished with fresh buffer. Each withdrawn buffer solution was analyzed by fluorescence spectroscopy to determine the released albumin concentration. The excitation wavelength was set to 295 nm to prevent overlapping excitation of tyrosine residues and the emission spectrum was recorded in the range of 305 - 450 nm on a Tecan infinite M1000 fluorescence plate reader. The excitation and emission bandwidths were both 5 nm. Black Greiner 96-well plates were used. 5 w/v% Dex70k(VS6)-PEG hydrogels were also prepared with HSA lacking chemical modification (5 w/v%) at the same concentration as a control.

CHEMOTHERAPEUTIC DRUG DELIVERY FROM DEX(VS)-SHSA-PEG HYDROGELS

The ability of Dex(VS)-sHSA-PEG hydrogels to deliver therapeutic cargo was evaluated using doxorubicin hydrochloride (DOX) as a model drug. To prepare the drug loaded hydrogels, DOX (either 75 μg, 130 nmol or 150 μg, 260 nmol) was pre-mixed with 100 μL of a sHSA solution (15 mg, 225 nmol) and incubated for 1 hour at 25 °C or 37 °C. Subsequently, 100 μL of a PEG (5.1 mg, 1.5 μmol) solution was added, and the mixture was combined with 100 μL of a Dex(VS) polymer solution (10.8 mg, 154 nmol) to form a 0.5 or 1 mg/mL DOX-loaded 10 w/v% Dex70k(VS6)-sHSA-PEG gelation solution of which 200 μL was left to gelate overnight in an appropriate vessel.

First, a drug release assay was performed. The DOX-loaded Dex(VS)-sHSA-PEG gels (200 μL) were layered with phosphate buffer saline (1 mL) and incubated at either 25 °C or 37 °C for 24 hours. The supernatant buffer solution (800 μL) was collected and replaced with fresh phosphate buffer saline (800 μL) every 24 hours. The collected buffer solutions were analyzed by UV-Vis at 480 nm to determine the concentration of DOX released by its molar extinction coefficient (ε = 11 500 M^{-1} cm^{-1}). All drug release experiments were performed in triplicate.

MCF-7 cells were seeded in a 24-well plate at a concentration of 25 000 cells / well in full growth medium (500 μL). The cells were allowed to grow for 24 hours (37 °C, 5% CO_2) before hydrogels (200 μL) prepared in Transwell® inserts with and without Doxorubicin (0.5 mg/mL) to assess cell death due to drug release and native gel toxicity. As a negative control cells were incubated for three days with a 1 μM solution of free Doxorubicin. The viability of the cells was assessed daily using an MTT assay in triplicate. The Transwell® inserts containing gels were removed and an MTT solution prepared in phosphate buffer saline (5 mg/mL, 20 μL) was added directly to the wells to be assayed. The cells were incubated for 4 hours with MTT to allow for the formation of formazan crystals. Subsequently, the medium was removed and the formazan crystals were dissolved in DMSO (500 μL) by gentle agitation. The amount of formazan formation was

quantified by UV-Vis spectroscopy using the absorbance at 570 nm. Cell viability was expressed as % viability and calculated using the ratio between treated and untreated cells (equation **2**):

$$Cell\ viability = \frac{A570\ cells\ treated}{A570\ cells\ untreated} * 100\% \qquad (\mathbf{2})$$

REFERENCES

1. Kearney C. J. and Mooney D. J., Macroscale delivery systems for molecular and cellular payloads, *Nature Materials*, 2013, **12**, 1004-1017.
2. Brudno Y. and Mooney D. J., On-demand drug delivery from local depots, *Journal of Controlled Release*, 2015, **219**, 8-17.
3. Siepmann J. and Siepmann F., Modeling of diffusion controlled drug delivery, *Journal of Controlled Release*, 2012, **161**, 351-362.
4. Dubose J. W., Cutshall C. and Metters A. T., Controlled release of tethered molecules via engineered hydrogel degradation: Model development and validation, *Journal of Biomedical Materials Research Part A*, 2005, **74**, 104-116.
5. Roy D., Cambre J. N. and Sumerlin B. S., Future perspectives and recent advances in stimuli-responsive materials, *Progress in Polymer Science*, 2010, **35**, 278-301.
6. Wang N. X. and Von Recum H. A., Affinity ‐ based drug delivery, *Macromolecular Bioscience*, 2011, **11**, 321-332.
7. Peng K., Cui C., Tomatsu I.*, et al.*, Cyclodextrin/dextran based drug carriers for a controlled release of hydrophobic drugs in zebrafish embryos, *Soft Matter*, 2010, **6**, 3778-3783.
8. Peng K., Tomatsu I., Korobko A. V.*, et al.*, Cyclodextrin-dextran based *in situ* hydrogel formation: A carrier for hydrophobic drugs, *Soft Matter*, 2010, **6**, 85-87.
9. Zhou J. and Ritter H., Cyclodextrin functionalized polymers as drug delivery systems, *Polymer Chemistry*, 2010, **1**, 1552-1559.
10. Liu C., Zhang Z., Liu X.*, et al.*, Gelatin-based hydrogels with β-cyclodextrin as a dual functional component for enhanced drug loading and controlled release, *RSC Advances*, 2013, **3**, 25041-25049.
11. Cai T., Yang W. J., Zhang Z.*, et al.*, Preparation of stimuli-responsive hydrogel networks with threaded β-cyclodextrin end-capped chains via combination of controlled radical polymerization and click chemistry, *Soft Matter*, 2012, **8**, 5612-5620.
12. Tada D., Tanabe T., Tachibana A.*, et al.*, Drug release from hydrogel containing albumin as crosslinker, *Journal of Bioscience and Bioengineering*, 2005, **100**, 551-555.
13. Kratz F., Albumin as a drug carrier: Design of prodrugs, drug conjugates and nanoparticles, *Journal of Controlled Release*, 2008, **132**, 171-183.
14. Cui M., Naczynski D. J., Zevon M.*, et al.*, Multifunctional albumin nanoparticles as combination drug carriers for intra-tumoral chemotherapy, *Advanced Healthcare Materials*, 2013, **9**, 1236-1245.
15. Wu Y., Ihme S., Feuringbuske M.*, et al.*, A core ‐ shell albumin copolymer nanotransporter for high capacity loading and two ‐ step release of doxorubicin with enhanced anti ‐ leukemia activity, *Advanced Healthcare Materials*, 2013, **2**, 884-894.
16. Kiick K. L., Peptide- and protein-mediated assembly of heparinized hydrogels, *Soft Matter*, 2008, **4**, 29-37.
17. Nie T., Akins R. E., Jr. and Kiick K. L., Production of heparin-containing hydrogels for modulating cell responses, *Acta Biomaterialia*, 2009, **5**, 865-875.
18. Baldwin A. D., Robinson K. G., Militar J. L.*, et al.*, *In situ* crosslinkable heparin-containing poly(ethylene glycol) hydrogels for sustained anticoagulant release, *Journal of Biomedical Materials Research Part A*, 2012, **100A**, 2106-2118.
19. Byrne M. E., Park K. and Peppas N. A., Molecular imprinting within hydrogels, *Advanced Drug Delivery Reviews*, 2002, **54**, 149-161.
20. Chen L., Xu S. and Li J., Recent advances in molecular imprinting technology: Current status, challenges and highlighted applications, *Chemical Society Reviews*, 2011, **40**, 2922-2942.

21. He X. M. and Carter D. C., Atomic structure and chemistry of human serum albumin, *Nature*, 1992, **358**, 209-215.
22. Wagner S., Rothweiler F., Anhorn M. G.*, et al.*, Enhanced drug targeting by attachment of an anti αv integrin antibody to doxorubicin loaded human serum albumin nanoparticles, *Biomaterials*, 2010, **31**, 2388-2398.
23. Wartlick H., Spänkuch-Schmitt B., Strebhardt K.*, et al.*, Tumour cell delivery of antisense oligonuclceotides by human serum albumin nanoparticles, *Journal of Controlled Release*, 2004, **96**, 483-495.
24. Bae S., Ma K., Kim T. H.*, et al.*, Doxorubicin-loaded human serum albumin nanoparticles surface-modified with tnf-related apoptosis-inducing ligand and transferrin for targeting multiple tumor types, *Biomaterials*, 2012, **33**, 1536-1546.
25. Hirose M., Tachibana A. and Tanabe T., Recombinant human serum albumin hydrogel as a novel drug delivery vehicle, *Materials Science and Engineering: C*, 2010, **30**, 664-669.
26. Kakinoki S., Taguchi T., Saito H.*, et al.*, Injectable *in situ* forming drug delivery system for cancer chemotherapy using a novel tissue adhesive: Characterization and *in vitro* evaluation, *European Journal of Pharmaceutics and Biopharmaceutics*, 2007, **66**, 383-390.
27. Tada D., Tanabe T., Tachibana A.*, et al.*, Albumin-crosslinked alginate hydrogels as sustained drug release carrier, *Materials Science and Engineering: C*, 2007, **27**, 870-874.
28. El-Sherif H., El-Masry M. and Taleb M. F. A., Ph-sensitive hydrogels based on bovine serum albumin for anticancer drug delivery, *Journal of Applied Polymer Science*, 2010, **115**, 2050-2059.
29. Oss-Ronen L. and Seliktar D., Photopolymerizable hydrogels made from polymer-conjugated albumin for affinity-based drug delivery, *Advanced Engineering Materials*, 2010, **12**, B45-B52.
30. Oss-Ronen L. and Seliktar D., Polymer-conjugated albumin and fibrinogen composite hydrogels as cell scaffolds designed for affinity-based drug delivery, *Acta Biomaterialia*, 2011, **7**, 163-170.
31. Boere K. W. M., Soliman B. G., Rijkers D. T. S.*, et al.*, Thermoresponsive injectable hydrogels cross-linked by native chemical ligation, *Macromolecules*, 2014, **47**, 2430-2438.
32. Bakaic E., Smeets N. M. B. and Hoare T., Injectable hydrogels based on poly(ethylene glycol) and derivatives as functional biomaterials, *RSC Advances*, 2015, **5**, 35469-35486.
33. Mather B. D., Viswanathan K., Miller K. M.*, et al.*, Michael addition reactions in macromolecular design for emerging technologies, *Progress in Polymer Science*, 2006, **31**, 487-531.
34. Nair D. P., Podgorski M., Chatani S.*, et al.*, The thiol-michael addition click reaction: A powerful and widely used tool in materials chemistry, *Chemistry of Materials*, 2014, **26**, 724-744.
35. Nguyen L.-T. T., Gokmen M. T. and Du Prez F. E., Kinetic comparison of 13 homogeneous thiol–x reactions, *Polymer Chemistry*, 2013, **4**, 5527-5536.
36. Simpkins N. S., The chemistry of vinyl sulphones, *Tetrahedron*, 1990, **46**, 6951-6984.
37. Meadows D. C. and Gervay - Hague J., Vinyl sulfones: Synthetic preparations and medicinal chemistry applications, *Medicinal research reviews*, 2006, **26**, 793-814.
38. Chatani S., Nair D. P. and Bowman C. N., Relative reactivity and selectivity of vinyl sulfones and acrylates towards the thiol–michael addition reaction and polymerization, *Polymer Chemistry*, 2013, **4**, 1048-1055.
39. Masri M. S. and Friedman M., Protein reactions with methyl and ethyl vinyl sulfones, *Journal of protein chemistry*, 1988, **7**, 49-54.
40. Morales-Sanfrutos J., Lopez-Jaramillo J., Ortega-Muñoz M.*, et al.*, Vinyl sulfone: A versatile function for simple bioconjugation and immobilization, *Organic & biomolecular chemistry*, 2010, **8**, 667-675.
41. Wang H., Cheng F., Li M.*, et al.*, Reactivity and kinetics of vinyl sulfone-functionalized self-assembled monolayers for bioactive ligand immobilization, *Langmuir*, 2015.
42. Ortega-Muñoz M., Morales-Sanfrutos J., Megia-Fernandez A.*, et al.*, Vinyl sulfone functionalized silica: A

"ready to use" pre-activated material for immobilization of biomolecules, *Journal of Materials Chemistry*, 2010, **20**, 7189-7196.

43. Lopez-Jaramillo F. J., Ortega-Muñoz M., Megia-Fernandez A.*, et al.*, Vinyl sulfone functionalization: A feasible approach for the study of the lectin–carbohydrate interactions, *Bioconjugate chemistry*, 2012, **23**, 846-855.
44. Mosiewicz K. A., Kolb L., van der Vlies A. J.*, et al.*, *In situ* cell manipulation through enzymatic hydrogel photopatterning, *Nature Materials*, 2013, **12**, 1072.
45. Bae J. W., Lee E., Park K. M.*, et al.*, Vinyl sulfone-terminated peg− plla diblock copolymer for thiol-reactive polymeric micelle, *Macromolecules*, 2009, **42**, 3437-3442.
46. Zustiak S. P. and Leach J. B., Hydrolytically degradable poly (ethylene glycol) hydrogel scaffolds with tunable degradation and mechanical properties, *Biomacromolecules*, 2010, **11**, 1348-1357.
47. Jukes J. M., van der Aa L. J., Hiemstra C.*, et al.*, A newly developed chemically crosslinked dextran–poly (ethylene glycol) hydrogel for cartilage tissue engineering, *Tissue Engineering Part A*, 2009, **16**, 565-573.
48. Roberts M., Bentley M. and Harris J., Chemistry for peptide and protein pegylation, *Advanced drug delivery reviews*, 2012, **64**, 116-127.
49. Baldwin A. D. and Kiick K. L., Tunable degradation of maleimide–thiol adducts in reducing environments, *Bioconjugate chemistry*, 2011, **22**, 1946-1953.
50. Gao Y., Kieltyka R. E., Jesse W.*, et al.*, Thiolated human serum albumin cross-linked dextran hydrogels as a macroscale delivery system, *Soft matter*, 2014, **10**, 4869-4874.
51. Yu Y. and Chau Y., One-step "click" method for generating vinyl sulfone groups on hydroxyl-containing water-soluble polymers, *Biomacromolecules*, 2012, **13**, 937-942.
52. Hiemstra C., van der Aa L. J., Zhong Z.*, et al.*, Novel *in situ* forming, degradable dextran hydrogels by michael addition chemistry: Synthesis, rheology, and degradation, *Macromolecules*, 2007, **40**, 1165-1173.
53. Hiemstra C., van der Aa L. J., Zhong Z.*, et al.*, Rapidly *in situ*-forming degradable hydrogels from dextran thiols through michael addition, *Biomacromolecules*, 2007, **8**, 1548-1556.
54. Osada Y. and Khokhlov A., *Polymer gels and networks*, CRC Press, 2001.
55. Lee J. B., Chun K. W., Yoon J. J.*, et al.*, Controlling degradation of acid-hydrolyzable pluronic hydrogels by physical entrapment of poly(lactic acid-co-glycolic acid) microspheres, *Macromolecular Bioscience*, 2004, **4**, 957-962.
56. Tacar O., Sriamornsak P. and Dass C. R., Doxorubicin: An update on anticancer molecular action, toxicity and novel drug delivery systems, *Journal of Pharmacy and Pharmacology*, 2013, **65**, 157-170.
57. Agudelo D., Bourassa P., Bruneau J.*, et al.*, Probing the binding sites of antibiotic drugs doxorubicin and *N*-(trifluoroacetyl) doxorubicin with human and bovine serum albumins, *PLoS ONE*, 2012, **7**, e43814.
58. Ellman G. L., Tissue sulfhydryl groups, *Archives of Biochemistry and Biophysics*, 1959, **82**, 70-77.
59. Habeeb A. F. S. A., [37] reaction of protein sulfhydryl groups with ellman's reagent, *Methods in Enzymology*, 1972, **25**, 457-464.

SUPPORTING INFORMATION

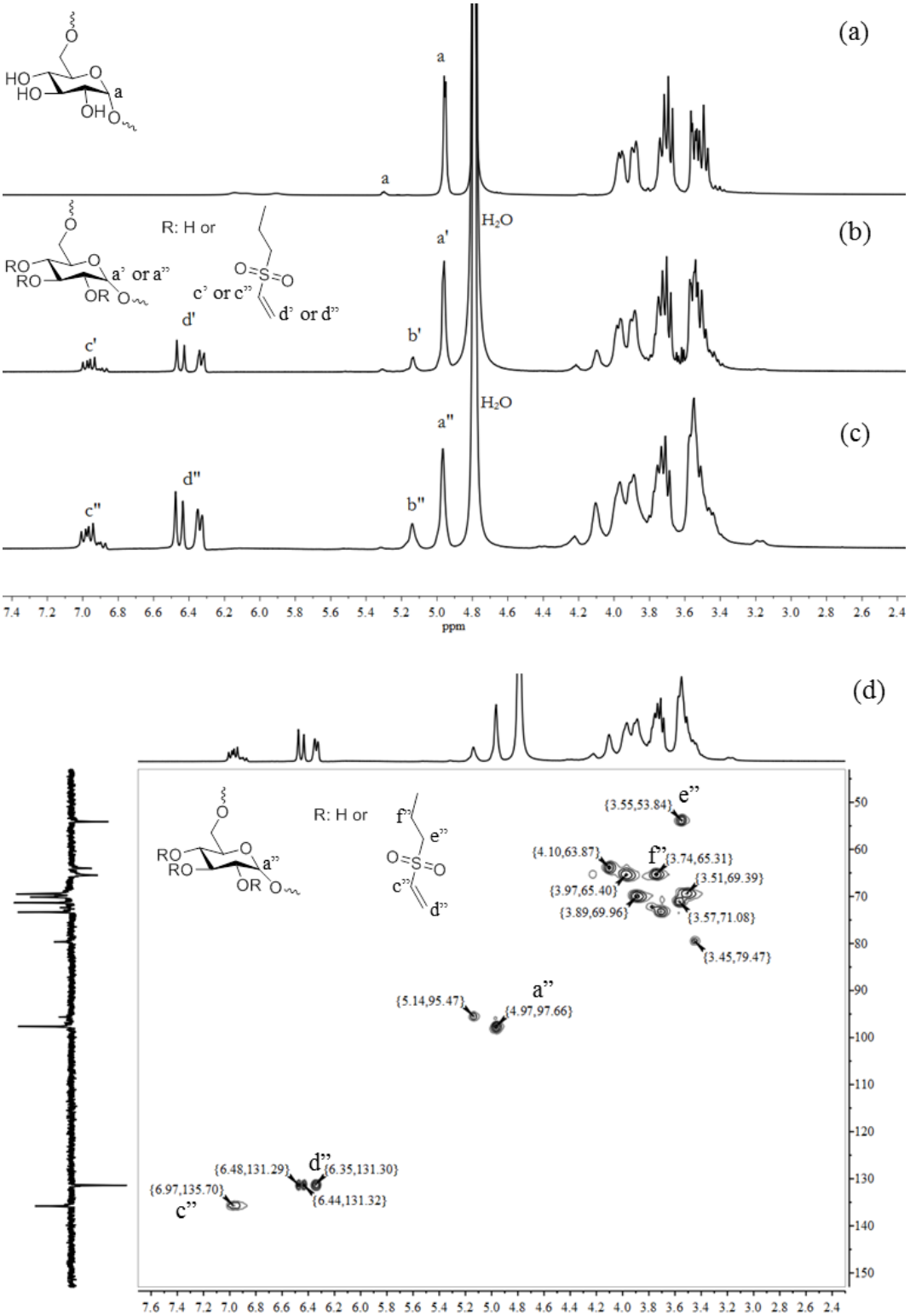

Figure S1. *^{1}H NMR spectra in D_2O: (a) unfunctionalized dextran, 20 kDa, (b) Dex20k-VS (DS=31.4) and (c) Dex20k-VS (DS=17.5). (d) 2D HSQC NMR spectrum (D_2O) of Dex20k-VS (DS=31.4).*

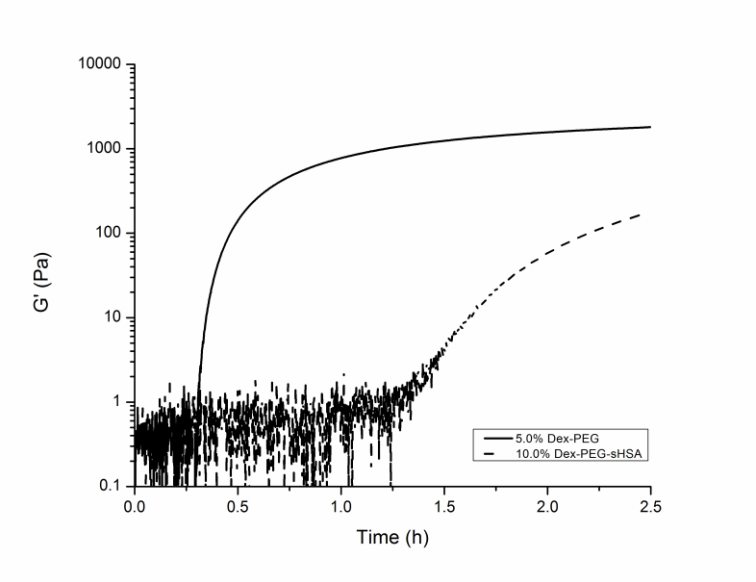

Figure S2. *Oscillatory rheology time sweeps of the gelation processes of 10 w/v% Dex70k(VS6)-sHSA-PEG hydrogels (dash line) and 5 w/v% Dex70k(VS6)-PEG hydrogels (solid line) using an equivalent molar concentration of functional groups.*

CHAPTER 4

ZEBRAFISH EMBRYO TOXICITY ASSAY USING A CYCLODEXTRIN-MODIFIED DEXTRAN-PEG POLYMERIC DRUG CARRIER

High-throughput screening assays based on zebrafish embryos have been applied in toxicology and drug discovery studies. However, concerns over the predictive capacity for specific compounds, such as neurotoxic compounds, conducted by the zebrafish embryo toxicity assay have been raised because the uptake of compounds through the membranes of zebrafish embryos varies thereby affecting the observed toxicity. In this chapter, a drug carrier mediated zebrafish embryo toxicity assay was developed, which improves the uptake of the model drug valproate through the gastrointestinal tract. The polymeric drug carrier used in this study is obtained by crosslinking maleimide modified dextran with poly(ethylene glycol) dithiol, wherein cyclodextrins were conjugated to the dextran backbone to provide drug binding cavities. By applying this macromolecular drug carrier the sensitivity of the zebrafish embryo toxicity assay toward the model drug valproate is significantly enhanced.

INTRODUCTION

Comprehensive safety data is essential for industrial chemicals, biocides, food additives, pharmaceuticals and other commercial chemicals, thus a wide variety of toxicity assays have been developed over years, varying from *in vitro* cell-based assays to *in vivo* assessments in whole animal models.[1] Typically, *in vitro* cell-based assays enable automated high-throughput screening of toxicity and are relatively cost-effective. However, *in vitro* cell-based models lack relevant whole-animal physiology thereby failing to fully resemble the complexities of *in vivo* models. To provide a better assessment, it would be optimal to evaluate results obtained from *in vitro* assays together with results obtained from *in vivo* assays in whole animal models such as rodents, dogs or monkeys. Considering the great number of compounds that need to be tested, ethical issues have been raised regarding the use of vertebrate animals in research and testing.[2, 3] Therefore, alternative toxicity assays that can bridge the gap in this field between cell assays and whole animal assays are required.[4-6]

To date, zebrafish (*Danio rerio*) embryos have been used predominantly in the fields of developmental biology, molecular genetics, toxicology and drug discovery.[7-10] The zebrafish model provides several remarkable advantages including their small size, high fecundity, fast development and transparent body in early stage embryos, which allows high-throughput screening based for various applications.[11-15] Moreover, zebrafish are sensitive to chemical exposure especially during early development.[7, 16, 17] Exposure of zebrafish embryos to chemical compounds can be achieved by addition of the chemical of interest at a physiological dose to the embryos' aquarium. Since embryonic development of zebrafish has been well characterized [18, 19] and the optically transparent embryos enable live observation under a light microscope, zebrafish embryos have become a promising model for developmental and reproductive toxicity screening,[20, 21] bridging the gap between simple cell-based assays and biological validation in whole animals such as rodents. For example, zebrafish have been used as a model to screen the acute toxicity of organic compounds,[22-24] nanoparticles,[25-28] various biomaterials[29] and heavy metals.[30-33]

However, regarding zebrafish embryo based toxicity assays concerns have been raised in their predictive capacity for specific compounds. Considering that organs of zebrafish embryos are not fully developed, ineffective uptake of certain molecules may result in false negative and/or unreliable results. It has been observed that fish embryos are relatively insensitive to neurotoxic compounds thereby failing to predict acute toxicity.[34-35] For example, valproate (i.e. 2-n-propylpentanoic acid) is an anti-epileptic drug traditionally used for the treatment of certain types of seizures. Although studies indicate that more adverse effects are observed in pregnancies with valproate exposure than other antiepileptic drugs, including fetal death and malformations[26], the zebrafish embryo toxicity assay is rather non-sensitive to assess the toxicity of valproate. Zebrafish embryos exposed to valproate from 6 hpf (hours post-fertilization) to 5 dpf (days post-fertilization)

showed only moderate malformations when exposed to 1 mM valproate.[24] In contrast, zebrafish embryos exposed to 0.4 mM valproate from 6 hpf to 4 dpf with daily solution changes followed by growth in the absence of valproate showed full mortality of the embryos.[36, 37] Recent studies indicated that the ineffective uptake of valproate into zebrafish embryos may be due to the poor membrane permeability as well as metabolism of valproate, resulting in the observed weak toxicity of zebrafish embryos toward this drug.[38] To improve the uptake efficiency of a variety of drugs, hydrophobic drug-hydrophilic polymer conjugates were tested in a toxicity assay using 7-dpf zebrafish embryos. This study showed a higher toxicity as compared to free drug.[39]

Previously, injectable hydrogel systems were developed based on mono-thiolated β-cyclodextrins (MSCD) conjugated to maleimide-bearing dextran crosslinked with linear poly(ethylene glycol) dithiols (PEG-DT) resulting in macromolecular networks (Figure 1).[40, 41] No severe phenotype abnormalities were observed upon injection of these Dex-CD/PEG drug carriers in zebrafish embryos. These drug loaded Dex-CD/PEG drug carriers are able to release the drugs in a sustained manner due to the reversible nature of the inclusion complexes between β-CD and drug molecules. In this work, the ability of Dex-CD/PEG polymeric drug carriers to mediate valproate uptake in zebrafish embryos was assessed.

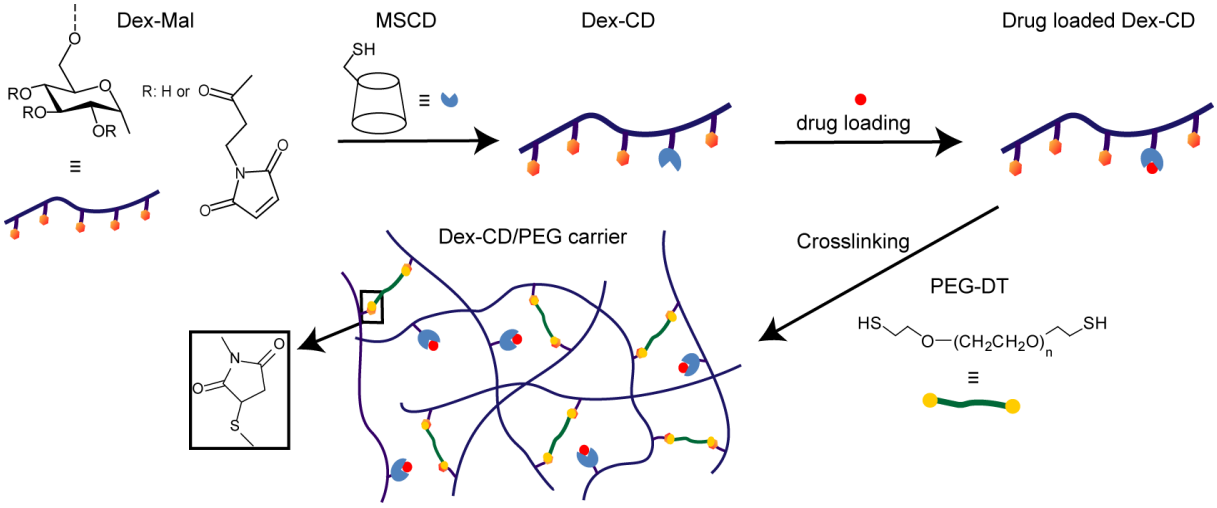

Figure 1. *Schematic representation of the preparation of the Dex-CD/PEG drug carrier.*

Results and Discussion

Interactions between valproate and b-cyclodextrin

Cyclodextrins have been studied and applied for drug delivery for decades due to their ability to form inclusion complexes with specific guest molecules.[42] Cyclodextrins have a relatively hydrophilic, truncated cone-shaped exterior and a hydrophobic hollow tapered cavity, permitting

the formation of an inclusion complex with specific hydrophobic guest molecules enhancing their solubility, stability and bioavailability. First, the interaction between β-CD and valproate was studied to evaluate its ability to bind valproate.

An equimolar mixture of β-CD and valproate was prepared by mixing β-CD and valproate in D_2O and studied by ^{1}H-NMR spectroscopy. Figure 2 shows the assignment of proton signals of the β-CD/valproate mixture. Formation of the valproate/β-CD inclusion complex was shown by 2D NOESY NMR, cross-peaks revealed the interaction between H_4, H_4' of valproate molecules and H_3, H_5 of β-CD (Figure 2C). Cross-peaks also revealed interaction between H_2, H_2' of valproate molecules and H_5 of β-CD. These correlations revealed that valproate indeed is bound inside the cavity of β-CD.[43]

EXPOSURE OF DEXTRAN DERIVATIVES TO ZEBRAFISH EMBRYOS

Fluorescent labelled dextrans are membrane impermeable and often used to study membrane fusion and endocytosis processes.[44-46] Here, zebrafish embryos were exposed to rhodamine B labelled dextrans (dex-RhoB) in order to study the biodistribution and uptake of these soluble macromolecules. Fluorescent dex-RhoB was synthesized by esterification of some of the hydroxyl groups of dextran (M_w = 20 000 Da) with rhodamine B carboxylic acid. The obtained conjugate was purified using a Sephadex G-25 column to remove unreacted dye. Figure 3A shows the UV-Vis spectra of dextran (1 mg/mL), rhodamine B (4 μM) and dex-RhoB (1 mg/mL) conjugates, respectively. The absorption maximum of rhodamine B redshifted 9 nm upon conjugation to dextran, in accordance with Zhang *et al.* who showed a similar shift upon esterification of the carboxyl acid group on the phenyl ring of rhodamine B.[47]

Zebrafish embryo develops rapidly in the initial 100 hours post fertilization. At 72-hpf (i.e. 3-dpf) zebrafish embryo development is at a protruding-mouth stage.[19] At this stage, the mouth of the embryo opens and protrudes anteriorly. Also, the liver and bile cells become visible at this time point. Thus, it becomes probable that zebrafish embryos are able to take up soluble (macro)molecules through the oral route from 3 dpf onwards.

To evaluate the uptake of dextran derivatives, solutions of dextran (1 mg/mL) and dex-RhoB (1 mg/mL) were prepared in egg water, and added to 3-dpf zebrafish embryos, while egg water without dextran was used as a control group. Twelve embryos were used in each group and the zebrafish were observed for 48 hours. The viability of zebrafish embryos was determined every 24 hours and fluorescent microscopy images of zebrafish embryos of the dex-RhoB group were taken. During this 48-hour exposure period, no toxicity was observed and dex-RhoB was observed in the gut of zebrafish embryos. Dex-RhoB fluorescence appeared in the mouth region of embryos after 24 hours (Figure 4A) while fluorescence appeared in the gut region of embryos after 48 hours

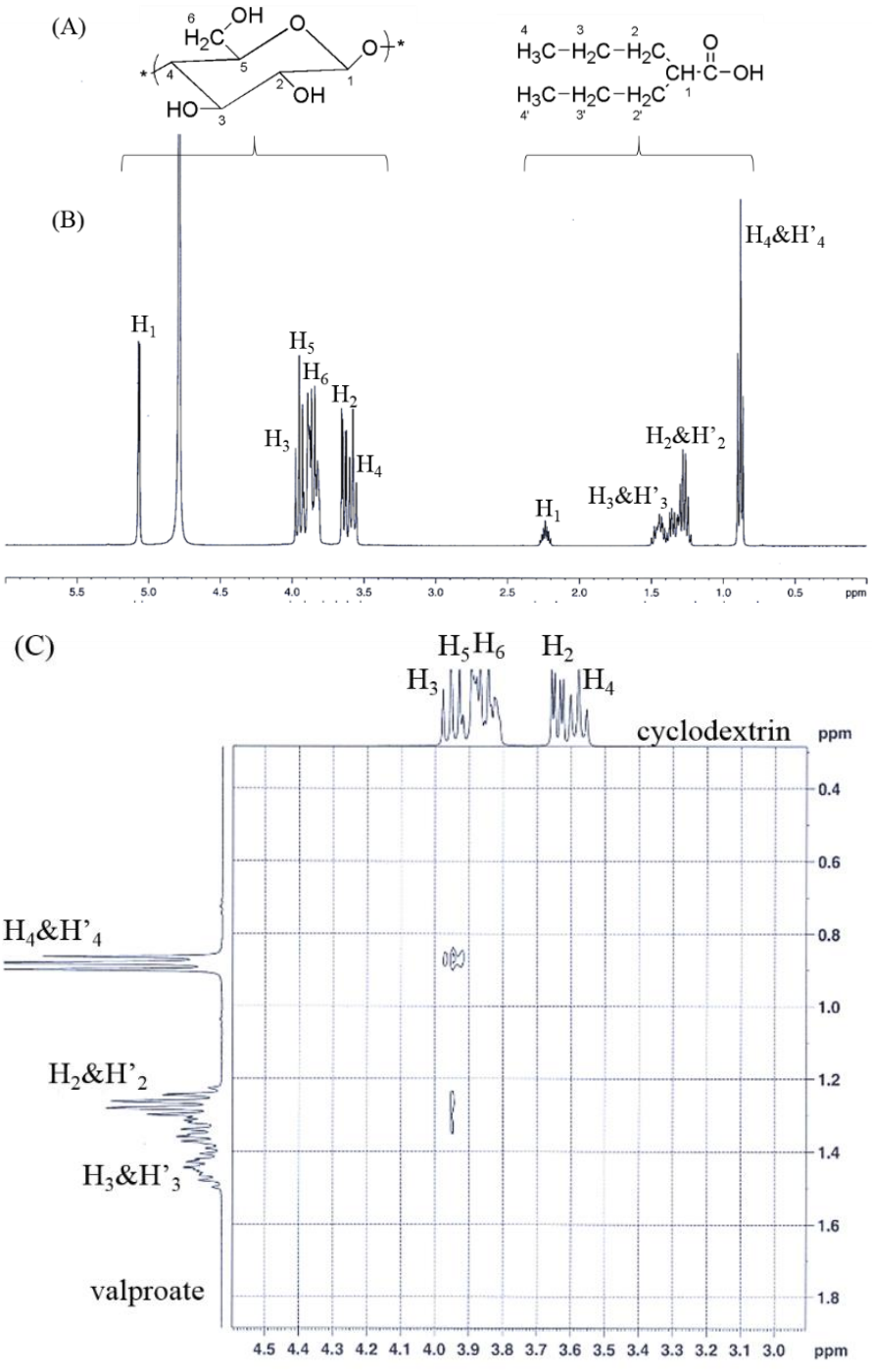

Figure 2. *(A) Molecular structure of β-CD and valproate. (B) Protons of the ^{1}H NMR spectrum of the mixture of β-CD and valproate in D_2O. (C) Cross-peaks between protons of the valproate and the β-CD moieties shown in the NOESY NMR spectrum of the valproate/β-CD complex in D_2O.*

(Figure 4B). This reveals that dextran and dextran derivatives are taken up by 3-dpf zebrafish embryos into the gastrointestinal tract *via* the oral route. However, 50% of the embryos showed no uptake of dex-RhoB after a 24-hour exposure period, which may be due to differences among the exact hatching time of each embryo in the testing group. Therefore, instead of 3-dpf zebrafish embryos, 4-dpf zebrafish embryos were used in the following studies in order to minimize the developmental differences among embryos and to facilitate oral uptake.

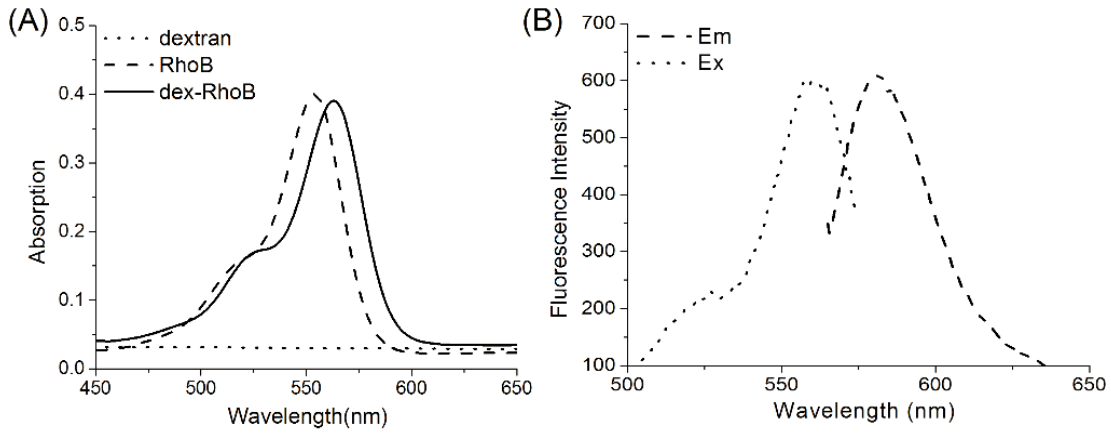

Figure 3. *(A) UV-vis spectra of dextran, rhodamine B and dex-RhoB conjugate in PBS buffer (pH 7.4). (B) Fluorescence excitation and emission spectra of 0.2 mg/mL dextran-RhoB in PBS buffer (pH 7.4) (λ_{ex} = 563 nm, λ_{em}=580 nm).*

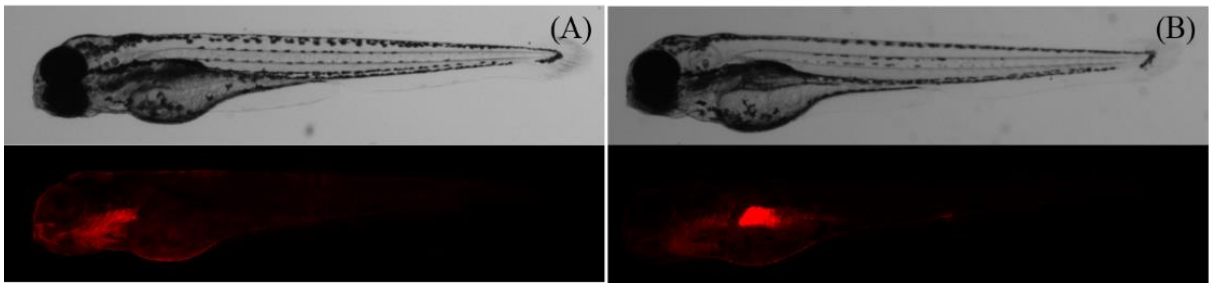

Figure 4. *Optical and fluorescent images of 3-dpf zebrafish embryos exposed to 1 mg/mL dex-RhoB after (A) 24-hour exposure and (B) 48-hour exposure.*

EXPOSURE OF ZEBRAFISH EMBRYOS TO DEX-CD/PEG

To utilize the valproate binding properties of β-CD and the oral uptake of dextran derivatives by zebrafish embryos, a previously reported Dex-CD/PEG polymeric drug carrier was applied to deliver valproate as a new zebrafish embryos toxicity assay.[40] The synthesis of Dex-CD/PEG includes the following steps: (1) functionalization of dextran (M_w = 20 kDa) with maleimide sidegroups to obtain dextran-maleimides (Dex-Mal); (2) conjugation of mono-thiolated β-cyclodextrins (MSCD) to 10% of the maleimide groups yielding dextran-cyclodextrin (Dex-CD);

and (3) mixing Dex-CD and linear PEG dithiols (PEG-DT, M_w = 3400 Da) aqueous solutions at an equimolar ratio of maleimide/thiol groups to obtain crosslinked Dex-CD/PEG polymeric drug carriers. Moreover, polymeric fluid could be obtained by decreasing the concentration of Dex-CD/PEG below the gelling point,[40] enabling their use in zebrafish toxicity assays.

Dex-CD/PEG (DS[Mal]=7, 7 maleimide groups per 100 glucopyranose residues) showed to be viscoelastic fluid at 2.5 wt%. No linear viscoelastic region was found in a range of 0.1-100% strain in the oscillatory amplitude sweep of the 2.5 wt% Dex-CD/PEG sample (Figure 5). By increasing the oscillatory strain, the storage modulus of the 2.5 wt% Dex-CD/PEG sample dropped to be lower than its loss modulus, showing a cross-over point at 6% strain. No valid data was obtained from dynamic light scattering (DLS) measurements due to very high polydispersity, suggestive of the presence of large particles or aggregates in the sample.

To investigate whether Dex-CD/PEG could be administered to 4-dpf zebrafish embryos *via* the oral route, N-(5-Fluoresceinyl)maleimide was conjugated to some of the thiols of PEG-DT (0.03 mol%) prior to the addition of Dex-CD yielding fluorescein labelled Dex-CD/PEG (2.5 wt%).

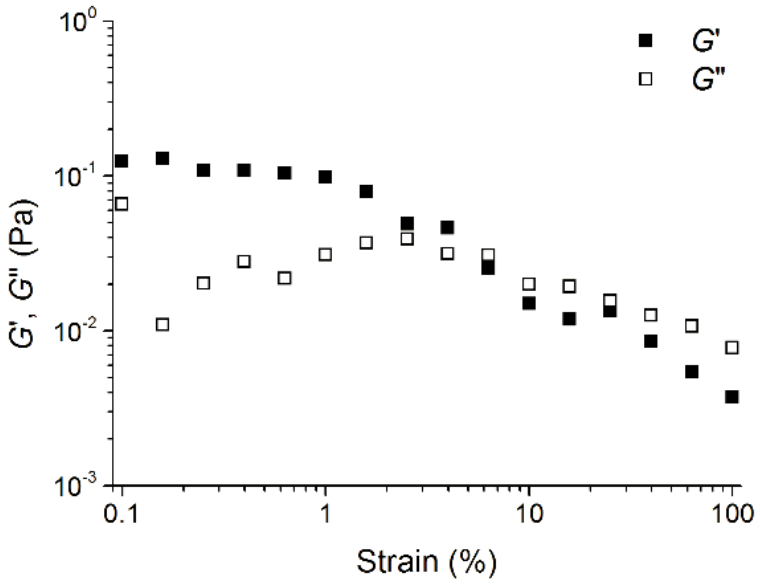

Figure 5. *Oscillatory amplitude sweep of 2.5 wt% Dex-CD/PEG carriers from 0.1 to 100 rad/s with 1% strain at 25°C.*

The fluorescent polymeric drug carrier was diluted with Danieau buffer (pH 7.2) and added a 96-well plate containing one zebrafish embryo per well. Next zebrafish viability and malformation were studied using light microscopy. After a 24-hour exposure period, fluorescein labelled Dex-CD/PEG was observed in the gut of all tested zebrafish embryos (Figure 6), indicating the efficient uptake of Dex-CD/PEG. Furthermore, by using 4-dpf embryos instead of 3-dpf embryos, the uptake of dextran-based carriers occurred already in the initial 24 hours of the exposure. After a 48-hour exposure period, all tested zebrafish embryos were viable and showed no malformation in

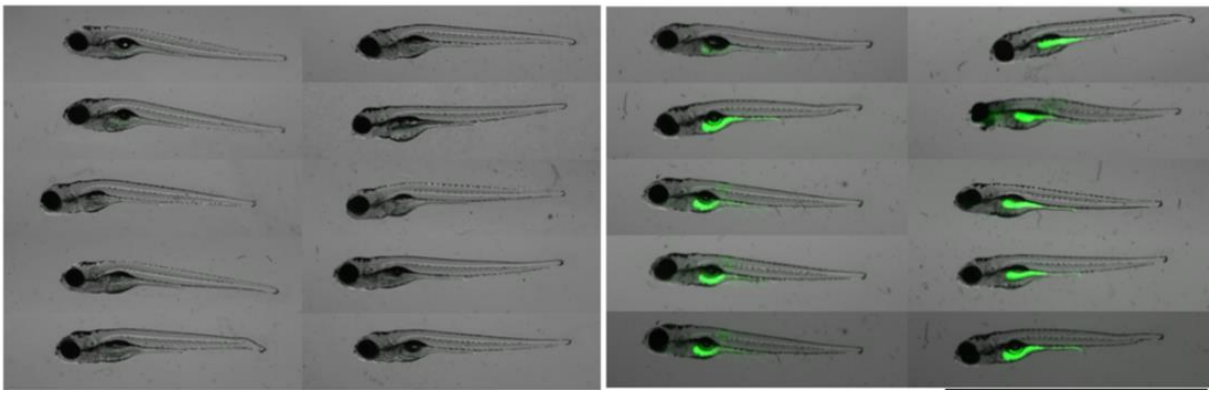

Figure 6. *Images of zebrafish embryos (5-dpf) taken by fluorescent microscopy after 24-hour exposure to egg water control group (left) and fluorescein labelled 2.5 wt% Dex-CD/PEG carriers group (right).*

presence of the Dex-CD/PEG revealing that this polymeric drug carrier is non-toxic to 4-dpf zebrafish embryos, which is in agreement with previous work.[40]

Zebrafish embryo at the early stage of development (i.e. 0 - 120 hpf) mainly relies on endogenous feeding, thus the uptake of test compounds in a toxicity assay can only occur *via* diffusion through the surface of the zebrafish embryo.[38, 48] However, after 3-dpf the larvae has completed most of its morphogenesis and mouths of 3-dpf zebrafish embryos have protruded.[19, 49] The 4-dpf zebrafish embryos continue growing rapidly and the gut tube drops more ventrally which can be easily observed.[19, 50] Belanger *et al.* reported that fluorescence appeared in the gut of 5-dpf zebrafish embryos after feeding the embryos with fluorescent protozoa which is indicative of exogenous feeding.[51] The ability of exogenous feeding is considered as the transition from the eleuthero embryo to larva interval in fish development. Moreover, these zebrafish studies were conducted at 25°C and it is likely that at a warmer temperature the development of the zebrafish embryo will be accelerated.[51] In this study fertilization and hatching of embryos was performed at 28.5 °C, thus it is likely that 4-dpf zebrafish embryos already developed faster enabling uptake *via* the oral route. The location of the fluorescence in zebrafish embryos proves that the oral uptake of soluble polymers can occur during the transition from the eleuthero embryo to larva interval in zebrafish development (see Figure 4 and 6).

DRUG CARRIER MEDIATED ZEBRAFISH EMBRYO TOXICITY ASSAY

The uptake of relatively polar compounds such as valproate by diffusion through membranes is inefficient and malformations of zebrafish embryos (e.g. oedema, brain deformities, bent tail) were observed only when the zebrafish embryos were exposed to valproate at a concentration of 1 mM.[36, 38] Thus, to have a comparable toxicity evaluation, zebrafish embryo viability upon a 48-hour exposure to various concentrations of valproate (from 10 μM to 1 mM) was tested. When 4-dpf zebrafish embryos were exposed to 100 μM valproate, no obvious signs of toxicity were observed,

while at 500 μM malformations became apparent However, no mortality was observed at this high concentration.

Next Dex-CD/PEG (2.5 wt%) loaded with valproate was prepared for the zebrafish embryo toxicity assay. For this, valproate (final concentration = 100 uM) was added in the Dex-CD solution prior to the addition of PEG-DT and kept overnight. Surprisingly, zebrafish embryo viabilty dropped to only 8 percent after a 48-hour exposure period and pericardial edema in zebrafish larvae were observed revealing valproate's toxicity (see Figure 7B-E).

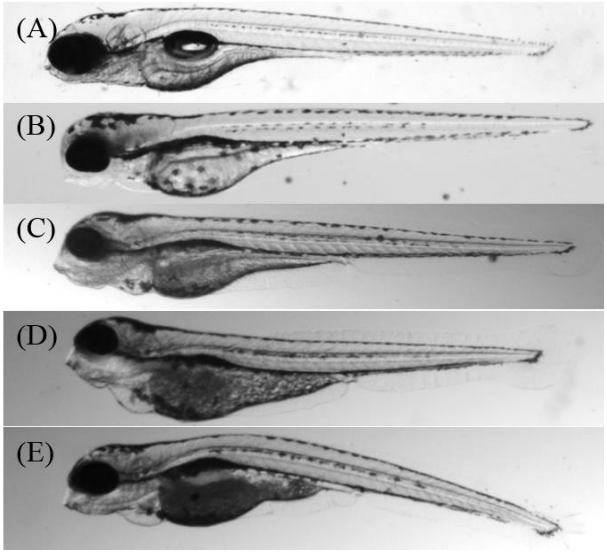

Figure 7. *Zebrafish embryos upon exposure to 100 μM valproate loaded 2.5% Dex-CD/PEG carriers: (A) normal zebrafish embryo; (B-E) zebrafish embryos with pericardial edema.*

In contrast, no death or malformation of embryos was observed in either the egg water control group, the 100 μM valproate group, or the 100 μM valproate mixed with 2.5 wt% Dex-CD/PEG group (Figure 8). Furthermore, no death or malformation of embryos was observed in 2.5 wt% Dex-CD/PEG carriers. Thus, the observed toxicity of 100 μM valproate encapsulated in Dex-CD/PEG can only be attributed to the interaction between the 2.5 wt% Dex-CD/PEG carriers and valproate. This data strongly suggests that the valproate/CD host-guest complex within Dex-CD/PEG plays a pivotal role, as evidenced by the efficient uptake and concomitant toxicity in this zebrafish embryo toxicity assay through the oral route. Most likely Dex-CD/PEG increases the internal concentration of the valproate compound, thereby changing the toxicokinetic profile of the valproate compound to zebrafish embryos.

INFLUENCE OF DEX-CD/PEG COMPOSITIONS

To study whether the composition of Dex-CD/PEG carriers influences the toxicity of the carriers and the response of the zebrafish embryos toward valproate, the composition of Dex-CD/PEG

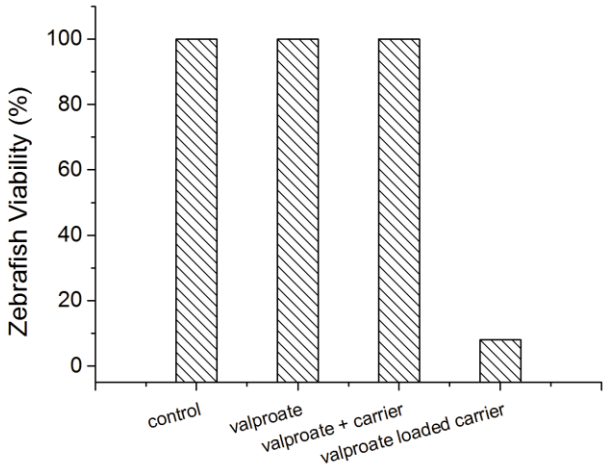

Figure 8. *Viability of zebrafish embryos after 48-hour exposure to the egg water (control group), 100 μM valproate, 100 μM valproate mixed with 2.5 wt% Dex-CD/PEG carriers, and 100 μM valproate loaded 2.5 wt% Dex-CD/PEG carriers respectively.*

carriers was varied. A library of Dex-CD/PEG carriers was synthesized in which the degrees of substitution of the applied Dex-Mal polymers (DS[Mal]) was varied. Table 1 provides an overview of compositions of prepared Dex-CD/PEG carriers. For the zebrafish embryos toxicity assay, the valproate concentration was kept constant and loaded into each drug carrier group prior to the crosslinking reaction between Dex-Mal and PEG-DT. The final concentration of valproate was 100 μM. For each Dex-CD/PEG carrier, a control group without valproate was also exposed to 4-dpf zebrafish embryos for 48 hours. The viability of zebrafish embryos was examined after a 48-hour exposure period, providing information about the uptake efficiency of valproate by the zebrafish embryos. The viscosity of each Dex-CD/PEG carriers was measured by a U-tube viscometer to obtain its dynamic viscosity which is related to valproate delivery properties of the drug carrier.

For Dex-CD/PEG carriers prepared with Dex-Mal4 (DS[Mal] of 4), no toxicity was observed after 48 hours when the concentration was below 2 wt% (Figure 9). However, the viscosity of Dex-CD/PEG carriers increased as a function of Dex-CD/PEG carriers concentration going from 0.5 wt% to 2 wt%. At 3 wt%, the viability of zebrafish embryos dropped from 100% to 50% after a 48-hour exposure period. At this concentration the liquid became too viscous to be measured with a U-tube viscometer.

Similar trends were also observed in the group of Dex-CD/PEG carriers prepared with Dex-Mal7 (DS[Mal] of 7) (Figure 9). After exposure for 48 hours the viability of zebrafish embryos maintained to be 100% for Dex-CD/PEG carriers having a concentration below 2 wt%, while the viscosity of Dex-CD/PEG carriers doubled when the concentration of Dex-CD/PEG carriers increased from

Table 1. *Compositions of Dex-CD/PEG carriers applied in the zebrafish embryo toxicity assay.*

Gel Samples	DEX-MAL		CD(mg)	PEG-DT(mg)	Buffer volume (mL)	Dynamic viscosity (cP)	Zebrafish viability
	DS[Mal]	Dex-Mal(mg)					
0.5 wt%	4	5	0.17	2.2	1	1.0990	100%
1.0 wt%	4	10	0.33	4.4	1	1.4974	100%
1.5 wt%	4	15	0.50	6.7	1	2.6666	100%
2.0 wt%	4	20	0.67	8.9	1	6.2535	100%
2.5 wt%	4	25	0.83	11.1	1	-	83.3%
3.0 wt%	4	30	1.00	13.3	1	-	50%
0.5 wt%	7	5	0.25	3.3	1	1.2376	100%
0.75 wt%	7	7.5	0.37	5.0	1	1.2376	100%
1.0 wt%	7	10	0.50	6.6	1	1.9683	100%
1.5 wt%	7	15	0.75	9.9	1	2.6953	100%
2.0 wt%	7	20	0.99	13.2	1	-	58.3%
2.5 wt%	7	25	1.24	16.5	1	-	8%
0.5 wt%	11	5	0.40	5.3	1	1.4829	100%
0.75 wt%	11	7.5	0.60	8.0	1	2.4804	75%
1.0 wt%	11	10	0.80	10.7	1	3.8541	66.7%

0.5 wt% to 1.5 wt%. Upon increasing the concentration of Dex-CD/PEG carriers to 2 wt%, the viability of zebrafish embryos dropped from 100% to 58%. Analysis of the dynamic viscosity at these concentrations could not be determined.

The group of Dex-CD/PEG carriers prepared with Dex-Mal11 (DS[Mal] of 11) showed a similar trend) (Figure 9). When the concentration of Dex-CD/PEG carriers increased from 0.5 wt% to 1.5 wt%, the viability of zebrafish embryos decreased from 100% to 67% after exposure for 48 hours. The viscosity of Dex-CD/PEG carriers increased with the concentration of Dex-CD/PEG

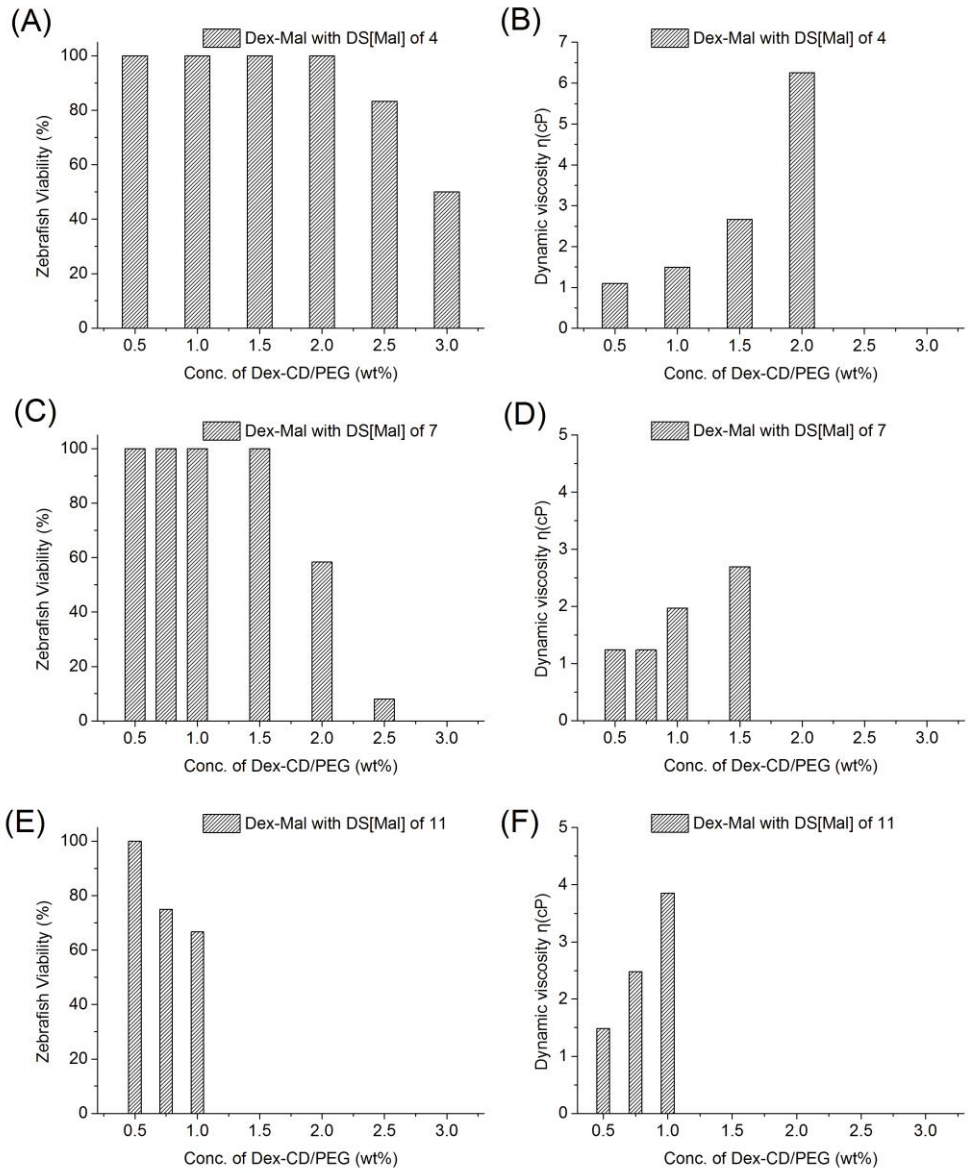

Figure 9. *Viability of 4-dpf zebrafish embryos after 48-hour exposure to 100 μM valproate encapsulated in Dex-CD/PEG carriers prepared by Dex-Mal with (A) DS[Mal] of 5, (C) DS[Mal] of 7, and (E) DS[Mal] of 11. Dynamic viscosities of Dex-CD/PEG carriers prepared by Dex-Mal with (B) DS[Mal] of 5, (D) DS[Mal] of 7, and (F) DS[Mal] of 11.*

carriers in each group. For the control groups of each Dex-CD/PEG carrier without loading valproate, no death of the tested zebrafish embryos was observed.

From these experiments, it became apparent that there is a correlation between the observed valproate toxicity and the viscosity of the Dex-CD/PEG carrier. Although the measured viscosity is not obtained for every Dex-CD/PEG carrier, it is well accepted that higher concentrations of functional groups from the precusors (such as Dex-Mal and PEG-DT) generate crosslinked systems with higher viscosity. When the viscosity of the applied Dex-CD/PEG carrier was too low, the loaded valproate rapidly released into the culture medium thus limited amount of valproate

could be taken up by zebrafish embryos together with the Dex-CD/PEG carriers.

Regarding the influence of the DS[Mal], it was found that Dex-CD/PEG carriers prepared with higher DS[Mal] (such as DS[Mal]=11) were capable of affecting the valbility of tested zebrafish embryos at a lower viscosity. Since mono-thiolated β-CD molecules were conjugated to the Dex-Mal polymers at 0.1 equivalent to the maleimide groups, Dex-CD/PEG carriers prepared with higher DS[Mal] have more β-CD moieties attached for valproate binding. As mentioned above, the same amount of valproate was loaded in each Dex-CD/PEG carriers to maintain a final concentration of 100 μM valproate, thus more β-CD moieties in the Dex-CD/PEG carriers may improve the drug delivery effiency during the toxicity assay. In other words, for Dex-CD/PEG carriers prepared at the same concentration, a higher DS[Mal] of applied Dex-Mal provides more binding sites for valproate delivery, thereby improving the uptake efficiency of valproate into the zebrafish embryos.

Therefore, the composition of Dex-CD/PEG carrier affects the viability of zebrafish embryos exposed to the corresponding 100 μM valproate encapsulated in Dex-CD/PEG. Hence the uptake efficiency of valproate in the zebrafish embryo toxicity assay depends on the viscosity and the density of drug binding sites of Dex-CD/PEG carriers.

CONCLUSIONS AND PERSPECTIVES

In this work, we explored the potential of dextran based crosslinked drug carriers to control the observed toxicity of valproate in a zebrafish embryo toxicity assay. We showed that the Dex-CD/PEG carriers can be internalized by 4-dpf zebrafish embryos into the gastrointestinal tract. Zebrafish embryos exposed to valproate encapsulated in Dex-CD/PEG became more sensitive toward the drug. Thus Dex-CD/PEG significantly improves the uptake of valproate in zebrafish embryos and should be applicable to any other drug that is able to form an inclusion complex with cyclodextrin.

Furthermore the observed toxicity of valproate depends on the composition of the applied Dex-CD/PEG carrier. It was shown that only polymeric carriers with sufficient viscosity and valproate binding sites can effectively improve oral uptake in a zebrafish embryo toxicity assay. However, more study is required to valdiate these findings with other existing *in vitro*/*in vivo* toxicity assays.

EXPERIMENTAL

MATERIALS

Dextran (M_w = 20 000 Da) was purchased from Pharmacia (Upsala, Sweden) and stored in a vacuum oven at 30 °C. Maleimide modified dextrans (Dex-Mal) with different degree of substitutions were synthesized as described previously.[52] Poly(ethylene glycol) dithiol (M_w = 3 400 Da, PEG-SH), sodium valproate, N-(5-Fluoresceinyl)maleimide, Rhodamine B (RhoB), 1,1'-carbonyldiimidazole (CDI), dimethylaminopyridine (DMAP), dimethyl sulfoxide (DMSO) were purchased from Sigma-Aldrich. Mono-thiolated β-cyclodextrin (MSCD) was provided by Ke Peng.[40] Danieau buffer (pH=7.2) was obtained from the Biology department. ^{1}H and 2D NOESY spectra were obtained in D_2O using a Bruker DRX-400 (400 MHz) spectrometer.

PREPARATION OF DRUG CARRIERS

Dex-CD/PEG carriers were prepared following a previously published protocol.[40] For example, to prepare 1 mL 2.5 wt% Dex-CD/PEG carriers (DS[Mal]=7), 1.3 mg MSCD (0.1 eq with respect to the maleimide groups) was added into 0.5 mL PBS buffer solution of Dex-Mal (25 mg, M_w = 20 000 Da, DS[Mal]=7) and the resulted Dex-CD solution was vortexed for 5 minutes. Then 0.5 mL PBS buffer solution of PEG-DT (16.5 mg, 0.9 eq to the maleimide groups) was mixed with the Dex-CD solution by vortexing and kept at room temperature overnight. The final concentration of Dex-Mal in the resulting Dex-CD/PEG carriers was about 2.5 wt%.

To prepare FITC labelled Dex-CD/PEG carriers, a 10 mg/mL stock solution of FITC was firstly prepared in DMSO. Taking the FITC labelled 2.5 wt% Dex-CD/PEG carriers for example, 12.5 μL FITC stock solution (0.03 eq with respect to the thiol groups) was added into the 0.5 mL PBS buffer solution of PEG-DT (16.5 mg) prior to the crosslinking reaction.

To prepare valproate loaded Dex-CD/PEG carriers, 100 mM valproate stock solution was prepared in Danieau buffer (pH 7.2). Droplets of 100 mM valproate stock solution were added to Dex-CD solution and incubated for 2 hours before the preparation of Dex-CD/PEG carriers. Taking the 100 μM valproate encapsulated 2.5 wt% Dex-CD/PEG carriers for example, 10 μL of the 100 mM valproate stock solution was added into 0.5 mL PBS buffer solution of Dex-Mal (25 mg). The resulted valproate loaded Dex-CD solution was vortexed for 5 minutes and incubated for 2 hours. Then 0.5 mL PBS buffer solution of PEG-DT (16.5 mg, 0.9 eq to the maleimide groups) was mixed with the valproate loaded Dex-CD solution by vortexing and kept at room temperature overnight for the zebrafish embryo assay.

OSCILLATORY RHEOLOGY

The mechanical properties of 2.5 wt% Dex-CD/PEG carriers (DS[Mal]=7) were measured on a DHR-2 rheometer (TA Instruments) at 25 °C using a parallel plate-plate geometry (40 mm diameter). 900 μL Dex-CD/PEG carriers were loaded on the bottom plate and the geometry was lowered to the gap distance of 700 μm. Time sweep measurements were performed to follow gelation process at a frequency of 1 rad s^{-1} with 1% strain. The linear viscoelastic regime (LVE) was determined for each sample using an amplitude sweep measurement at 1 rad s^{-1} from 0.1% to 100% strain. Frequency sweep measurements were conducted from 100 to 0.1 rad s^{-1} with 1% strain in the linear viscoelastic regime. The mechanical properties of other Dex-CD/PEG carriers listed in Table 1 were measured by a U-tube viscometer to calculate the dynamic viscosity of each carrier.

ZEBRAFISH EMBRYO TOXICITY ASSAY

All zebrafish were handled in compliance with the local animal welfare regulations and maintained according to standard protocols (zfin.org). Larvae were raised in egg water (60 g/ml Instant Ocean sea salts) at 28.5 °C. All protocols adhered to the international guidelines specified by the EU Animal Protection Directive 2010/63/EU.

96-well plates were applied for housing zebrafish embryos during the toxicity assay. In each well, one zebrafish embryo and 250 μL egg water containing the testing dose of valproate alone or encapsulated in the Dex-CD/PEG carriers were added. To prevent sample bias, embryos from collected clutches were pooled, then individual 4-dpf embryos were randomly assigned to individual wells of 96-well plates. Therefore, for each experiment, all embryos were taken from the same mating pairs. Both exposure methods used a total of 12 embryos per dose. Control embryos (exposed to egg water only) were included as references of normal embryonic development. These 96-well plates were kept in the incubator at 28 °C and the mortality of treated and control embryos were assessed daily over 48 hours after treatment.

REFERENCES

1. Judson R. S., Richard A. M., Dix D. J., *et al.*, The toxicity data landscape for environmental chemicals, *Environmental Health Perspectives*, 2009, **117**, 685-695.
2. Parliament E., Directive 2010/63/eu of the european parliament and of the council of 22 september 2010 on the protection of animals used for scientific purposes, 2010, 34-35.
3. Strahle U., Scholz S., Geisler R., *et al.*, Zebrafish embryos as an alternative to animal experiments. A commentary on the definition of the onset of protected life stages in animal welfare regulations, *Reproductive Toxicology*, 2012, **33**, 128-132.
4. Piersma A. H., Validation of alternative methods for developmental toxicity testing, *Toxicology Letters*, 2004, **149**, 147-153.
5. Piersma A. H., Alternative methods for developmental toxicity testing, *Basic & Clinical Pharmacology & Toxicology*, 2006, **98**, 427-431.
6. Hamm J., Sullivan K., Clippinger A. J., *et al.*, Alternative approaches for identifying acute systemic toxicity: Moving from research to regulatory testing, *Toxicology in Vitro*, 2017, **41**, 245-259.
7. Hill A. J., Teraoka H., Heideman W., *et al.*, Zebrafish as a model vertebrate for investigating chemical toxicity, *Toxicol Sci*, 2005, **86**, 6-19.
8. Ali S., Champagne D. L., Spaink H. P., *et al.*, Zebrafish embryos and larvae: A new generation of disease models and drug screens, *Birth Defects Research Part C-embryo Today-reviews*, 2011, **93**, 115-133.
9. Tamplin O. J., White R. M., Jing L., *et al.*, Small molecule screening in zebrafish: Swimming in potential drug therapies, *Wiley Interdisciplinary Reviews-Developmental Biology*, 2012, **1**, 459-468.
10. Basu S. and Sachidanandan C., Zebrafish: A multifaceted tool for chemical biologists, *Chemical reviews*, 2013, **113**, 7952-7980.
11. Pardomartin C., Chang T., Koo B. K., *et al.*, High-throughput *in vivo* vertebrate screening, *Nature Methods*, 2010, **7**, 634-636.
12. Rihel J., Prober D. A., Arvanites A. C., *et al.*, Zebrafish behavioral profiling links drugs to biological targets and rest/wake regulation, *Science*, 2010, **327**, 348-351.
13. Delvecchio C., Tiefenbach J. and Krause H. M., The zebrafish: A powerful platform for *in vivo*, hts drug discovery, *Assay and Drug Development Technologies*, 2011, **9**, 354-361.
14. Letamendia A., Quevedo C., Ibarbia I., *et al.*, Development and validation of an automated high-throughput system for zebrafish *in vivo* screenings, *PLOS ONE*, 2012, **7**.
15. George S., Xia T., Rallo R., *et al.*, Use of a high throughput screening approach coupled with *in vivo* zebrafish embryo screening to develop hazard ranking for engineered nanomaterials, *ACS Nano*, 2011, **5**, 1805-1817.
16. Peterson R. E., Theobald H. M. and Kimmel G. L., Developmental and reproductive toxicity of dioxins and related compounds: Cross-species comparisons, *Critical Reviews in Toxicology*, 1993, **23**, 283-335.
17. Woltering D. M., The growth response in fish chronic and early life stage toxicity tests: A critical review, *Aquatic Toxicology*, 1984, **5**, 1-21.
18. Kimmel C. B., Genetics and early development of zebrafish, *Trends Genet.*, 1989, **5**, 283-288.
19. Kimmel C. B., Ballard W. W., Kimmel S. R., *et al.*, Stages of embryonic development of the zebrafish, *Developmental Dynamics*, 1995, **203**, 253-310.
20. Mccollum C. W., Ducharme N. A., Bondesson M., *et al.*, Developmental toxicity screening in zebrafish, *Birth Defects Research Part C-embryo Today-reviews*, 2011, **93**, 67-114.
21. He J., Gao J., Huang C., *et al.*, Zebrafish models for assessing developmental and reproductive toxicity, *Neurotoxicology and Teratology*, 2014, **42**, 35-42.

22. Kienle C., Kohler H. R. and Gerhardt A., Behavioural and developmental toxicity of chlorpyrifos and nickel chloride to zebrafish (danio rerio) embryos and larvae, *Ecotox Environ Safe*, 2009, **72**, 1740-1747.
23. Zhang W., Zhang Y. T., Zhang H. X.*, et al.*, Sex differences in transcriptional expression of fabps in zebrafish liver after chronic perfluorononanoic acid exposure, *Environ Sci Technol*, 2012, **46**, 5175-5182.
24. Huang Q. Y. and Huang H. Q., Alterations of protein profile in zebrafish liver cells exposed to methyl parathion: A membrane proteomics approach, *Chemosphere*, 2012, **87**, 68-76.
25. Zhu X., Zhu L., Duan Z.*, et al.*, Comparative toxicity of several metal oxide nanoparticle aqueous suspensions to zebrafish (danio rerio) early developmental stage, *Journal of environmental science and health. Part A, Toxic/hazardous substances & environmental engineering*, 2008, **43**, 278-284.
26. Asharani P. V., Lian Wu Y., Gong Z.*, et al.*, Toxicity of silver nanoparticles in zebrafish models, *Nanotechnology*, 2008, **19**, 255102.
27. Bai W., Zhang Z. Y., Tian W. J.*, et al.*, Toxicity of zinc oxide nanoparticles to zebrafish embryo: A physicochemical study of toxicity mechanism, *J Nanopart Res*, 2010, **12**, 1645-1654.
28. Bar-Ilan O., Albrecht R. M., Fako V. E.*, et al.*, Toxicity assessments of multisized gold and silver nanoparticles in zebrafish embryos, *Small*, 2009, **5**, 1897-1910.
29. Fako V. E. and Furgeson D. Y., Zebrafish as a correlative and predictive model for assessing biomaterial nanotoxicity, *Adv Drug Deliver Rev*, 2009, **61**, 478-486.
30. Richetti S. K., Rosemberg D. B., Ventura-Lima J.*, et al.*, Acetylcholinesterase activity and antioxidant capacity of zebrafish brain is altered by heavy metal exposure, *Neurotoxicology*, 2011, **32**, 116-122.
31. Senger M. R., Rosemberg D. B., Seibt K. J.*, et al.*, Influence of mercury chloride on adenosine deaminase activity and gene expression in zebrafish (danio rerio) brain, *Neurotoxicology*, 2010, **31**, 291-296.
32. Ling X. P., Zhang Y. H., Lu Y. H.*, et al.*, Superoxide dismutase, catalase and acetylcholinesterase: Biomarkers for the joint effects of cadmium, zinc and methyl parathion contamination in water, *Environ Technol*, 2011, **32**, 1463-1470.
33. Chan K. M., Ku L. L., Chan P. C. Y.*, et al.*, Metallothionein gene expression in zebrafish embryo-larvae and zfl cell-line exposed to heavy metal ions, *Mar Environ Res*, 2006, **62**, S83-S87.
34. Klüver N., König M., Ortmann J.*, et al.*, Fish embryo toxicity test: Identification of compounds with weak toxicity and analysis of behavioral effects to improve prediction of acute toxicity for neurotoxic compounds, *Environ Sci Technol*, 2015, **49**, 7002-7011.
35. Knöbel M., Busser F. J. M., Rico-Rico Á.*, et al.*, Predicting adult fish acute lethality with the zebrafish embryo: Relevance of test duration, endpoints, compound properties, and exposure concentration analysis, *Environ Sci Technol*, 2012, **46**, 9690-9700.
36. Herrmann K., Effects of the anticonvulsant drug valproic acid and related substances on the early development of the zebrafish (brachydanio rerio), *Toxicology in vitro*, 1993, **7**, 41-54.
37. Cowden J., Padnos B., Hunter D. L.*, et al.*, Developmental exposure to valproate and ethanol alters locomotor activity and retino-tectal projection area in zebrafish embryos, *Reproductive Toxicology*, 2012, **33**, 165-173.
38. Brox S., Seiwert B., Kuster E.*, et al.*, Toxicokinetics of polar chemicals in zebrafish embryo (danio rerio): Influence of physicochemical properties and of biological processes, *Environ Sci Technol*, 2016, **50**, 10264-10272.
39. Yan D., Ni L., Chen H. L.*, et al.*, Amphiphilic nanoparticles of resveratrol-norcantharidin to enhance the toxicity in zebrafish embryo, *Bioorganic & Medicinal Chemistry Letters*, 2016, **26**, 774-777.
40. Peng K., Cui C., Tomatsu I.*, et al.*, Cyclodextrin/dextran based drug carriers for a controlled release of hydrophobic drugs in zebrafish embryos, *Soft Matter*, 2010, **6**, 3778-3783.
41. Peng K., Tomatsu I., Korobko A. V.*, et al.*, Cyclodextrin-dextran based *in situ* hydrogel formation: A carrier

for hydrophobic drugs, *Soft Matter*, 2010, **6**, 85-87.

42. Uekama K., Hirayama F. and Irie T., Cyclodextrin drug carrier systems, *Chemical reviews*, 1998, **98**, 2045-2076.
43. Trapani G., Cutrignelli A., Latrofa A.*, et al.*, Valproic acid - hydrophilic cyclodextrin complexes and valproic acid - solid dispersions: Evaluation of their potential pharmaceutical use, *Drug Development and Industrial Pharmacy*, 2004, **30**, 53-64.
44. Stutzin A., A fluorescence assay for monitoring and analyzing fusion of biological membrane vesicles *in vitro*, *FEBS Letters*, 1986, **197**, 274-280.
45. Arvinte T., Wahl P. and Nicolau C., Resonance energy-transfer and fluorescence intensity studies of the transport of liposome-encapsulated molecules into isolated mouse liver nuclei, *Biochemistry*, 1987, **26**, 765-772.
46. Tian T., Zhu Y., Zhou Y.*, et al.*, Exosome uptake through clathrin-mediated endocytosis and macropinocytosis and mediating mir-21 delivery, *Journal of Biological Chemistry*, 2014, **289**, 22258-22267.
47. Zhang X., Zhang Y. and Liu L., Fluorescence lifetimes and quantum yields of ten rhodamine derivatives: Structural effect on emission mechanism in different solvents, *Journal of Luminescence*, 2014, **145**, 448-453.
48. Berghmans S., Butler P., Goldsmith P.*, et al.*, Zebrafish based assays for the assessment of cardiac, visual and gut function — potential safety screens for early drug discovery, *Journal of Pharmacological and Toxicological Methods*, 2008, **58**, 59-68.
49. Parichy D. M., Elizondo M. R., Mills M. G.*, et al.*, Normal table of postembryonic zebrafish development: Staging by externally visible anatomy of the living fish, *Developmental Dynamics*, 2009, **238**, 2975-3015.
50. Holmberg A., Olsson C. and Holmgren S., The effects of endogenous and exogenous nitric oxide on gut motility in zebrafish danio rerio embryos and larvae, *The Journal of Experimental Biology*, 2006, **209**, 2472-2479.
51. Belanger S. E., Balon E. K. and Rawlings J. M., Saltatory ontogeny of fishes and sensitive early life stages for ecotoxicology tests, *Aquatic Toxicology*, 2010, **97**, 88-95.
52. Gao Y., Kieltyka R. E., Jesse W.*, et al.*, Thiolated human serum albumin cross-linked dextran hydrogels as a macroscale delivery system, *Soft Matter*, 2014, **10**, 4869-4874.

CHAPTER 5

CHEMICALLY CROSSLINKED POLYMER NETWORKS ASSIST THE FORMATION OF GIANT UNILAMELLAR VESICLES

Giant Unilamellar Vesicles (GUVs) have become popular as cell membrane model systems for biophysical studies. However, preparation of GUVs is not trivial. The quality, size and yield strongly depends on their preparation method. Here we present a novel method for GUV growth using gentle hydration of a lipid film from a chemically crosslinked dextran–poly(ethylene glycol) hydrogel substrate, wherein the hydrogel was formed by the thiol-Michael addition reaction. Polymer and additive-free GUVs were prepared rapidly under physiological ionic strength conditions in high yield without the need of special equipment. By modulating the physicochemical properties of the hydrogels, the GUV growth can be controlled in terms of yield, size and size distribution. The influence of the molar ratio of thiols and maleimides functional groups, the molecular weight and structure of thiolated poly(ethylene glycol) and the degree of substitution of maleimide modified dextran on GUV formation was studied. Chemical reagents and/or biomacromolecules can be encapsulated during formations and the obtained GUVs can be used for biophysical studies.

Part of this chapter was published in *Chemical Communications*, **2014**, 50, 1953-1955 and *Soft Matter*, **2017**, 13, 5580-5588.

INTRODUCTION

Cell membranes, as the frontier between the cell and its environment, play an important role in cellular phenomena such as mass transfer, energy transformation and signal transduction.[1, 2] Cell membranes are comprised of self-assembled lipid bilayers, hosting a variety of membrane proteins and multi-subunit assemblies. Due to their high degree of sophistication and functionality, cell membranes have long fascinated researchers in Physics, Chemistry and Biology. To study the properties of cell membranes, various simplified biomimetic models of cell membranes have been developed over the past one hundred years.[2, 3]

Giant unilamellar vesicles (GUVs) are widely used model systems for investigating various properties of cell membranes,[4-6] because they approximate the size and membrane curvature of living cells and offer the flexibility to visualize and probe biophysical phenomenon of one single vesicle under an optical microscope. GUVs are typically prepared by gentle hydration[7] or the electroformation methods.[8] The gentle hydration method usually involves evaporation of a lipid-containing organic solvent on a glass substrate and subsequent exposure to a buffer solution results in vesicle formation. In order to form vesicles at a moderate ionic strength (200 mOsm/kg), there must be 10-20% negatively charged lipids in the lipid composition and a heating step is required to bring the lipid solution above its phase transition temperature. In some cases, it is also necessary to add monosaccharaides in the dry lipid film to promote lamellar repulsion.[9] The main disadvantage of the gentle hydration method is the variable size and relatively low yield of produced vesicles and the gentle hydration method is not suitable for all lipid compositions. On the other hand, the electroformation method is the most widely used vesicle formation method and can provide a high GUV yield with a narrow size distribution.[10] Lipid mixtures are able to swell and grow in non-electrolytic solutions when an electric field is applied. However, to prepare GUVs under high ionic strength conditions, higher electric field frequencies and longer hydration times are required leading to potential lipid hydrolysis and peroxidation.[11, 12]

Recently, researchers have found that the traditional gentle hydration method can be significantly improved using a hydrogel film. Horger *et al.* demonstrated that by applying an agarose gel film on a glass slide, GUVs were formed when a lipid film was hydrated on this substrate under physiological conditions.[13] However, GUV contamination occurred due to dissolution of agarose in the hydration process. Traces of agarose were found both inside and spanning the GUV membrane, which modified the mechanical properties and membrane permeability.[14] Poly(vinyl alcohol) hydrogels were used as an alternative to prevent GUV contamination by the gel components, but a high yield of GUVs was only obtained in presence of sucrose.[15]

To enable GUV formation under physiological conditions, we developed a chemically crosslinked

hydrogel matrix to be used as a substrate covalently anchored to a glass surface. The hydrogel network consists of dextran and poly(ethylene glycol) (PEG) polymers crosslinked *via* a thiol-Michael addition reaction and anchored to a thiolated glass surface. Using this method, GUVs can be formed from various lipid compositions under additive-free, physiological ionic strength conditions. Moreover, we studied the influence of the physiochemical properties of the hydrogel with respect to the molar ratio of the thiol and maleimide functional groups, the molecular weight of thiolated PEG and the degree of substitution of both thiolated PEG and Dex-Mal on GUV formation. Dex-PEG hydrogels were characterized by oscillatory rheology, swelling experiments and cryo-SEM imaging. The yield and size distribution of formed GUVs were analyzed by the fluorescence microscopy and fluorescence activated cell sorting (FACS). Based on these results, we developed a chemically crosslinked hydrogel system for GUV growth under physiological conditions without artifacts intercalated or encapsulated within the membrane. Additionally, we found that modulation of the physicochemical properties of the Dex-PEG hydrogel resulted in the potential for control over GUV growth in terms of yield and size.

RESULTS AND DISCUSSION

HYDROGEL SYNTHESIS

Dex-PEG hydrogels were prepared by reacting aqueous solutions of Dex-Mal and thiolated PEG (PEG-SH) using the thiol-Michael addition reaction (Scheme 1). Since no initiator or catalyst is required to facilitate the reaction, contamination of the GUVs or biomolecule-encapsulated GUVs formed using these hydrogel films is prevented.

Oscillatory time sweeps were used to probe the rate of network formation and its final mechanical properties, while amplitude and frequency sweeps were used to confirm the formation of a chemically crosslinked network. Typically, solutions of 3.5% (w/v) Dex70k-Mal5.5 (M_w=70 kDa, DS[Mal]=5.5) and PEG2k-2SH (M_w=2 kDa, 2 thiol end groups) were loaded on the rheometer plate and the storage modulus (*G*') and the loss modulus (*G*") were followed as a function of time. Within a few seconds, *G*' increased dramatically and became higher than *G*", indicative of the formation of a viscoelastic material. Once a plateau in *G*' was attained, amplitude and angular frequency sweeps were conducted. *G*' and *G*" remained nearly constant with *G*' being two orders of magnitude greater than *G*" in both amplitude and frequency sweeps, consistent with the formation of a chemically crosslinked network (Figure 1).

In order to grow GUVs from these hydrogel films, a solution of Dex70k-Mal and thiolated PEG was drop-casted on a thiolated glass slide at 40 °C until a thin hydrogel layer was formed through a Michael addition reaction between the polymers and the glass surface. By visual inspection,

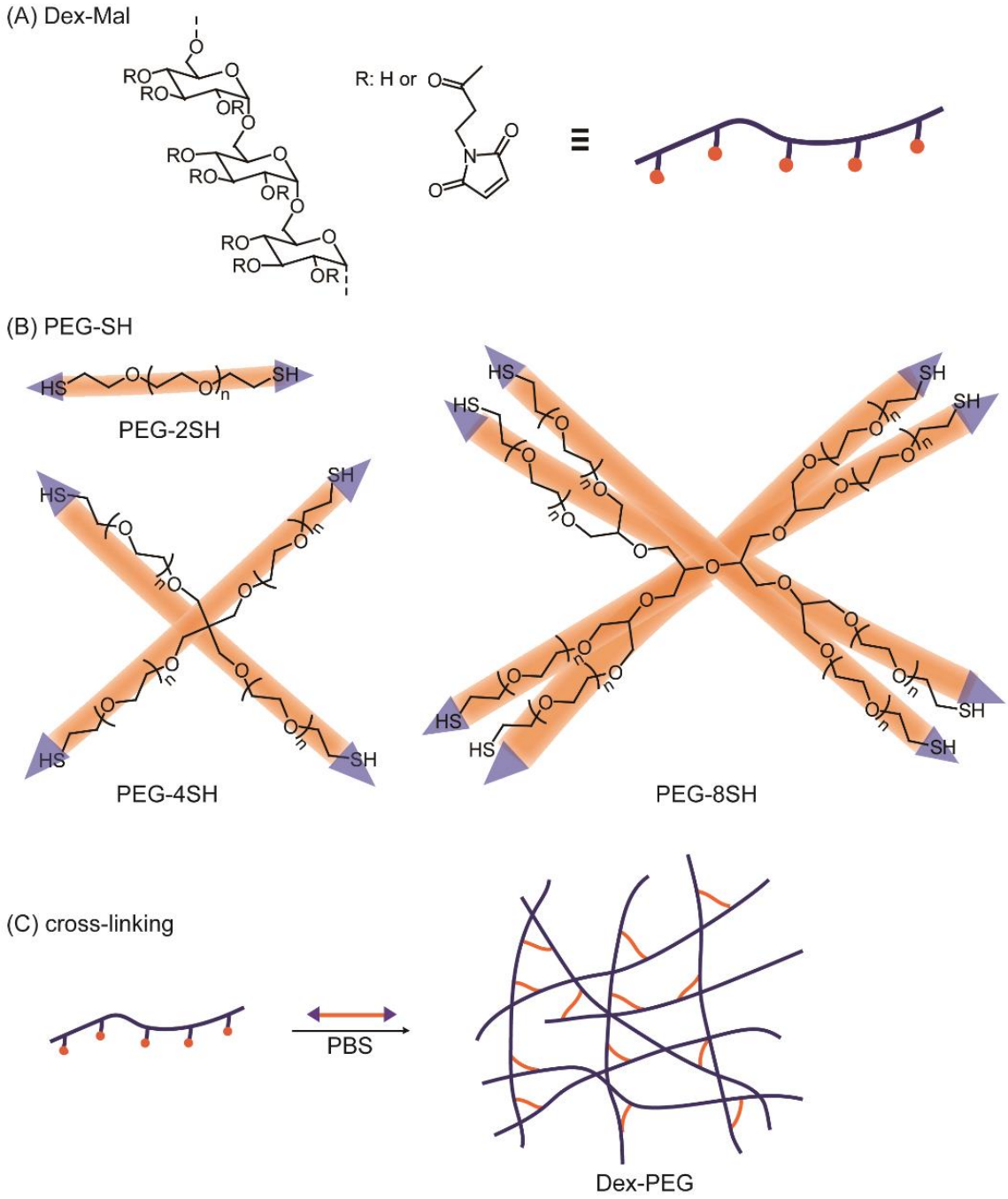

Scheme 1. *Molecular structures of (A) Dex-Mal and (B) PEG-SH (linear, 4 arms and 8 arms). (C) Formation of the Dex-PEG hydrogel by crosslinking Dex-Mal and PEG-SH.*

different combinations of polymer precursors resulted in distinct appearances of hydrogel films formed on the glass slides. Dex-PEG gels prepared from Dex70k-Mal with DS[Mal] of 2~4 resulted in transparent and homogeneous layers on glass surfaces. In contrast, Dex70k-Mal with a DS[Mal] greater than 5 led to the formation of a inhomogeneous film. We found that the surface roughness affected the GUV yield and size (*vide infra*). Moreover, the hydrogel coated glass slides

were examined for their capacity to swell upon rehydration by their immersion in PBS buffer at room temperature. The swollen weight of hydrogels prepared by various DS[Mal] of Dex70k-Mal attached onto glass slides was measured over time. The weight of all swollen samples reached a plateau within an hour, suggestive of rapid swelling kinetics (Figure S1).

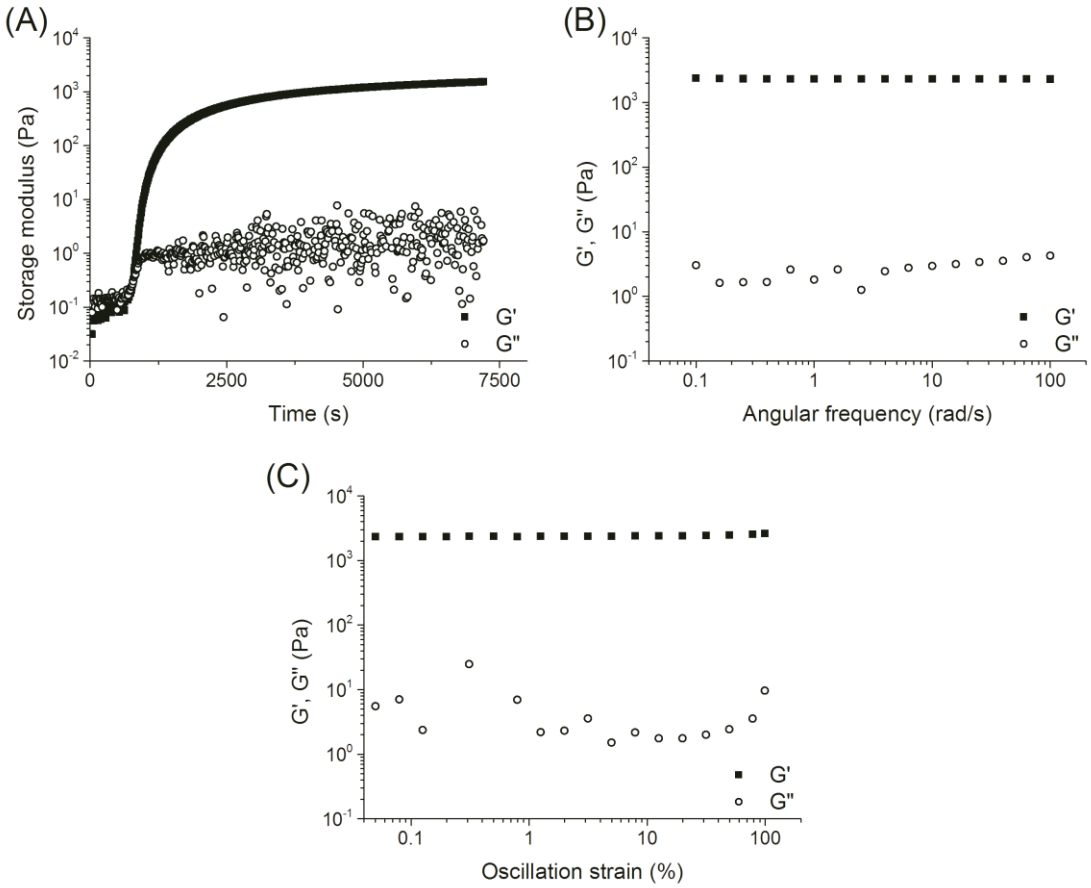

Figure 1. *Oscillatory rheology measurements of Dex-PEG hydrogels composed of 3.5% (w/v) Dex70k-Mal5.5 crosslinked with PEG2k-2SH at 25 ˚C. (A) Time sweep using 1% strain at 1 rad/s. (B) Amplitude sweep from 0.1 to 100 rad/s with 1% strain. (C) Angular frequency measurement from 0.1% to 100% strain at 1 rad/s.*

GIANT VESICLE PREPARATION USING CROSSLINKED DEX-PEG FILMS

To evaluate the potential of the chemically crosslinked hydrogel for assisting GUV growth, several buffers and lipid compositions were tested for this purpose. 1% (w/v) Dex70k-Mal4 (M_w=70 kDa, DS[Mal]=4) and PEG3.4k-2SH (M_w=3.4 kDa, 2 thiol end groups) were mixed together to produce the gel layer for the following studies.

Vesicle production in buffer systems of physiological ionic strength was first examined. The osmolality of phosphate buffered saline (PBS) and HEPES buffered saline (HBS) was 310 mOsm/kg and 320 mOsm/kg, respectively, which are on par with buffers found and used in

biology and physiological fluids (300 mOsm/kg). For both buffers, free floating vesicles were obtained in high yield without any extra reagents or special requirements regarding the lipid composition.

The capacity of Dex-PEG gel to promote GUV formation with various lipid compositions was subsequently assayed. Lipid compositions with different percentages of cholesterol (CH), negatively charged lipids (POPG and DOPS) and liquid ordered lipid phases (DPPC) were deposited on gel-coated glass slide (See Table 1) to yield vesicles as described earlier. In presence of CH (Table 1: a, b and h), free floating GUVs with a spherical morphology (Figure 2: A, B and F) were prepared in good yields in contrast to previous reports[17] where the use of the gentle hydration method showed exclusive formation of tubular morphologies (POPC with 5–30% CH in HEPES). The content of anionic lipids was increased up to 50% using the Dex-PEG hydrogel method, which is in contrast to the gentle hydration methods where this value is kept below 10% to promote growth (Table 1: c, d and e). More specifically, in presence of relatively high percentage of POPG or DOPS, spherical vesicles were successfully formed in high yield by our method (Figure2: C, D and E). When using lipids that form liquid ordered lipid phases, it is known that

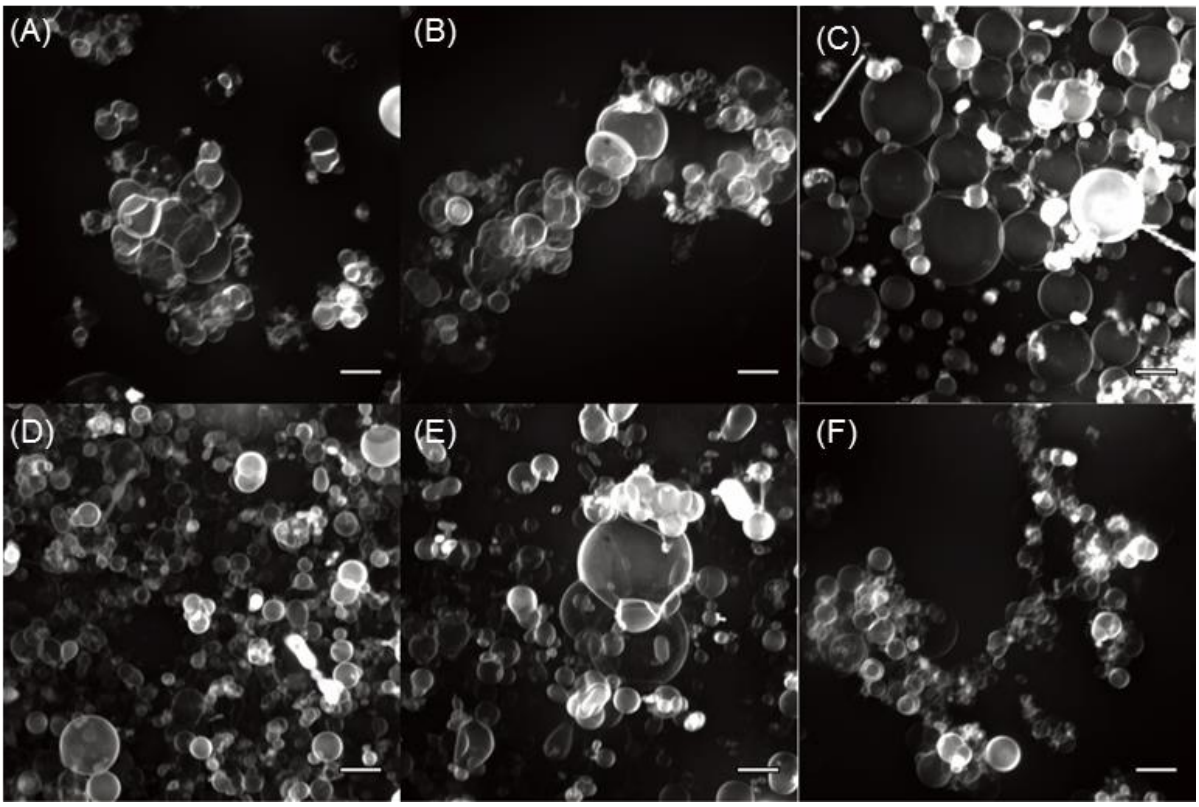

Figure 2. *Formation of GUVs from Dex-PEG hydrogel coated glass slides with various lipid compositions (scale bar: 10 μm). (A) 90% POPC : 10% CH, (B) 80% POPC : 20% CH, (C) 90% POPC : 10% POPG, (D) 50% POPC : 50% POPG, (E) 90% POPC : 10% DOPS and (F) 50% DOPC : 25% DOPE : 25% CH. Reproduced from ref. [16].*

lipid mixtures can undergo phase separation through phase coexistence of liquid ordered (L_o) and liquid disordered (L_d) phases.[18] Thus far, phase separated GUVs have only been formed under non-physiological conditions (KCl, 50 mM).[19] On our hydrogel matrices, phase-separated GUVs consisting of 30-50% DPPC were easily grown at 50 °C (Figure S2). Hence, we demonstrated that the Dex-PEG gel-assisted hydration method can successfully produce GUVs from different types of lipids showing its potential to enable their facile growth.

Table 1. *Lipid compositions examined for GUV growth on Dex-PEG at physiological ionic strength conditions (>300 mOsm/kg).*

No.	Lipid composition (% mol)	Buffer system	
		PBS	HBS
a	90% POPC / 10% CH	√	√
b	80% POPC / 20% CH	√	√
c	90% POPC / 10% POPG	√	√
d	50% POPC / 50% POPG	√	√
e	90% POPC / 10% DOPS	√	√
f	50% DOPC / 25% DOPE / 25% CH	√	√
g	50% DOPC / 50% DPPC	√	√
h	33.3% DOPC / 33.3% DPPC / 33.3% CH	√	√
i	50% DOPC / 20% DOPE / 5% PEG2000-PE / 25% CH	√	√

INFLUENCE OF THE HYDROGEL PHYSICOCHEMICAL PROPERTIES ON GUV PRODUCTION

Since the pioneering work by Horger *et al.* on the gel-assisted hydration method for GUV growth,[13] few research groups have studied and improved this advanced technique with various types of gels.[14, 15] The mechanism of giant vesicle formation *via* this method, especially the role of the hydrogel films, is however still unclear. According to Horger *et al.*, the swelling of the hydrogel film is a key step in the formation of the lipid lamellae, the growth of liposomes and their fusion.[13] Because the degree of hydrogel swelling strongly depend on the crosslinking density (ϱ_x) of the network,[20] we hypothesized that the production of GUVs could be controlled by the polymeric structure of Dex-PEG hydrogels. Starting from the initially developed Dex-PEG gel film composition for GUV formation (hydrogel prepared from 1% Dex70k-Mal4 and PEG3.4k-2SH

at equimolar thiol to maleimide), we modulated the physicochemical properties of Dex-PEG hydrogels using three parameters: the molar ratio of thiol to maleimide (MR[SH:Mal]), the molecular weight and architecture of thiolated PEG, and the degree of substitution of the maleimide modified dextran (DS[Mal]). The obtained GUVs were analyzed by fluorescence microscopy and the fluorescence-activated cell sorting (FACS). To gain insight into the effect of these three factors on GUV production, we further examined the difference in the network properties of the hydrogels using oscillatory rheology, swelling experiments and cryo-SEM imaging.

THIOL-MALEIMIDE MOLAR RATIO

To study the effect of the molar ratio of thiol to maleimide groups (MR[SH:Mal]), Dex70k-Mal4 was crosslinked with PEG2k-2SH at a molar ratio of thiol to maleimide of 0.5, 0.75, 1 and 1.25. In these experiments, the molar concentration of maleimides was kept at 8 mM while the molar concentration of thiols was varied.

The gelation kinetics of Dex-PEG hydrogels (3.5%, w/v) with 4 different SH:Mal ratios were followed by oscillatory rheology using time sweep measurements. Significant differences in gel formation kinetics and plateau moduli were observed (Figure 3A). When the molar ratio of SH:Mal was decreased from 1 to 0.75, the Dex-PEG hydrogel formed more slowly reaching a lower plateau modulus (260 Pa). When the molar ratio of SH:Mal was further decreased to 0.5, the gelation time of Dex-PEG hydrogels was two times slower in comparison to the 1:1 sample with final storage modulus one order of magnitude lower (20 Pa). When the molar ratio of SH:Mal was increased to 1.25, the gelation of Dex-PEG hydrogels proceeded faster than other three samples, however the final storage modulus did not exceed samples prepared with MR[SH:Mal] of 1. The formation of viscoelastic materials by all samples was confirmed by amplitude and angular frequency sweeps.

The equilibrium mass swelling ratio (q) of different hydrogel systems with different molar ratios of thiol to maleimide were compared. As shown in Figure 3B, the value of q increased when the hydrogel formulation departed from a 1:1 stoichiometry. For Dex-PEG hydrogels prepared with a large excess of maleimide groups (0.5 molar ratio) the greatest amount of swelling is observed with a two-fold increase in q.

Combining the results of the rheological and swelling measurements, modulation of the molar ratio of thiol to maleimide groups can result in significant changes in hydrogel physicochemical properties in terms of mechanical strength and swelling behavior. These properties are influenced by the crosslinking density (ρ_x) of the network. When one of the functional groups is in excess a network with fewer crosslinks is obtained, resulting in lower storage moduli and higher equilibrium swelling ratios. This trend is on par with a previously reported polymeric hydrogel system synthesized by the azide-alkyne click reaction.[21] The stoichiometric imbalance of functional groups

in the Dex-PEG system may promote the formation of closed loops, which is formed by thiols on the same PEG chain of the PEG-SH crosslinker reacted to maleimides on the same Dex-Mal chain. These closed loops, called primary cycles, do not connect to the crosslinked network but only dangle within it, decreasing the hydrogel crosslinking density resulting in spatial inhomogeneity of hydrogel networks.[22]

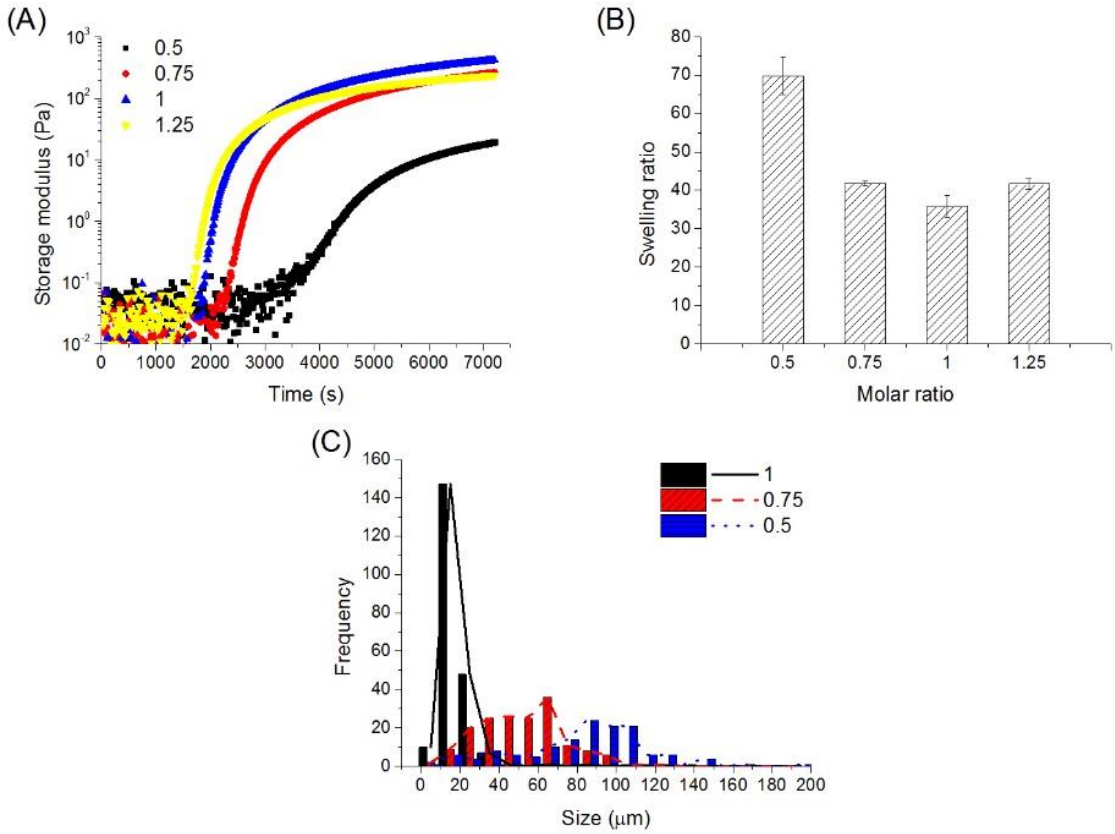

Figure 3. *The effect of the thiol to maleimide molar ratio in the Dex-PEG hydrogel composed of 3.5% (w/v) Dex70k-Mal4 and PEG2k-2SH on (A) the gelation kinetics and mechanical strength, (B) the equilibrium swelling ratio. (C) The size distribution of generated GUVs (lipid composition: 50% DOPC : 25% DOPE : 25% CH, wherein Dex-PEG hydrogel films for the hydration process were prepared by 1% (w/v) Dex70k-Mal4 and PEG2k-2SH with a molar ratio of thiol to maleimide at 0.75, 0.5, 1 and 1.25). Reproduced from ref. [16, 23].*

Hydrogel films were prepared from 1% (w/v) Dex70k-Mal4 and PEG2k-2SH with a molar ratio of thiol to maleimide of 0.5, 0.75 and 1 and were attached to glass slides for GUV formation. With a molar ratio of thiol to maleimide of 1, a very narrow size distribution of GUVs were obtained with an average size of 15 μm. When the hydrogel film departed from a 1:1 stoichiometry, the GUV size distribution broadened (Figure 3C) and the value of the average peak size turned greater. This observation confirms that the size distribution and the diameter of obtained GUVs by gel-assisted hydration method is related to the polymeric structure of Dex-PEG hydrogels. On the

other hand, decreasing the molar ratio of thiol to maleimide of the gel network led to the formation of a more inhomogeneous network with the formation of GUVs (50 – 100 μm) that were larger and more polydisperse in size.

PEG MOLECULAR WEIGHT AND ARCHITECTURE

To study the effect of crosslinker architecture and size, five different thiolated PEG (PEG-SH) crosslinkers (Scheme 1B and Table 2) were reacted with 3.5% (w/v) Dex70k-Mal4 at a 1:1 molar ratio of thiol to maleimide in PBS buffer. By oscillatory rheology, more rapid gelation kinetics and a higher mechanical strength were observed for hydrogels prepared from thiolated PEG with a higher molecular weight (Figure 4A). By increasing the M_w of the linear PEG-dithiols from 2 kDa to 10 kDa (i.e. PEG2k-2SH and PEG10k-2SH), the storage modulus of the Dex-PEG hydrogels increased one order of magnitude. Hydrogels prepared from PEG10k-SH (M_w=10 kDa) with a non-linear architecture and an increased number of functional groups provided a more complicated trend. Compared to PEG10k-2SH (M_w=10 kDa, 2 thiol-ending groups), PEG10k-4SH (M_w=10 kDa, 4 thiol ending groups) increased the gelation rate and improved the mechanical strength of the obtained Dex-PEG hydrogel. However, the use of PEG10k-8SH (M_w=10 kDa, 8 thiol-ending groups) resulted in a lower storage modulus in comparison to PEG10k-4SH.

Table 2. *Thiol functionalized PEGs used to prepare Dex-PEG hydrogels.*

Sample	Molecular weight	SH per molecule
PEG2k-2SH	2 kDa	2
PEG3.4k-2SH	3.4 kDa	2
PEG10k-2SH	10 kDa	2
PEG10k-4SH	10 kDa	4
PEG10k-8SH	10 kDa	8

This observation was in accordance with results of the viscosity measurement performed on mixtures composed of 0.5% (w/v) Dex70k-Mal2.5 and various thiolated PEG (Figure S3). Crosslinked polymer samples containing the 4-arm PEG10k-4SH showed the highest dynamic viscosity, while similar values were obtained from the 8-arm PEG10k-8SH and the linear PEG-2SH. Equilibrium swelling measurements displayed a similar trend to the oscillatory rheology data after reaction of Dex70k-Mal4 with various thiolated PEG (Figure 4B). By increasing the molecular weight of the linear PEG-2SH molecules (i.e. PEG2k-2SH, PEG3.4k-2SH and PEG10k-2SH), the equilibrium mass swelling ratio (*q*) of obtained hydrogels decreased. When the molecular weight of

the linear PEG-2SH polymer increased four-fold, *q* decreased 54%. Conversely, when the molecular weight of PEG-SH was maintained at 10 kDa, *q* increased with its modulation of its architecture. In the case of the 8-arm PEG10k-8SH, a 68% increase of *q* was recorded in comparison to the linear PEG variant (PEG10k-2SH).

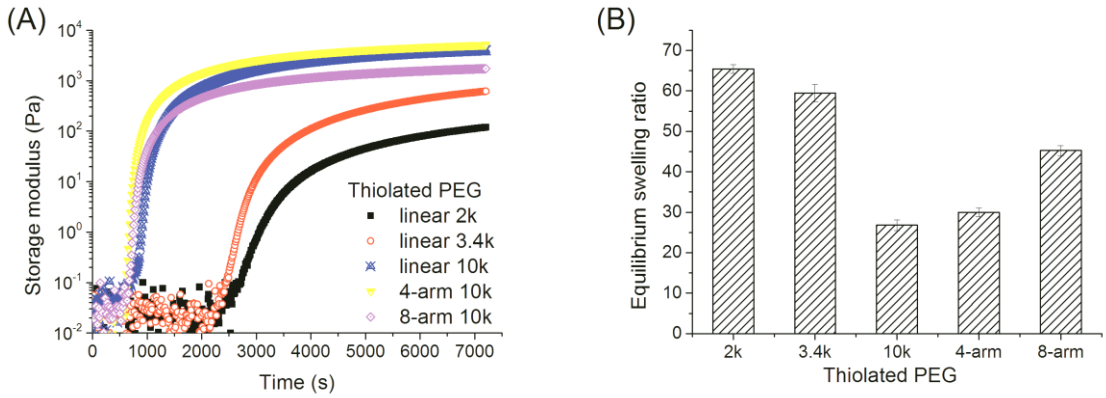

Figure 4. *Effect of molecular weight and architecture of various thiolated PEGs on (A) the gelation process and the mechanical strength and (B) the equilibrium swelling ratio of Dex-PEG hydrogels. Hydrogels were prepared by reacting 3.5% (w/v) Dex70k-Mal4 with various thiolated PEG at a MR[SH:Mal] of 1 in PBS. Thiolated PEGs used to prepare Dex-PEG hydrogels: PEG2k-2SH (black), PEG3.4k-2SH (red), PEG10k-2SH (blue), PEG10k-4SH (yellow) and PEG10k-8SH (purple). Reproduced from ref. [23].*

Cryo-SEM images of the Dex-PEG hydrogel films prepared using the various types of PEG-SH crosslinkers provided insight into their microstructure (Figure 5). For linear PEG-2SH with the lowest molecular weight (PEG2k-2SH), the porous structure was discontinuous. On the other hand, hydrogels prepared with PEG3.4k-2SH, PEG10k-4SH or PEG10k-8SH presented a more homogeneous microstructure having interconnected pores similar to honeycombs.

The experimental results described above show the molecular weight and the architecture of the thiolated PEG precursor also strongly influence the effective crosslinking density of the network. As mentioned earlier, the formation of inhomogeneities in the network is strongly related to the presence of primary cycles and other non-idealities formed during the gelation process precluding effective crosslinks from forming. Moreover, according to a study by Elliott, the formation of primary cycles in the polymeric network can be lessened by increasing the size of the crosslinking agent and the precursor concentration.[24] Similarly, Metters reported that decreasing the crosslinker concentration and functionality generated more non-idealities in the network.[22] It became evident that we also encountered a similar phenomenon at low concentrations of precursors when preparing the thin hydrogel films for GUV formation. The steric accessibility of the functional groups and kinetics of the thiol-maleimide addition reaction play a significant role in formation of the network. After one end of the linear PEG-2SH is chemically ligated to Dex-Mal, the other reactive group will react with the closest maleimide unit. For a linear PEG-2SH of a relatively low

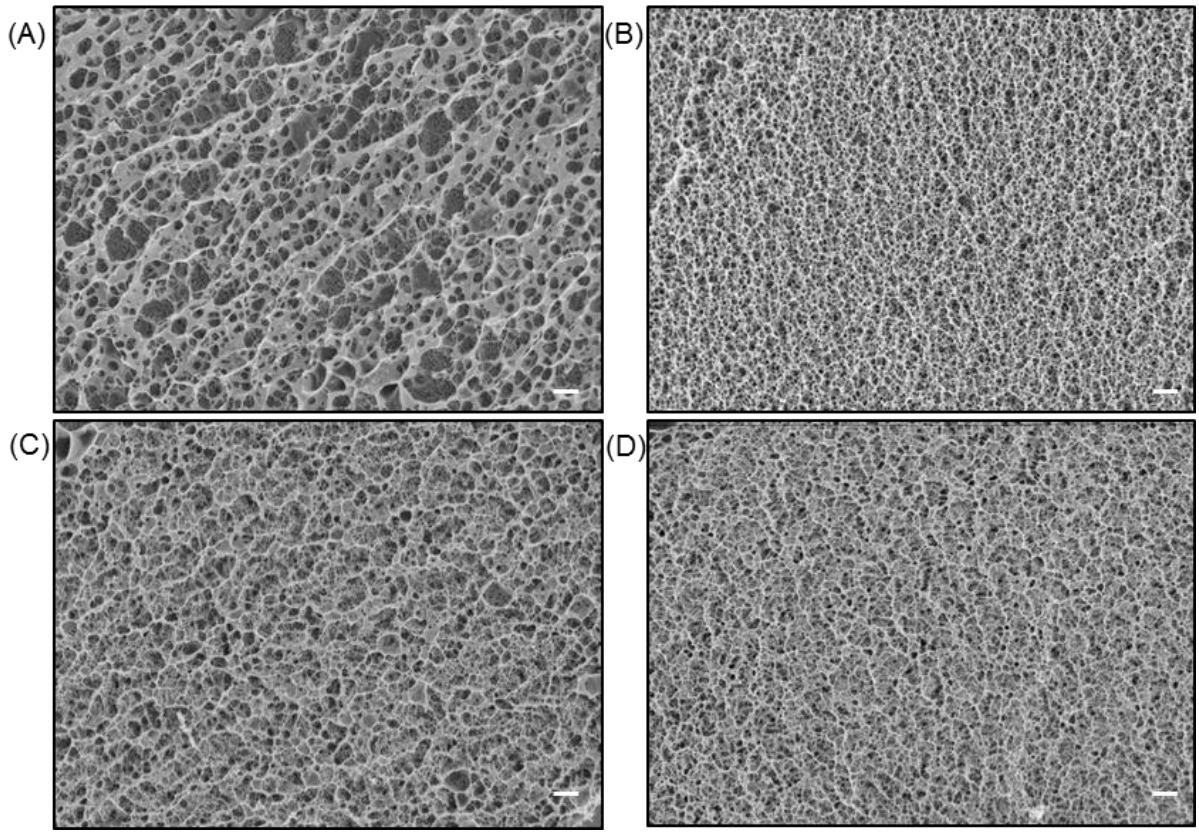

Figure 5. *Cryo-SEM images of Dex-PEG hydrogels prepared by 1% (w/v) Dex70k-Mal4 crosslinked to various PEG-SH. (A) PEG2k-2SH, (B) PEG3.4k-2SH, (C) PEG10k-4SH and (D) PEG10k-8SH. Scale bar: 1 μm. Reproduced from ref. [23].*

molecular weight, such as PEG2k-2SH, the second thiol group is more likely to react with a maleimide group on the same Dex-Mal chain or remain unreacted due to its short chain length, thus generating primary cycles and other inhomogeneities in the network. The effect of the polymeric architecture of thiolated PEG on hydrogel properties can be explained by the same hypothesis. In comparison to the linear PEG10k-2SH and the 4-arm PEG10k-4SH, the size of PEG10k-8SH is more compact, thus the accessibility of reactive thiols is restricted. Therefore, it is reasonable that hydrogels prepared with PEG10k-8SH display lower crosslinking density and, thus weaker mechanical properties and higher equilibrium swelling ratios than that of hydrogels prepared with PEG10k-2SH and PEG10k-4SH. In summary, polymeric networks of Dex-PEG hydrogels show strong dependence on the molecular weight and the architecture of the reactive PEG-SH polymers and, therefore the design of the hydrogel system is important in order to maximize GUV growth. Based on the effect of the molecular weight and architecture of PEG-SH on the formation of the hydrogel networks, films of various samples were prepared to study their influence on GUV formation. Two different lipid compositions, 75 mol% POPC : 20 mol% cholesterol : 5 mol% PEG2000-PE and 80 mol% POPC : 20 mol% cholesterol, were used to prepare GUVs and the yields of GUVs were quantified by FACS (Figure 6A). It was found that

hydrogel films made from 1% Dex70Mal4 and PEG10k-4SH resulted in the lowest yield of GUVs for both lipid compositions. Considering PEG10k-4SH preformed a much lower equilibrium mass swelling ratio than other types of thiolated PEG, this result indicates that the swelling of Dex-PEG hydrogel film is crucial to the formation of GUVs during the hydration of the lipid and hydrogel film. In contrast, although hydrogels made weak mechanical property, relatively high yields of GUVs were obtained. Thus a higher equilibrium mass swelling ratio facilitates GUV production.

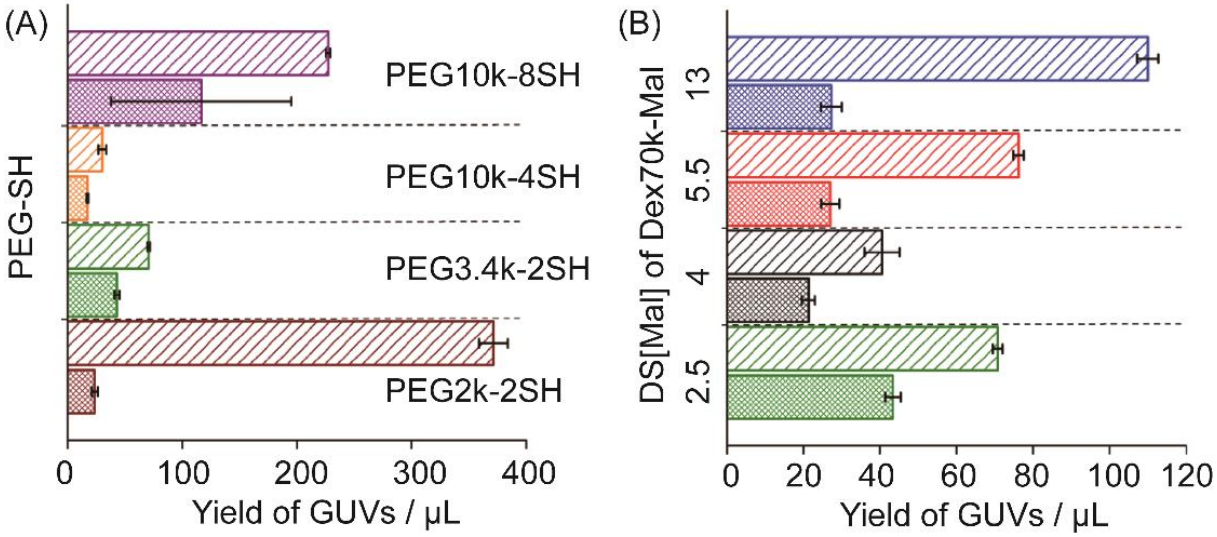

Figure 6. *Yields of GUVs produced on Dex-PEG hydrogel films composed of (A) 1% (w/v) Dex70k-Mal4 and various thiolated PEG (PEG2k-2SH, PEG3.4k-2SH, PEG10k-4SH and PEG10k-8SH) at an equimolar ratio of thiol to maleimide; (B) 1% (w/v) Dex70k-Mal with different DS[Mal] (Dex70k-Mal2.5, Dex70k-Mal4, Dex70k-Mal5.5 and Dex70k-Mal13) and PEG3.4k-2SH at an equimolar ratio of thiol to maleimide. Line patterned bars represent GUVs with a lipid composition of 75 mol% POPC : 20 mol% cholesterol : 5 mol% PEG2000-PE. Cross-hatched bars represent GUVs with a lipid composition of 80 mol% POPC : 20 mol% cholesterol. Reproduced from ref. [16, 23].*

MODULATION OF THE DEGREE OF SUBSTITUTION OF THE DEX-MAL POLYMER

The effect of the degree of substitution of maleimide (DS[Mal]) of the Dex-Mal polymer on the physiochemical properties of Dex-PEG gels was examined using PEG2k-2SH crosslinked to Dex70k-Mal with various degree of substitution (DS[Mal]=4, 5.5 and 9) at a stoichiometric ratio of thiols to maleimides in PBS. It should be noticed that the set-up of hydrogel systems prepared from Dex-Mal with different DS[Mal] is crucial to the resulting trend, which will be discussed below in detail.

3.5% (w/v) Dex70k-Mal4, Dex70k-Mal5.5 and Dex70k-Mal9 were crosslinked to PEG2k-2SH respectively and measured by oscillatory rheology. Dex70k-Mal with higher DS[Mal] displayed faster gelation process and resulted in stronger hydrogels (Figure 7A). The oscillation time sweep curves seems to indicate a positive correlation between the DS[Mal] and the final storage modulus

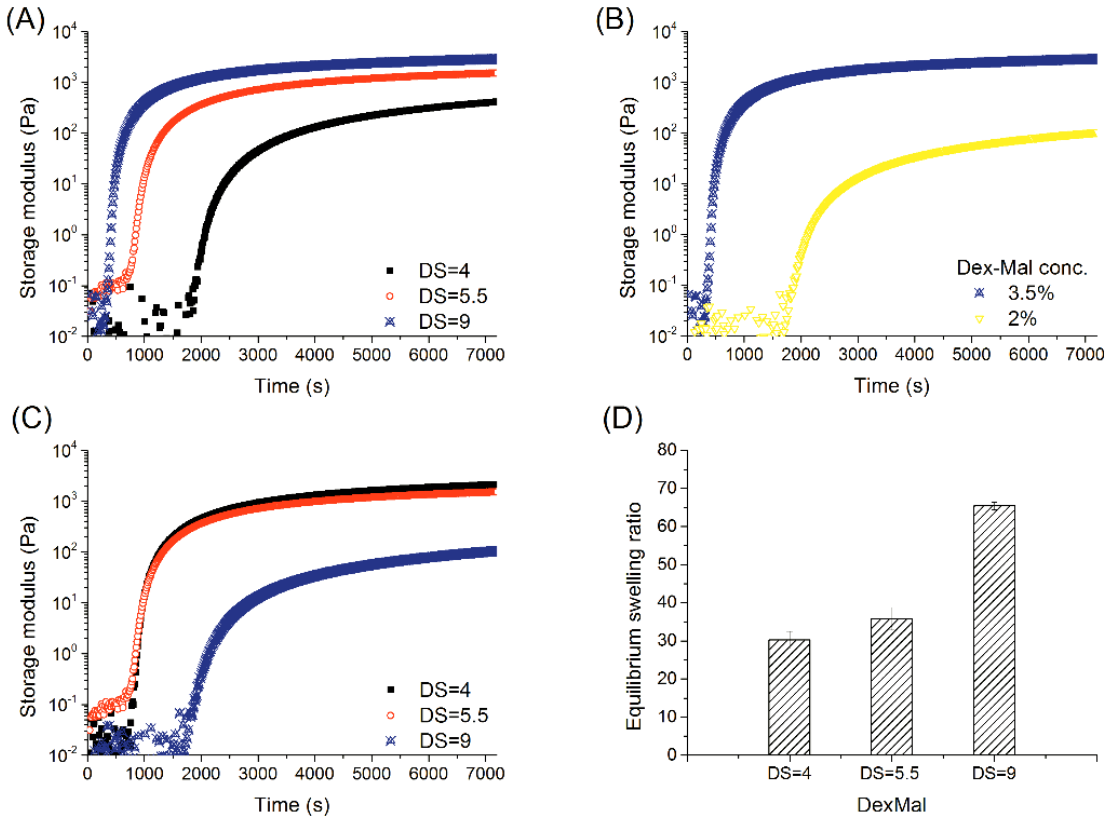

Figure 7. *Oscillatory rheology time sweep profiles of Dex-PEG hydrogels prepared by (A) 3.5% (w/v) Dex70k-Mal crosslinked to PEG2k-2SH wherein Dex70k-Mal4, Dex70k-Mal5.5 and Dex70k-Mal9 were used respectively; (B) 1% and 3.5% (w/v) Dex70k-Mal9 crosslinked to PEG2k-2SH; (C) 1.1% (w/v) PEG2k-2SH crosslinked to Dex70k-Mal wherein Dex70k-Mal4, Dex70k-Mal5.5 and Dex70k-Mal9 were used respectively; (D) The equilibrium swelling ratio of hydrogels prepared using 1.1% (w/v) PEG2k-2SH and Dex70k-Mal wherein Dex70k-Mal4, Dex70k-Mal5.5 and Dex70k-Mal9 were used respectively. The molar ratio of thiol to maleimide was kept at 1 in all samples.*

of the corresponding hydrogel. However, the influence of the DS[Mal] of Dex-Mal polymers cannot be assessed due to different functional group concentrations of these hydrogel systems. In fact, when the concentration of Dex-Mal in all three hydrogel systems (DS[Mal]=4, 5.5 and 9) was kept at 3.5% (w/v), different numbers of maleimide groups per dextran chain led to various concentrations of maleimide groups in each system. The observed trend (Figure 7A) is probable caused by the functional group concentration instead of the architecture of the Dex-Mal polymer. To verify this, hydrogels composed of 2% (w/v) Dex70k-Mal9 crosslinked to PEG2k-2SH were prepared and measured by oscillatory rheology (Figure 7B). As shown in Figure 7B, the gelation was slowed down and the final storage modulus of 2% gels was one order of magnitude smaller than that of 3.5% gels. Also, high similarity in oscillation time sweep curves was observed between the Dex-PEG gel prepared from 2% Dex70k-Mal9 and the Dex-PEG gel prepared from 3.5% Dex70k-Mal4. These results showed that the observed trend in Figure 7A may be dominated by

the concentration of maleimide, making it difficult to assess the influence of DS[Mal] on the resulting hydrogel properties.

Therefore the concentration of PEG2k-2SH was maintained to 1.2% for the preparation of 1%Dex-PEG hydrogels using Dex70k-Mal4, Dex70k-Mal5.5 and Dex70k-Mal9 respectively at an equimolar ratio of thiol to maleimide. The concentration of Dex-Mal in each hydrogel system was not the same, Dex70k-Mal4 (5.1%), Dex70k-Mal5.5 (3.5%) and Dex70k-Mal9 (1%). Figure 7C shows that hydrogels prepared from Dex70k-Mal with a higher DS[Mal] displayed a slower gelation process resulting in a weaker hydrogel. When the DS[Mal] of Dex-Mal increased from 4 to 9, the gelation process was retarded and the final storage modulus of resulting hydrogels decreased by one order of magnitude. The swelling experiments also revealed that the equilibrium mass swelling ratio (q) of hydrogels doubled when the DS[Mal] of Dex-Mal increased from 4 to 9 (Figure 7D). As the viscoelastic property of dextran solution is nearly independent of dextran concentration at such a low concentration of dextran (below 5%), any obvious change in the oscillatory rheology and swelling experiments is due to the DS[Mal] rather than the concentration of Dex-Mal. Thus these results indicate that hydrogels prepared from Dex-Mal with higher DS[Mal] have a lower effective crosslinking density.

Cryo-SEM images of Dex-PEG hydrogels prepared by 1% Dex70k-Mal with various DS[Mal] (from 4 to 13) and PEG3.4k-2SH displayed differences in the hydrogel microstructure (Figure 8). For the sample prepared from Dex70k-Mal4 and Dex70k-Mal5.5, multiple layers of continuous pores were observed. The pore size seemed to increase with the DS[Mal] of the applied Dex-Mal. For the sample prepared from Dex70k-Mal4 an average pore size around 200 nm was observed. For the sample prepared from Dex70k-Mal5.5, an average pore size around 1 μm was observed. However, a further increase of the DS[Mal] to 9 led to the formation of inhomogeneous network (Figure 8C). When Dex70k-Mal13 was used, the sample presented a poorly connected structure lacking well defined pores (Figure 8D).

Taken together, too high DS[Mal] of Dex-Mal may reduce the effective crosslinking density of prepared hydrogels. For example, when the DS[Mal] of Dex-Mal increases from 4 to 9, the amount of maleimide groups on each dextran polymer chain increases from 17 to 39 (Table 3), thus too many maleimide functional groups are substituted on the same polymer chain. In the case of applying Dex70k-Mal9 (DS[Mal]=9), once one of these maleimide groups on the dextran chain reacts to one thiol group of the thiolated PEG, the accessibility of other maleimide groups on the same dextran chain decreases. For each maleimide group on the same dextran chain, the probability to be reacted to different thiolated PEG also decreases. Thus using Dex-Mal with a higher DS[Mal] for Dex-PEG hydrogel preparation may lead to a drop of the number of effective crosslinks. Furthermore, the hydrophobicity of Dex-Mal may increase with the DS[Mal], resulting a more

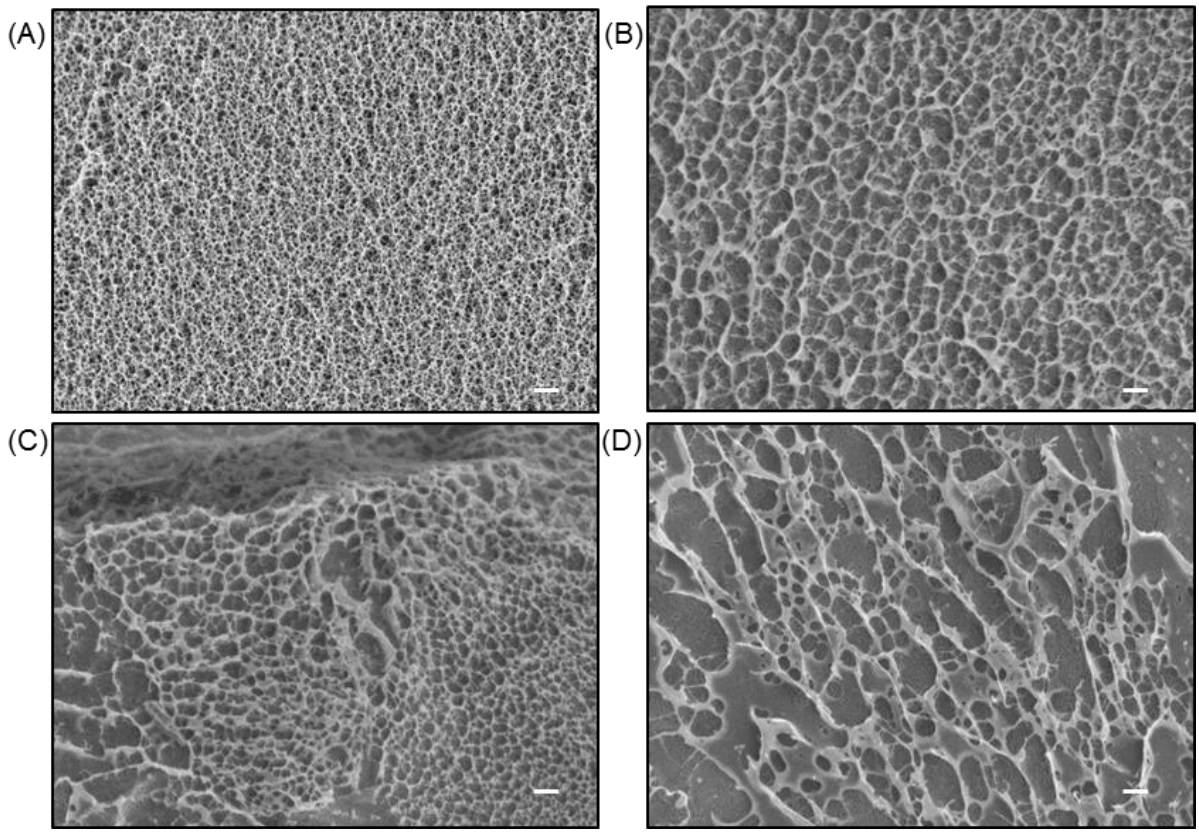

Figure 8. *Cryo-SEM images of Dex-PEG hydrogels prepared from 1% (w/v) (A) Dex70k-Mal4, (B) Dex70k-Mal5.5, (C) Dex70k-Mal9 and (D) Dex70k-Mal13 crosslinked to PEG3.4k-2SH. An equimolar ratio of thiol to maleimide was maintained in all samples. Scale bar: 1 μm. Reproduced from ref. [23].*

Table 3. *List of prepared Dex-Mal polymers with increasing degree of substitution.*

	Number of maleimide groups on dextran	
Sample	per 100 glucopyranose units (DS[Mal])	per dextran chain
Dex70k-Mal2.5	2.5	10.8
Dex70k-Mal4	4	17.3
Dex70k-Mal5.5	5.5	23.8
Dex70k-Mal9	9	38.9
Dex70k-Mal13	13	54.9

compact conformation of the Dex-Mal polymer in the solution. Such compact conformation may hinder part of the maleimide groups to react with the thiolated PEG.

The influence of the DS[Mal] of Dex-Mal on the yield of GUV production was investigated using Dex-PEG hydrogel films prepared from various Dex70k-Mal (Dex70k-Mal2.5, Dex70k-Mal4, Dex70k-Mal5.5 and Dex70k-Mal13) and PEG3.4k-2SH at an equimolar ratio of thiol to maleimide.

It was found that the hydrogel films prepared from Dex70Mal4 resulted in the lowest yield of GUVs while the hydrogel films prepared from Dex70Mal13 resulted in the highest yield of GUVs. Such results are similar to the observation discussed in the above section related to the type of thiolated PEG. It seems that hydrogel films having relatively high equilibrium mass swelling ratios assist the formation of GUVs more efficiently during the hydration.

In summary, the generation of GUVs depends on the physicochemical properties of the hydrogel films in the gel-assisted hydration method. Swelling properties of the hydrogel film, such as the equilibrium swelling ratio, influence on the yield of GUVs. As the swelling process of the hydrogel film influences the hydration of the lipid, interactions between lipids and the hydrophilic environment of the hydrogel film is also important for the GUV formation.

CONCLUSION

We developed a chemically crosslinked Dex-PEG hydrogel to improve the GUV growth method using gentle hydration. Polymer and additive-free GUVs can be made rapidly under physiological ionic strength conditions in high yield without any special equipment. This approach makes it possible to prepare GUVs in PBS from various lipid compositions showing important advantages for certain lipid compositions that are otherwise difficult for vesicle formation.

Dex-PEG hydrogels are prepared by mixing two functionalized hydrophilic polymers in aqueous buffer. Compared to physical gels, the gelation of the covalent Dex-PEG hydrogel system proceeds rapidly to form stable hydrogels with a controllable structure. The GUVs production was systematically investigated by controlling the molar ratio of the thiol and maleimide functional groups, the molecular weight of thiolated PEG and the architecture of both thiolated PEG and Dex-Mal. We found that to produce GUVs in high yield, it is essential for Dex-PEG gel films to have a relatively high equilibrium swelling ratio. These hydrogel films may promote the interaction between the lipid components and hydrophilic polymeric network, which is likely the key factor for successful GUV formation.

We have explored the Dex-PEG hydrogel film-assisted hydration method for encapsulation of chemical reagents, biomacromolecules and even polymersomes.[23] This simple and versatile approach has facilitated the visualization and quantification of transmembrane activities[25] and the study of membrane proteins. We anticipate that this method can be useful to research areas such as biomimetic chemistry, biomembrane physics and artificial cell mimics.

EXPERIMENTAL

MATERIALS

Cholesterol (CH), 1,2-dioleoyl-*sn*-glycero-3-phosphocholine (DOPC), 1,2-dioleoyl-*sn*-glycero-3-phosphoethanolamine (DOPE), 1-palmitoyl-2-oleoyl-*sn*-glycero-3-phosphocholine (POPC), 1-palmitoyl-2-oleoyl-*sn*-glycero-3-phospho-(1'-rac-glycerol) (sodium salt) (POPG), 1,2-dioleoyl-*sn*-glycero-3-phosphoethanolamine-N-[methoxy(polyethylene glycol)-2000] (ammonium salt) (PEG2000-PE), 1,2-dioleoyl-*sn*-glycero-3-phosphoethanolamine-N-(lissamine rhodamine B sulfonyl) (ammonium salt) (PE-LR) were purchased from Avanti Polar Lipids. 1,2-Dipalmitoyl-*sn*-glycero-3-phosphocholine (DPPC), maleic anhydride, *p*-toluene sulfonic acid monohydrate (PTSA) 4-nitrophenyl disulfide, 4-(dimethylamino) pyridine (DMAP), dextran (70 kDa), N,N'-diisopropylcarbodiimide (DIC), dimethyl sulfoxide (DMSO), poly(ethylene glycol) dithiols (M_w=3.4 kDa) were purchased from Sigma-Aldrich. Poly(ethylene glycol) dithiols (M_w=2 kDa, M_w=10 kDa) were purchased from NANOCS (USA), 4-arm poly(ethylene glycol) thiols and 8-arm poly(ethylene glycol) thiols (M_w=10 kDa) were purchased from Jenkem Technology (USA). Phosphate buffered saline (PBS) was composed of 150 mM NaCl, 15 mM K_2HPO_4 and 5 mM KH_2PO_4. HEPES buffered saline (HBS) was composed of 150 mM KCl and 20 mM HEPES.

Dextran was dried in a vacuum oven (30 °C) and DMSO was dried over 4Å molecular sieves before use. 3-maleimidopropionic acid and 4-(dimethylamino)pyridinium 4-toluenesulfonate (DPTS) were synthesized as previously reported.[26, 27] Dialysis membranes (MWCO 3.5-5 kDa) were obtained from Spectrum Laboratories Inc.

SYNTHESIS OF DEX-MAL

Dex-Mal was synthesized by DIC mediated esterification of the hydroxyl groups of dextran with N-maleoyl-β-alanine. Briefly, N-maleoyl-β-alanine (313 mg, 1 eq.), DPTS (86.8 mg, 0.15 eq.) and DIC (434.9 μL, 1.5 eq.) were dissolved in anhydrous DMSO (15 mL). The mixture was stirred at room temperature for two hours, followed by the addition of a dextran solution in DMSO (15 mL). After stirring overnight at room temperature, the formed N, N'-dialkylurea was removed by filtration and the crude product was obtained by precipitation in cold isopropanol. The precipitate was dissolved in water and dialyzed against Milli-Q water five times over two days and subsequently lyophilized. ^{1}H NMR (400 MHz, D_2O): δ 3.3-4.0 (m, dextran glucopyranosyl ring protons), 4.9 (s, dextran anomeric proton), 6.8 (s, maleimide).

The degree of substitution of Dex-Mal (DS[Mal]) is defined as the number of maleimide groups per 100 glucopyranose residues of dextran, which was calculated from the ^{1}H NMR spectra based on the protons of the maleimides (δ 6.8) and the anomeric proton (δ 4.9). The DS[Mal] of Dex-

Mal was controlled by the molar ratio between dextran and N-Maleoyl-β-alanine.

DEX-PEG HYDROGELS PREPARATION

Dex-Mal and thiolated PEG were dissolved in PBS individually and then mixed together using a pipette to prepare the hydrogel samples. Compositions of the Dex-PEG hydrogel are shown below (Table 4).

Table 4. *Composition of Dex-PEG hydrogels.*

Gel conc. (w/v)	Dex70-Mal		Thiolated PEG			Molar ratio	Buffer
	DS [Mal]	Weight (mg)	Type	Mw	Weight (mg)	SH:Mal	Volume (mL)
1.0%	4	10.0	linear	3400	3.9	1	1
3.5%	4	35.6	linear	2000	8.2	1	1
3.5%	4	35.6	linear	2000	6.2	0.75	1
3.5%	4	35.6	linear	2000	4.1	0.5	1
3.5%	4	35.6	linear	2000	10.3	1.25	1
3.5%	4	35.6	linear	2000	8.2	1	1
3.5%	4	35.6	linear	3400	13.9	1	1
3.5%	4	35.6	linear	10000	20.5	1	1
3.5%	4	35.6	4-arm	10000	10.3	1	1
3.5%	4	35.6	8-arm	10000	45.8	1	1
3.5%	5.5	35.6	linear	2000	12.0	1	1
2.0%	9	21.1	linear	2000	12.0	1	1
5.0%	4	52.0	linear	2000	12.0	1	1

GEL-ASSISTED GUV FORMATION

The surface of a microscope glass slide was functionalized with 3-mercaptopropyl trimethoxysilane according to a previously reported method[28] (Figure 9, step 1) and sequentially drop-casted by a mixture of the Dex-Mal solution and thiolated PEG at 40 °C (Figure 9, step 2) until a homogeneous hydrogel film was formed and anchored to the glass surface. The molar ratio of maleimides to thiols was 1:1 in all samples unless otherwise stated. After the hydrogel layer was fully gelated, a lipid solution (14 mM, 10 μL) was deposited on the top of the hydrogel film. The lipid and hydrogel film was dried in a vacuum oven for 30 minutes at 35 °C or under a gentle stream of nitrogen gas

which prevented lipid oxidation at room temperature (Figure 9, step 3). In the hydration step, a liquid chamber was made by placing a 15 mm (OD) glass O-Ring on top of the hydrogel film and sealed with high vacuum silicon grease. PBS (or HBS) buffer solution (400 µL) was added to the chamber and the film (Figure 9, step 4) was allowed to swell for 1-2 hours at room temperature resulting in free-floating vesicles (Figure 9, step 5). Swelling of the film was performed above the T_m of all lipids. For samples containing solely unsaturated lipids, this swelling was performed at room temperature. For mixtures containing saturated lipids, swelling was performed at 50 °C. The formed free floating GUVs were transferred into an eppendorf tube for further analysis.

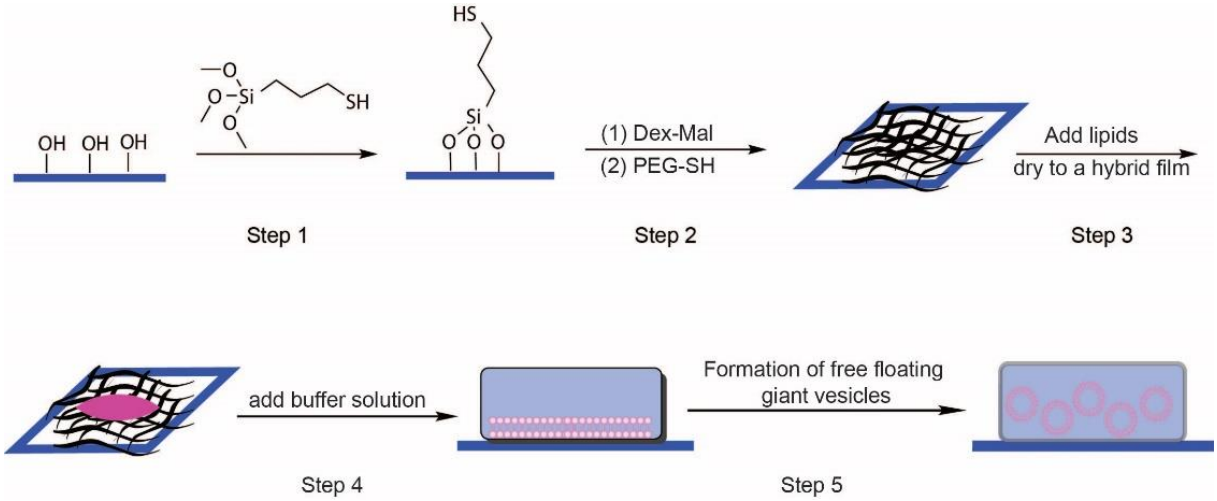

Figure 9. *Procedure of the preparation of GUVs from Dex-PEG hydrogel coated glass slide. Reproduced from ref. [16].*

The contact angle of the original, thiolated and gel-coated glass slide surfaces were measured by using the LBADSA plugin in ImageJ software. The osmolality of buffer solutions were determined from the freezing point depression using an Osmometer Roebling Type 13. The osmometer was calibrated using 100 mOsm/kg NaCl standard solution. The confocal imaging of the GUV growth was performed by a TI-Eclipse inverted microscope (Nikon, Japan) equipped with a 16-bit Cascade II 512 EMCCD camera (Photometrics, USA). Spinning-disc confocal microscopy was executed using a CSUX confocal head (Yokogawa, Japan). Illumination was provided by a 50 mW solid-state laser at 561 nm (Coherent Inc., Germany). Fluorescence was imaged through a bandpass filter centered at 595 nm. Epifluorescence was measured with a 40× objective and confocal microscopy was carried out using a 60× NA1.43 Plan-Apo Nikon oil-immersion objective. The size and yields of the obtained GUVs were visualized by a Zeiss axiovert-200 inverted microscope equipped with a Chroma TRITC and DAPI BP 445/50 fluorescence filter sets. Images were recorded with a black and white CCD camera (AxioCam NRm).

OSCILLATORY RHEOLOGY

The mechanical properties of the Dex-PEG hydrogels were measured on a DHR-2 rheometer (TA

Instruments) at 25 °C using a parallel plate-plate geometry (25 mm diameter). Solutions of Dex-Mal and PEG-SH (150 μL of each) were loaded on the bottom plate and the geometry was lowered to the gap distance of 600 μm. Time sweep measurements were performed to follow gelation process at a frequency of 1 rad s^{-1} with 1% strain. The linear viscoelastic regime (LVE) was determined for each sample using an amplitude sweep measurement at 1 rad s^{-1} from 0.1% to 100% strain. Frequency sweep measurements were conducted from 100 to 0.1 rad s^{-1} with 1% strain in the linear viscoelastic regime.

SWELLING TEST

Hydrogels (200 μL) were prepared in PBS buffer at room temperature (22 °C) according to the gelation protocol in glass vials. 2 mL PBS buffer (0.01% NaN_3, pH=7.4) was added on top of each hydrogel at room temperature. At various time points, the buffer was removed from the top of hydrogels, then each swollen hydrogel was weighed and fresh buffer was put on top afterwards. When the weight of swollen hydrogel reached a plateau, the equilibrium mass swelling ratio (q) was calculated using the equation below:

$$q = \frac{W_s}{W_d}$$

Where W_s is the equilibrium swollen weight and W_d the dry weight of the hydrogel. Each set of hydrogels were measured in triplicate.

CRYO-SCANNING ELECTRON MICROSCOPY (CRYO-SEM)

The morphologies of the hydrogels were imaged using a JEOL 6330 Cryo Field Emission Scanning Electron Microscope from the General Instrumentation Facility at Radboud University (Nijmegen, The Netherlands). 5 μL of Dex-PEG hydrogel was injected into a hollow cylindrical sample holder and immediately flash frozen in liquid nitrogen. The sample was inserted in the cold-stage of the SEM cryo-preparation chamber and cleaved to make a horizontal fracture plane. Water was sublimated during 15 minutes and the fracture plane was coated with a thin gold-palladium layer and subsequently the sample was transferred into the SEM chamber, where it remained frozen during the imaging.

REFERENCES

1. Edidin M., Lipids on the frontier: A century of cell-membrane bilayers, *Nature Reviews Molecular Cell Biology*, 2003, **4**, 414-418.
2. Zhao J., Zhao X., Jiang Z.*, et al.*, Biomimetic and bioinspired membranes: Preparation and application, *Progress in Polymer Science*, 2014, **39**, 1668-1720.
3. Chan Y.-H. M. and Boxer S. G., Model membrane systems and their applications, *Current opinion in chemical biology*, 2007, **11**, 581-587.
4. Menger F. M. and Angelova M. I., Giant vesicles: Imitating the cytological processes of cell membranes, *Accounts of chemical research*, 1998, **31**, 789-797.
5. Walde P., Cosentino K., Engel H.*, et al.*, Giant vesicles: Preparations and applications, *ChemBioChem*, 2010, **11**, 848-865.
6. Fenz S. F. and Sengupta K., Giant vesicles as cell models, *Integrative Biology*, 2012, **4**, 982-995.
7. Akashi K., Miyata H., Itoh H.*, et al.*, Preparation of giant liposomes in physiological conditions and their characterization under an optical microscope, *Biophysical Journal*, 1996, **71**, 3242-3250.
8. Angelova M. I. and Dimitrov D. S., Liposome electroformation, *Faraday discussions of the Chemical Society*, 1986, **81**, 303-311.
9. Tsumoto K., Matsuo H., Tomita M.*, et al.*, Efficient formation of giant liposomes through the gentle hydration of phosphatidylcholine films doped with sugar, *Colloid Surface B*, 2009, **68**, 98-105.
10. Bagatolli L. A., Parasassi T. and Gratton E., Giant phospholipid vesicles: Comparison among the whole lipid sample characteristics using different preparation methods: A two photon fluorescence microscopy study, *Chemistry and Physics of Lipids*, 2000, **105**, 135-147.
11. Pott T., Bouvrais H. and Meleard P., Giant unilamellar vesicle formation under physiologically relevant conditions, *Chemistry and Physics of Lipids*, 2008, **154**, 115-119.
12. Montes L. R., Alonso A., Goni F. M.*, et al.*, Giant unilamellar vesicles electroformed from native membranes and organic lipid mixtures under physiological conditions, *Biophysical Journal*, 2007, **93**, 3548-3554.
13. Horger K. S., Estes D. J., Capone R.*, et al.*, Films of agarose enable rapid formation of giant liposomes in solutions of physiologic ionic strength, *Journal of the American Chemical Society*, 2009, **131**, 1810-1819.
14. Lira R. B., Dimova R. and Rieke K. A., Giant unilamellar vesicles formed by hybrid films of agarose and lipids display altered mechanical properties, *Biophysical Journal*, 2014, **107**, 1609-1619.
15. Weinberger A., Tsai F.-C., Koenderink Gijsje H.*, et al.*, Gel-assisted formation of giant unilamellar vesicles, *Biophysical Journal*, 2013, **105**, 154-164.
16. Lopez Mora N., Hansen J. S., Gao Y.*, et al.*, Preparation of size tunable giant vesicles from cross-linked dextran(ethylene glycol) hydrogels, *Chemical Communications*, 2014, **50**, 1953-1955.
17. Nomura S.-i. M., Mizutani Y., Kurita K.*, et al.*, Changes in the morphology of cell-size liposomes in the presence of cholesterol: Formation of neuron-like tubes and liposome networks, *Biochimica et Biophysica Acta (BBA) - Biomembranes*, 2005, **1669**, 164-169.
18. Veatch S. L. and Keller S. L., Organization in lipid membranes containing cholesterol, *Physical Review Letters*, 2002, **89**.
19. Baumgart T., Hess S. T. and Webb W. W., Imaging coexisting fluid domains in biomembrane models coupling curvature and line tension, *Nature*, 2003, **425**, 821-824.
20. Peppas N. A., Ottenbrite R. M., Park K.*, et al.*, *Biomedical applications of hydrogels handbook*, Springer Science & Business Media, 2010.
21. DeForest C. A., Sims E. A. and Anseth K. S., Peptide-functionalized click hydrogels with independently

tunable mechanics and chemical functionality for 3d cell culture, *Chemistry of materials*, 2010, **22**, 4783-4790.

22. Metters A. and Hubbell J., Network formation and degradation behavior of hydrogels formed by michael-type addition reactions, *Biomacromolecules*, 2005, **6**, 290-301.
23. Mora N. L., Gao Y., Gutierrez M. G.*, et al.*, Evaluation of dextran(ethylene glycol) hydrogel films for giant unilamellar lipid vesicle production and their application for the encapsulation of polymersomes, *Soft Matter*, 2017, **13**, 5580-5588.
24. Elliott J. E. and Bowman C. N., Predicting network formation of free radical polymerization of multifunctional monomers, *Polymer Reaction Engineering*, 2002, **10**, 1-19.
25. Valkenier H., López Mora N., Kros A.*, et al.*, Visualization and quantification of transmembrane ion transport into giant unilamellar vesicles, *Angewandte Chemie International Edition*, 2015, **54**, 2137-2141.
26. Moore J. S. and Stupp S. I., Room-temperature polyesterification, *Macromolecules*, 1990, **23**, 65-70.
27. de Figueiredo R. M., Oczipka P., Frohlich R.*, et al.*, Synthesis of 4-maleimidobutyric acid and related maleimides, *Synthesis-Stuttgart*, 2008, 1316-1318.
28. Cras J. J., Rowetaitt C. A., Nivens D. A.*, et al.*, Comparison of chemical cleaning methods of glass in preparation for silanization, *Biosensors and Bioelectronics*, 1999, **14**, 683-688.

SUPPORTING INFORMATION

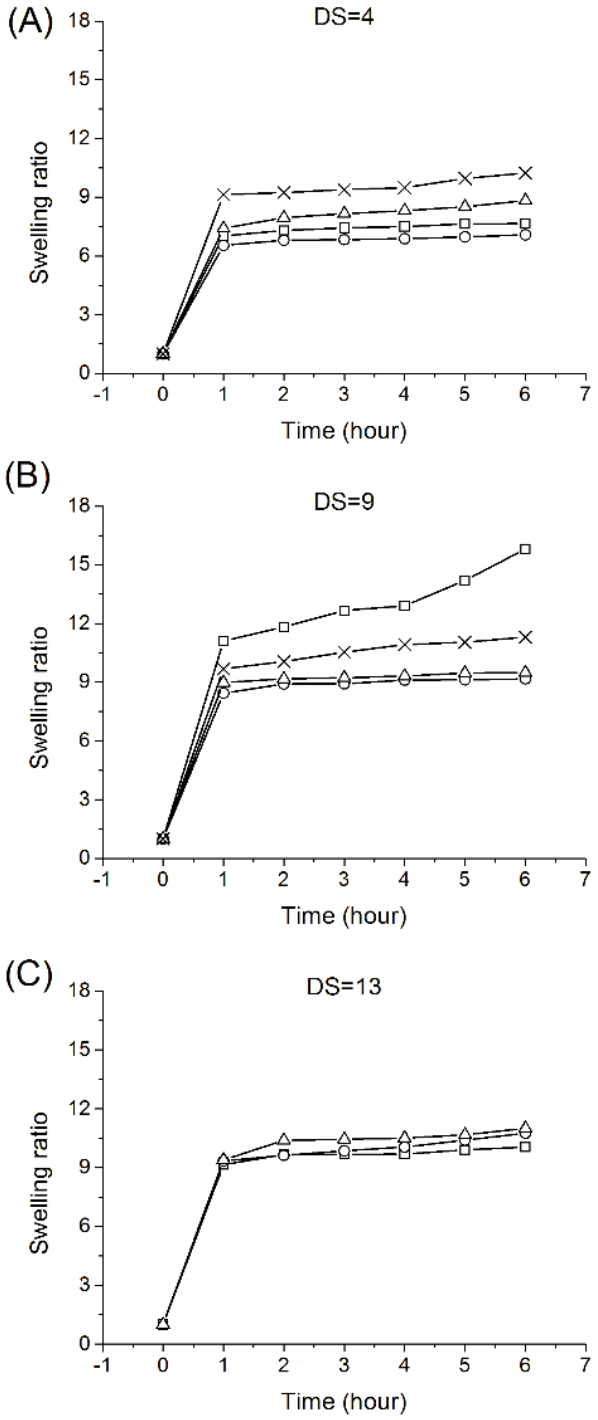

Figure S1. *Equilibrium swelling ratios of hydrogel-coated glass slides prepared with various compositions of 1% (w/v) Dex-PEG. (A) Dex70k-Mal4, (B) Dex70k -Mal9, and (C) Dex70k -Mal13 crosslinked with thiolated PEG (□: PEG2k-2SH. ○: PEG3.4k-2SH. ⊥: PEG10k-4SH. x: PEG10k-8SH) respectively.*

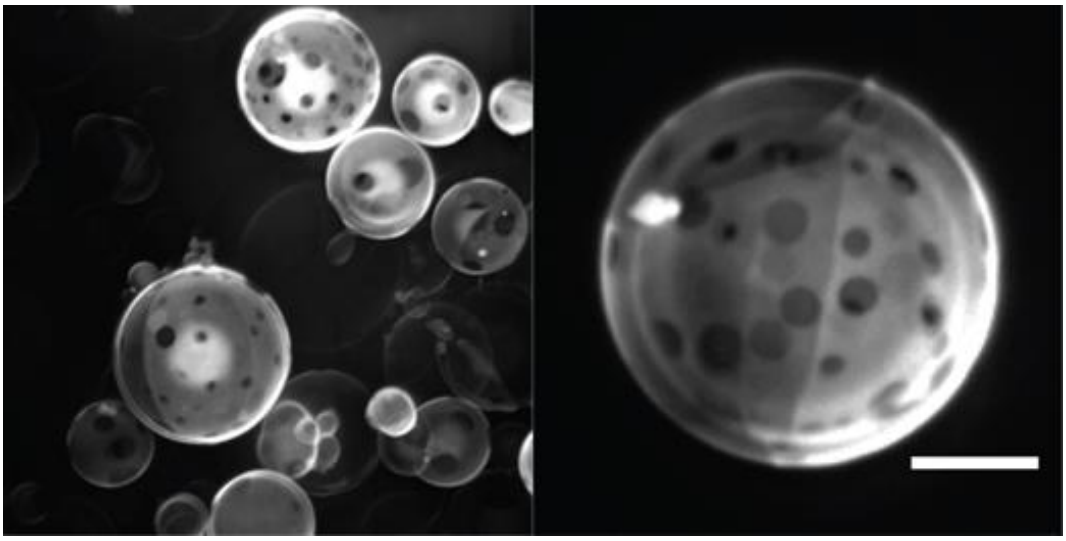

Figure S2. *Confocal microscopy Z-projections showing phase separated GUVs (lipid composition: 40% DPhPC : 40% DPPC : 20% CH, mol%) in PBS at physiological ionic strength (Scale bar: 10 μm). Images adopted from ref. [16].*

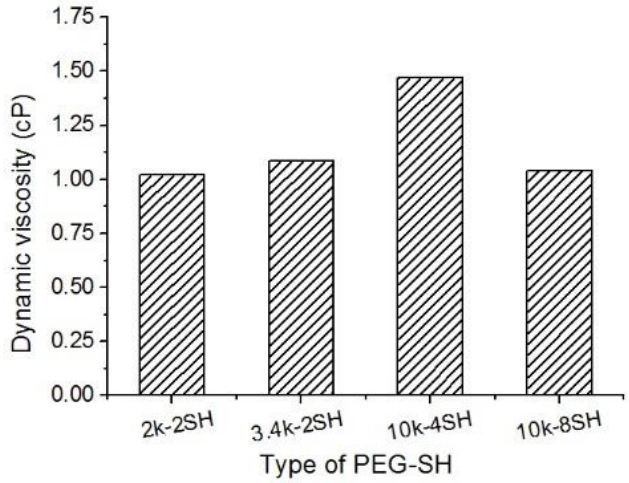

Figure S3. *Comparison of the dynamic viscosity of 0.5% (w/v) Dex70k-Mal2.5 crosslinked to PEG prepared by various thiolated PEG: PEG2k-2SH, PEG3.4k-2SH, PEG10k-4SH and PEG10k-8SH.*

CHAPTER 6

THE EFFECT OF COILED-COIL PEPTIDE CONJUGATION ON DEXTRAN SELF-ASSEMBLY

Dextran-peptide conjugates were prepared by grafting dextran polymers with a pair of coiled- coil peptides **E** and **K**. The effect of polymer conjugation on peptide conformation and coiled-coils interactions was investigated using circular dichroism (CD) spectroscopy, dynamic light scattering and fluorescence spectroscopy studies. It was found that the conformation of each peptide was altered upon bioconjugation to dextran. CD spectroscopy indicated homomeric coiled-coil formation in dextran-peptide **K** conjugates due to the high local concentration of peptide **K**. Dextran-peptide **E** and dextran-peptide **K** maintained the ability for coiled-coil formation with the complementary peptide. Upon mixing a pair of dextran-peptide **E** and dextran-peptide **K**, the hydrodynamic diameter increased to ~100 nm indicative of aggregate formation. Limited coiled-coil formation between the dextran-peptide **E** and the dextran-peptide **K** in the solution was observed, presumably because homomeric coiled-coil formation in dextran-peptide **K** conjugates and steric hindrance induced by the dextran backbones preventing efficient **E/K** coiled-coil formation.

INTRODUCTION

Bioconjugation of peptides or proteins to polymers can provide multiple benefits such as improved water solubility, enhanced stability, increased circulation time and reduced immune response.[1, 2] Moreover, by utilizing the unique structure and function of peptides or proteins, such as enzymatic activity and receptor recognition, smart hybrid materials responding to certain biological and nonbiological stimuli can be established by designing suitable polymer-peptide and/or polymer-protein conjugates.[3] Poly(ethylene glycol) (PEG) is the most commonly applied and prominent polymer in the field of bioconjugation.[4-6] PEGylation has been established as a powerful strategy to increase the serum half-life of biological molecules *in vivo* and many PEGylated drug candidates are currently in clinical trials or already on the market.[7] A drawback of PEG is its potential immunogenicity. Although PEG alone is not immunogenic, ovalbumin and some other PEGylated protein agents were found to elicit antibody formation against PEG in animal studies.[8, 9] Another drawback of the most used linear PEG is its poor loading capacity of biomolecules due to limited number of available functional groups for the bioconjugation. Multi-arm PEG precursors have been developed to introduce more functional groups. However, the number of functional groups is still limited to 8 for commercially available PEG polymers. In order to improve the biomolecule-loading-capacity of bioconjugated polymers, several alternative bioconjugate systems have been developed. Particularly, these alternative polymeric backbones provide multiple functional groups by their side chains instead of by terminal end groups of the main chain. One approach is to apply natural or synthetic polymeric backbones bearing multiple functional sites for the bioconjugation, such as polysaccharides, hydroxyethyl starch, poly(vinylpyrrolidinones) and poly(glutamic acid).[10, 11] In another approach grafted polymers were synthesized directly from peptide/protein macroinitiators by atom transfer radical polymerization (ATRP)[12-14] or reversible addition-fragmentation chain transfer (RAFT) polymerizations.[15, 16]

Dextran, a neutral polysaccharides consisting of an α-(1→6) linked D-glucose main chain, has been investigated as one of the potential alternatives for polymeric conjugates over last four decades due to its good water solubility, low toxicity, bioinertness and low immunogenicity.[5, 17-19] Dextran possesses multiple hydroxyl groups which can be applied to conjugate numerous therapeutic molecules such as drugs, peptides, enzymes, proteins, fluorescent indicators and imaging agents, resulting hybrid mixture with increased sensitivity or activity.[20-23] Typical methods for providing multiple functional groups on dextran polymers include direct esterification of hydroxyl group, periodate oxidation of dextran to produce Schiff base or its reduced form, and pre-activation of dextran by phosgene to produce carbonate or carbamate esters.[17, 18] Recently, a more flexible synthetic strategy has been developed based on the thiol Michael addition reaction.[20-22] By introducing vinyl groups (for example, maleimides, vinyl sulfones oracrylates) to dextran,

cysteinylated biomolecules can be coupled to the pre-functionalized dextran polymers in a controlled and efficient manner. The obtained multivalent biomolecule-dextran conjugates have shown improved biofunction compared to monomers and dimers of the corresponding biomolecule. For example, Morimoto reported an approximately 1000-fold increase for dextran-peptide conjugates in affinity between FLAG peptide and anti-FLAG mouse IgG1 antibody relative to the monomer.[21] Tang found that multivalent cationic peptides conjugated dextran led to achieve higher gene expression and lower cytotoxicity for gene delivery.[22] Shinchi observed improved immunostimulatory potency and pharmacodynamics by conjugating toll-like receptors to dextran.[24]

One of the basic folding motifs in natural proteins is the so-called coiled-coil motif. It is a left-handed superhelix formed through the winding of two or more right-handed α-helical peptides around each other.[25, 26] The primary amino acid sequence of coiled-coil forming peptides typically contains repetitions of seven amino acid residues (i.e. heptad repeats), which assemble to these specific noncovalent complexes in aqueous solution. Upon carefully design of the peptide sequence these self-assembled complexes can respond to external stimuli such as pH or temperature,[27] resulting them to function as "molecular switch" building blocks in reversible smart materials.[28-35] In previous work from our group, a heterodimeric coiled coil forming peptide pair comprised of peptide **E** $(EIAALEK)_3$ and peptide **K** $(KIAALKE)_3$ was used to form noncovalent triblock copolymers.[36] Reversible dissociation of the coiled coil could be induced by temperature control, resulting in the transition of rod-like micelles into spherical micelles. Moreover, the **E**/**K** coiled-coil motif was successfully used in other applications such as membrane fusion,[37-40] surface patterning[41] and drug delivery.[42]

In the present work, we investigated whether the coiled-coils binding motif could direct the interaction between dextran polymers. Two pairs of dextran-peptide **E** and dextran-peptide **K** bioconjugates were synthesized, wherein the dextran polymer was attached at the N-terminus of the peptides for one pair and at the C-terminus of the peptides for the other pair. The effect of conjugation on peptide conformation was studied by circular dichroism spectroscopy and fluorescence spectroscopy. The interaction between complementary dextran-peptide conjugates was studied by circular dichroism spectroscopy, fluorescence resonance energy transfer and dynamic light scattering measurements.

RESULTS AND DISCUSSION

SYNTHESIS OF DEXTRAN-PEPTIDE CONJUGATES

Firstly, the influence of dextran on the ability of equimolar **E**/**K** mixtures to form coiled-coil

heterodimers was studied. N-acetylated peptide **E** and dextran (M_w = 70 000 Da) were mixed in PBS (pH=7.4) to obtain a solution of 50 μM peptide **E** and 5 mg/mL dextran. Similarly, peptide **K** and dextran (M_w = 70 000 Da) were mixed in PBS (pH=7.4) to obtain a solution of 50 μM peptide **K** and 5 mg/mL dextran. Next, these solutions were mixed to obtain a solution of 50 μM peptides **E** and **K** and 5 mg/mL dextran and all solutions were analysed by circular dichroism (CD) spectroscopy (Figure 1B). For comparison peptide **E**, **K** and their equimolar mixture were also analyzed for comparison (Figure 1A). It was shown that peptide **E** adopted a predominantly random-coil conformation while peptide **K** exhibits a slightly more α-helical conformation.

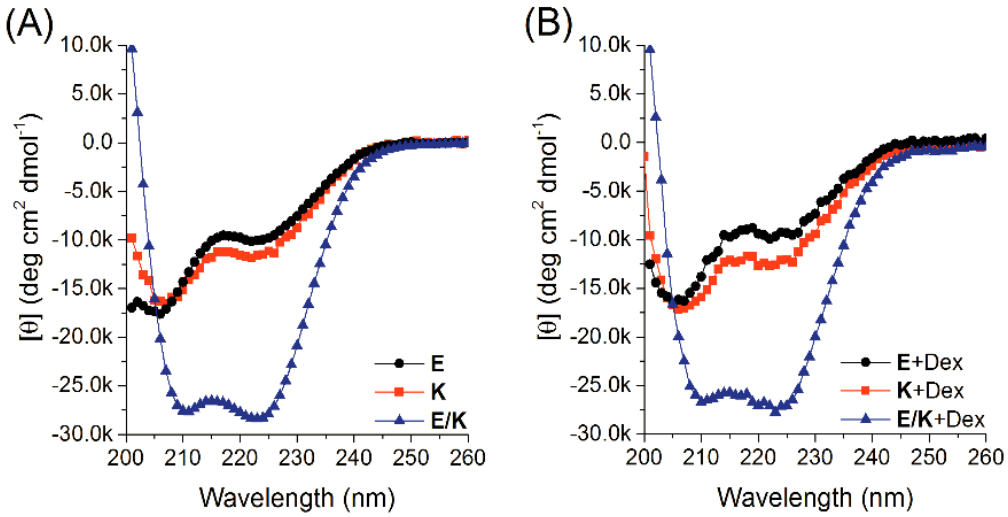

Figure 1. *Circular dichroism spectra at 25 °C of (A) peptide E, K, and their equimolar ratio E-K mixture in PBS (pH=7.4); (B) peptide E, K, and their equimolar ratio E-K mixture in presence of 5 mg/mL dextran in in PBS (pH=7.4. Total peptide concentration was kept at 50 μM in each sample.*

When peptides **E** and **K** were mixed in an equimolar ratio a significant increase in intensity at 222 nm was observed in the CD spectra, indicative of coiled-coil formation. In the presence of dextran polymers, no significant differences were observed in the CD spectra of **E**, **K** or **E/K**. The intensity at 222 nm increased upon mixing **E** and **K** in an equimolar ratio in the presence of dextran polymers, indicating that the formation of coiled-coils between peptide **E** and peptide **K** is not inhibited by the presence of this polysaccharide. However, it was noticed that the molar ellipticity at 222 nm varied slightly in each CD spectra in the presence of dextran. This variation may be related to potential hydrogen bonding between the dextran polymer and peptides **E** or **K** since unmodified glucose unit of the dextran polymer has three hydroxyl groups. This initial experiment revealed that coiled-coils formation was unaffected in presence of dextran polymers. Therefore we decided to conjugate these peptides to dextran in order to control its properties *via* coiled-coil formation.

Four dextran-peptide conjugates were synthesized using a Michael addition reaction between a

vinyl sulfone group attached to the dextran and a thiol group of the peptide (Scheme 1). One pair of the dextran-peptide conjugates consisted of **Dex-E** and **Dex-K**, wherein the N-terminus of the peptides was covalently attached to the dextran polymer. The other pair of the dextran-peptide conjugates consisted of **E-Dex** and **K-Dex**, wherein the C-terminus of the peptides was covalently attached to the dextran polymer. Dextran polymers (M_w = 70 000 Da) were functionalized with vinyl sulfone groups by a reaction between the electrophilic double bonds of divinyl sulfone and alkoxide ions of the hydroxyl groups on the dextran polymers in a 0.1M NaOH solution.[43] Using this approach, relatively stable ether linkages that can resist basic hydrolysis were formed between the dextran polymer backbone and vinyl sulfone groups, yielding vinyl sulfone grafted dextrans (**Dex-VS**). Both peptides **E** $(EIAALEK)_3$ and **K** $(KIAALKE)_3$ were synthesized with the previously reported amino acid sequences, and extended with a cysteine residue *via* a flexible oligo PEG linker.[31, 36] To facilitate the quantification of the molar peptide concentration in the dextran-peptide conjugates, a tyrosine (**Y**) was coupled to the N-terminus of peptide **E** and a tryptophan (**W**) was coupled to the N-terminus of peptide **K**. In addition, the tyrosine-tryptophan (**Y**-**W**) pair was used as a donor-acceptor couple to investigate interactions between dextran-peptide **E** and dextran-peptide **K** mixtures using fluorescence resonance energy transfer (FRET) measurements. Moreover, tetra(ethylene glycol), $(PEG)_4$, was introduced as a spacer between the peptide and dextran backbone. This $(PEG)_4$ spacer may increase the accessibility of the conjugated peptides and lower the steric hindrance of dextran influencing the formation of parallel heterodimers.[44, 45] Table 1 presents the dextran-peptide polymers used in this study, wherein the peptide sequences are written with the one-letter amino acid code.

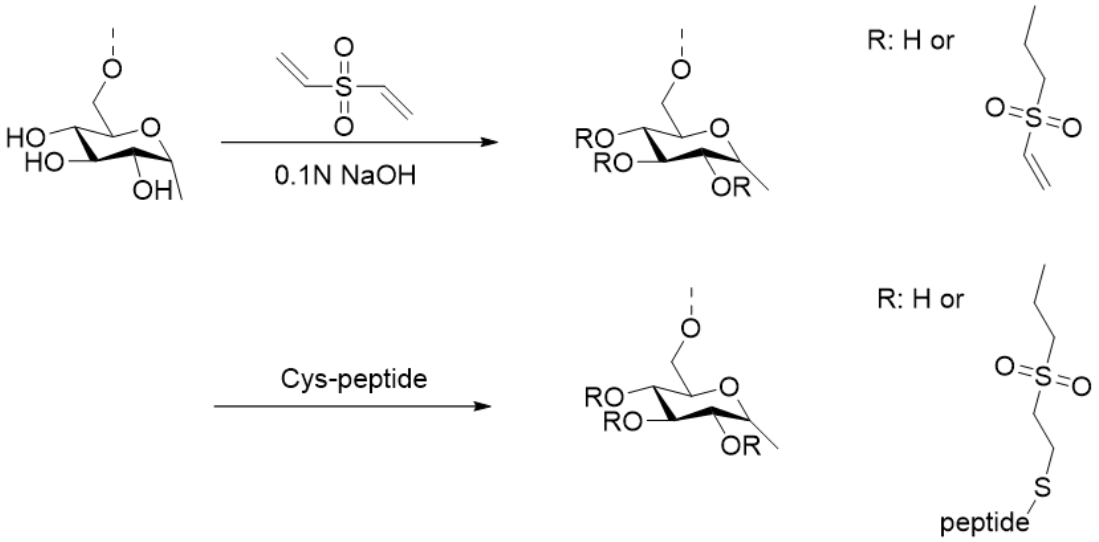

Scheme 1. *Synthesis of vinyl sulfone modified dextran (Dex-VS) and peptide-dextran conjugates.*

PROPERTIES OF DEXTRAN-PEPTIDE CONJUGATES

In CD spectra of peptide **E**, **Dex-E** and **E-Dex** shown in Figure 2A, **Dex-E** and **E-Dex** conjugates presented rather similar CD spectra with two minima centered around 208 and 222 nm respectively. Compared to peptide **E**, the intensity of the minimum at 208 nm of **Dex-E** and **E-Dex** conjugates was strongly decreased. In general, absorptions in the CD spectra between 240 nm and 190 nm relates to the peptide bonds including two types of electron transitions: an n→π* transition at around 222 nm and π→π* transitions at around 208 and 190 nm.[46, 47] Thus the secondary structure of peptide **E** was affected after conjugated to dextran polymers. Dynamic light scattering (DLS) measurements revealed for both **Dex-E** and **E-Dex** assemblies of ~10 nm in the absence of larger aggregates (Figure 3A).

Table 1. *List of prepared peptide-dextran conjugates Dex-E, Dex-K, E-Dex and K-Dex.*

Name	Sequence (from N to C terminus)[1]
Dex-K	**Dextran-VS-C-PEG$_4$-W(KIAALKE)$_3$**
Dex-E	**Dextran-VS-C-PEG$_4$-Y(EIAALEK)$_3$**
K-Dex	**W(KIAALKE)$_3$--PEG$_4$-C-VS-Dextran**
E-Dex	**Y(EIAALEK)$_3$-PEG$_4$-C-VS-Dextran**

[1]VS : vinylsulfone. PEG$_4$: tetra-ethyleneglycol

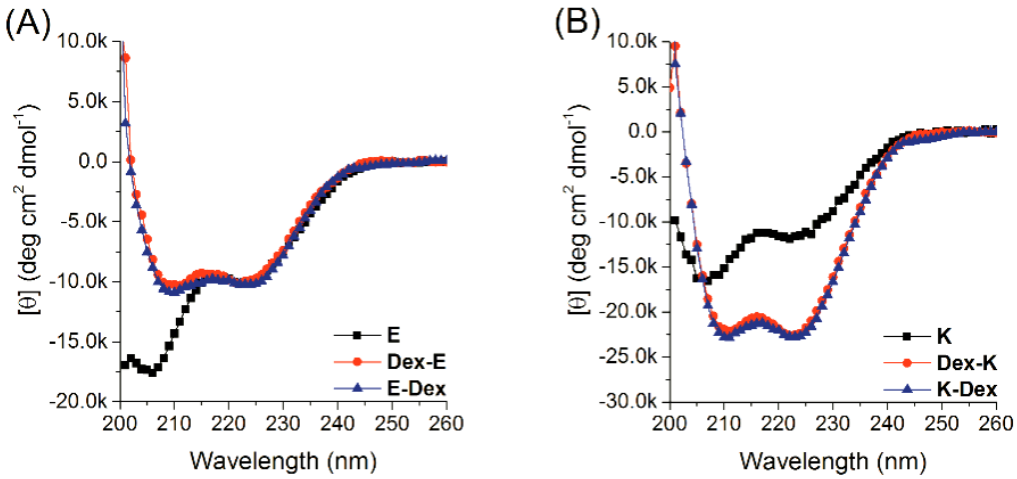

Figure 2. *Circular dichroism spectra at 25 ˚C of (A) peptide E, Dex-E and E-Dex; (B) peptide K, Dex-K and K-Dex in PBS (pH=7.4). The peptide concentration was kept at 50 μM in each sample.*

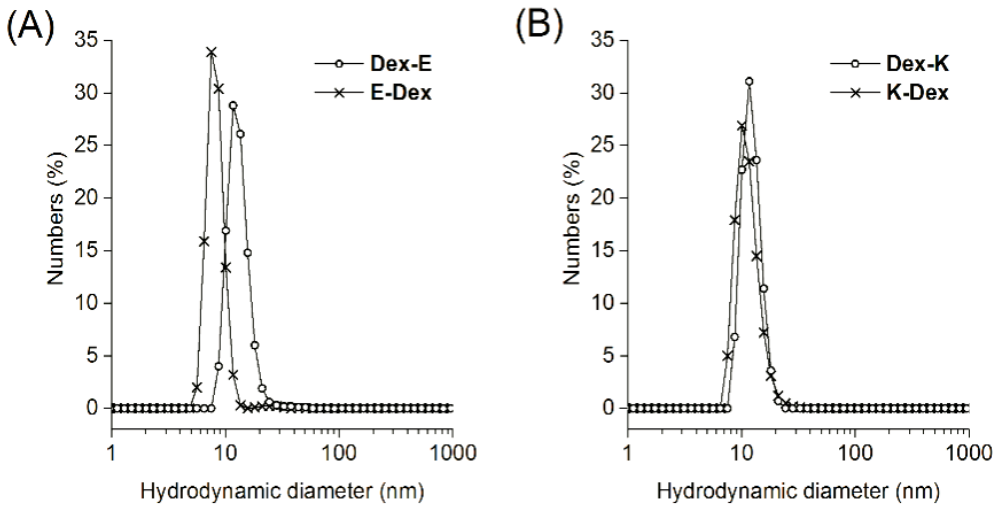

Figure 3. *DLS number distribution for (A) Dex-E and E-Dex, and (B) Dex-K and K-Dex in PBS (pH=7.4). The peptide concentration was kept at 50 μM in each sample.*

The CD spectra of **Dex-K** and **K-Dex** conjugates presented rather similar CD spectra with two minima centered around 208 and 222 nm respectively (Figure 2B). The minimum at 222 nm in the CD spectra of both **Dex-K** and **K-Dex** conjugates was enhanced dramatically compared to peptide **K**. As the molar ellipticity at 222 nm ($[\theta]_{222}$) is directly proportional to the amount of α-helical structure, the observed enhancement of $[\theta]_{222}$ points to an increase in α-helix secondary structure upon peptide conjugation to dextran.[48] The minimum at 208 nm was also enhanced for the polymer-peptide conjugates, resulting in an ellipticity ratio $[\theta]_{222}/[\theta]_{208}$ of about 1.1, indicative of coiled-coil formation.[49, 50] DLS measurements of both **Dex-K** and **K-Dex** revealed a hydrodynamic diameter of ~10 nm in the absence of larger aggregates (Figure 3B). According to the CD and DLS results of **Dex-K** and **K-Dex** conjugates, the formation of intramolecular homo coils (i.e. **K** dimerization or oligomerization) among grafted peptides **K** on the dextran backbone seems to occur.

This CD study revealed that the conformation of peptides in the aqueous solution varied significantly after conjugation to dextran polymers. When comparing this data to the CD spectra presented in Figure 1, the presence of dextran polymers alone has only a limited influence on conformation of peptides **E** and **K**. However, upon conjugation to the dextran backbone, the conformation of all four dextran-peptide conjugates was strongly influenced, which may due to a much closer distance between peptides **E** (or **K**) and the dextran backbone. This results in a relatively high local peptide concentration, which previously has shown to induce formation of homo coiled-coils.[37, 51-53]

To evaluate the coiled-coil forming potential of these four dextran-peptide conjugates in more

detail, each of **Dex-E**, **Dex-K**, **E-Dex** and **K-Dex** bioconjugates was mixed with its corresponding partner peptide **K** or **E** in an equimolar ratio and the peptide secondary structure was determined by CD spectroscopy (Figure 4A-D). The CD spectra of the resulting mixtures (i.e. **Dex-E/K**, **E-Dex/K**, **Dex-K/E** and **K-Dex/E**) indicate interactions between each dextran-peptide conjugate and its corresponding peptide partner resulting in coiled coil formation. To have a better comparison, we calculated the average CD spectra of each mixture based on the individual spectra. If dilution dominated the measured CD spectra, the estimated CD curve of the mixture solution would have a similar shape and amplitude to an average of the CD spectra of the two components. The estimated dilution curves were overlaid with the actual CD spectra of the **Dex-E/K**, **E-Dex/K**, **Dex- K/E** and **K-Dex/E** mixtures respectively.

According to the results shown in Figure 4E-H, each of the four dextran-peptide conjugates still maintains its potential for coiled-coil formation toward the complementary peptide probe. Using the **Dex-E/K** mixture as an example (Figure 4A/E), mixing **Dex-E** and **K** resulted in an amplification of $[\theta]_{222}$ and the ellipticity ratio $[\theta]_{222}/[\theta]_{208}$ increased to ~0.95. This indicates the formation of α-helical coiled-coils in the **Dex-E/K** mixture solution. Similarly, trends were observed for **E-Dex/K**, **Dex-K/E** and **K-Dex/E**.

In summary, the conformation of both peptides **E** and **K** changed upon conjugation to dextran. However, all four dextran-peptide conjugates still maintained their coiled-coil formation potential when mixed with their complementary peptide partner.

COILED-COIL FORMATION OF COMPLEMENTARY DEXTRAN-PEPTIDE CONJUGATES

Next, we investigated whether dextran-peptide **E** and dextran-peptide **K** may generate assemblies *via* coiled-coil interactions. Initially, mixtures of dextran-peptide conjugates having the dextran backbone coupled to the same terminus (i.e. N-terminus or C-terminus) were studied (i.e. **Dex-E/Dex-K** and **E-Dex/K-Dex**). The CD spectrum of **Dex-E/Dex-K** showed two minima around 208 and 222 nm respectively (Figure 4A) with $[\theta]_{222}/[\theta]_{208}$ ~1.1. As mentioned earlier, the ellipticity ratio $[\theta]_{222}/[\theta]_{208}$ of **Dex-E** was ~1 and ~1.1 for **Dex-K**, so the ellipticity ratios $[\theta]_{222}/[\theta]_{208}$ did not change significantly. Comparison to the calculated average CD spectrum assuming no interactions between **Dex-E** and **Dex-K** (Figure 5B), **E/K** interactions in the mixture are relatively weak. Surprisingly, the DLS measurements revealed the presence of larger assemblies (~100 nm) in solution for the mixture (Figure 6A), strongly suggesting that **Dex-E/Dex-K** do interact.

For the **E-Dex/K-Dex** mixture, similar trends in $[\theta]_{222}$, $[\theta]_{208}$ and the ellipticity ratio $[\theta]_{222}/[\theta]_{208}$ were observed (Figure 5C). When compared to the calculated average CD spectrum of **E-Dex** and **K-Dex**, a certain level of **E/K** interactions upon mixing equimolar **E-Dex** and **K-Dex** was

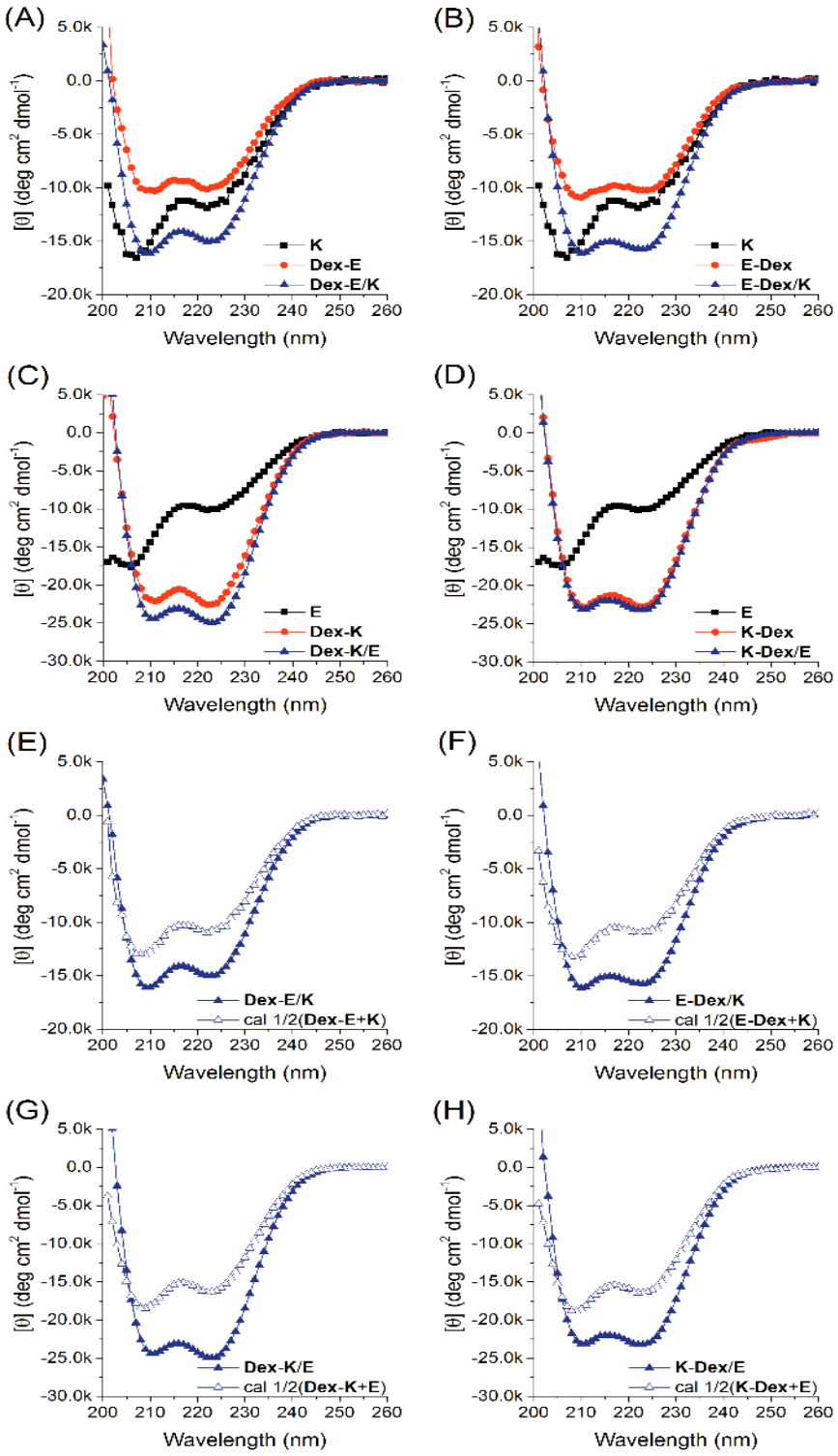

Figure 4. *Circular dichroism spectra at 25 °C of (A) peptide K, Dex-E, and Dex-E/K mixture; (B) peptide K, E-Dex, and E-Dex/K mixture; (C) peptide E, Dex-K and E/Dex-K mixture; (D) peptide E, K-Dex and E/K-Dex mixture in PBS (pH=7.4). Total peptide concentration was kept at 50 μM in each sample. In each mixture the peptide segments E and K were mixed in an equimolar ratio. Comparisons of the CD spectrum and the estimated diluting curves of (E) the Dex-E/K mixture; (F) the E-Dex/K mixture; (G) the E/Dex-K mixture; (H) the E/K-Dex mixture.*

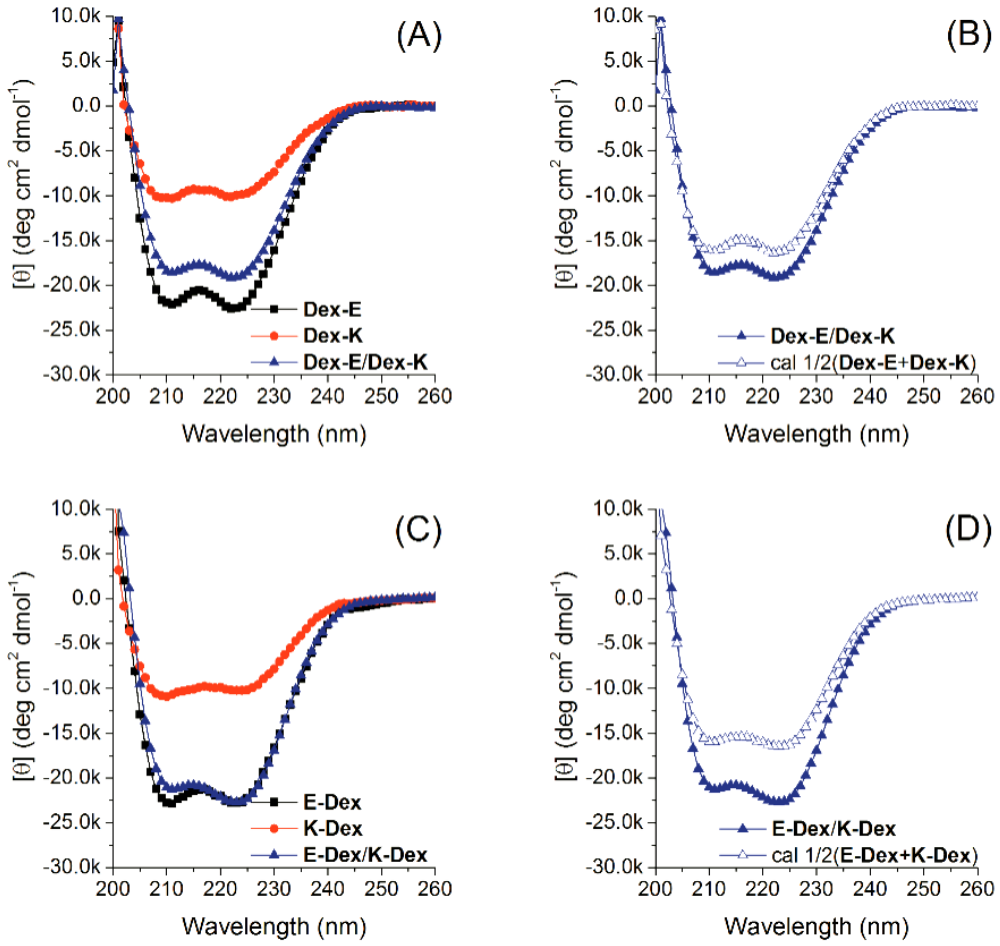

Figure 5. *Circular dichroism spectra at 25 °C of (A) Dex-E, Dex-K and the Dex-E/Dex-K mixture; (B) the Dex-E/Dex-K mixture and its estimated diluting curve; (C) E-Dex, K-Dex and the E-Dex/K-Dex mixture; (D) the E-Dex/K-Dex mixture and its estimated diluting curve. All experimental samples were prepared in PBS (pH=7.4) with a total peptide concentration at 50 μM. In each mixture the peptide segments E and K were mixed in an equimolar ratio.*

observed (Figure 5D). Moreover, DLS of the equimolar **E-Dex/K-Dex** mixture also revealed the formation of larger assemblies (>100 nm), indicating that noncovalent interactions occur (Figure 6B).

The interaction between the dextran-peptide **E** and the dextran-peptide **K** was further investigated by fluorescence spectroscopy. We utilized the tyrosine-tryptophan (**Y**-**W**) pair as a donor-acceptor couple to acquire structural information of dextran-peptide **E**/ dextran-peptide **K** mixtures using fluorescence resonance energy transfer (FRET) measurements.[54, 55] The Förster distance (R_0) for the **Y**/**W** pair is ~1.5 nm, at this distance the energy transfer efficiency between **Y** and **W** is 50%. When the distance between **Y** and **W** is on the order of or larger than $2R_0$, no energy transfer will occur.[56] Thus if parallel **E**/**K** coiled-coils occur between dextran-peptide **E** and dextran-peptide **K**, energy transfer can be observed in the emission spectrum of the mixture. Energy transfer between

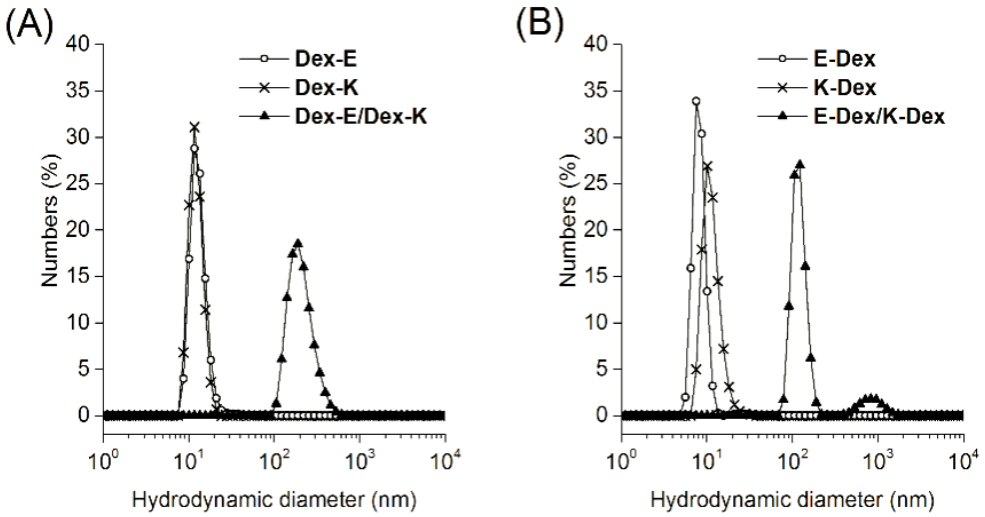

Figure 6. *DLS number distribution for (A) Dex-E, Dex-K and the Dex-E/Dex-K mixture, and (B) E-Dex, K-Dex and the E-Dex/K-Dex mixture in PBS (pH=7.4). In each mixture the peptide segments E and K were mixed in an equimolar ratio and the peptide concentration was kept at 50 μM in each sample.*

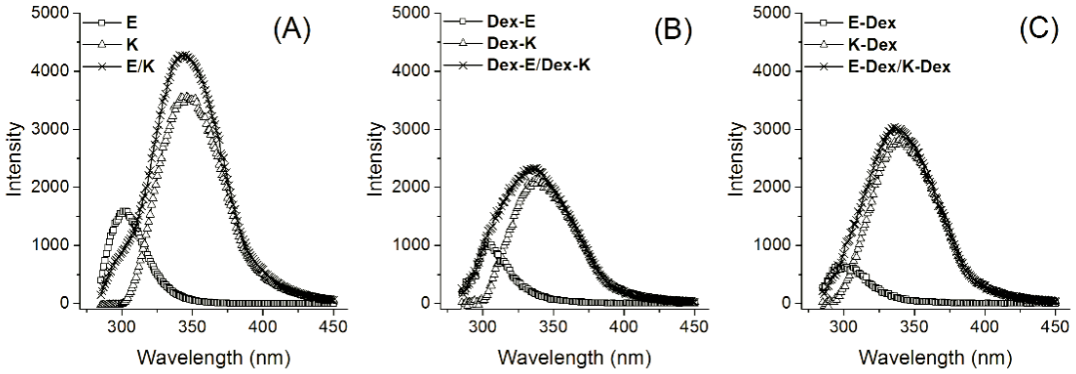

Figure 7. *Fluorescence emission spectra (excitation at 275 nm) of (A) peptide E (□), peptide K (⊿), and an equimolar mixture of peptides E and K (x); (B) Dex-E (□), Dex-K (⊿), and an equal peptide molar mixture of Dex-E and Dex-K (x); (C) E-Dex (□), K-Dex (⊿) and an equal peptide molar mixture of E-Dex and K-Dex (x) in PBS buffer (pH=7.4) at 25 °C. Each peptide concentration was kept at 50 μM.*

Y and **W** was observed for an equimolar mixture of **E** and **K** (Figure 7A). When the mixture was excited with light matching the donor **Y**'s absorption wavelength (275 nm), the presence of the acceptor **W** quenched the donor fluorescence in the emission spectrum, proving the formation of parallel coiled-coils. However in both **Dex-E**/**Dex-K** and **E-Dex/K- Dex** mixture, no quenching effect of the donor **Y** on **E-Dex** was observed (Figure 7B/C). These results seem to indicate that the distance between **Y** of **Dex-E** (or **E-Dex**) and **W** of **Dex-K** (or **K-Dex**) is on the order of or larger than $2R_0$. Thus the conjugation of peptides to the dextran backbone seems to prevent the

close proximity of peptide **E** and **K** and concomitant prevent efficient coiled coil formation.

Moreover, it was found from the fluorescence results that the conjugation of peptides to dextran backbone varies the micro-environment of the tryptophan residue (**W**). Comparison of the emission spectra of peptide **K**, **Dex-K** and **K-Dex** showed that the intensity of the emission of **K-Dex** conjugates was lower than that of peptide **K**, while the intensity of the emission of **Dex-K** conjugates was even lower than that of **K-Dex** conjugates (Figure 7). This decrease in emission intensity is indicative of a change of the environment of the tryptophan residue to a more polar environment in **Dex-K** and **K-Dex** conjugates.[57] The differences of the emission intensity between **Dex-K** and **K-Dex** conjugates might be explained by the position of the tryptophan residue relative to the dextran backbone. Considering that the tryptophan residue was coupled to the N-terminus of peptide **K** in both **Dex-K** and **K-Dex** conjugates, the tryptophan residue is in close proximity to the dextran backbone in **Dex-K** conjugates while the tryptophan residue is positioned at the far end of the grafting chain of **K-Dex** conjugates. Thus the micro-environment of the tryptophan residue of **Dex-K** conjugates seems to be more polar compared to **K-Dex** conjugates. The fluorescence results indicate changes of the micro-environment of the peptide terminus coupled to the dextran polymer, which may play a role in the interaction between the dextran-peptide **E** and the dextran-peptide **K**.

According to the CD, DLS and fluorescence data of equimolar **Dex-E**/**Dex-K** and **E-Dex**/**K-Dex** mixtures, each complementary dextran-peptide pair led to the formation of aggregates larger than 100 nm in the solution, but limited coiled-coil interactions of **E**/**K** was observed as shown by CD and FRET measurements. It is possible that coiled-coil formation is hampered by the micro-environment changes after the polymer-peptide conjugation. Also, the intramolecular homo coils of dextran-peptide **K** solution may still exist in the solution of the complementary dextran-peptide pair thereby preventing efficient heteromeric coiled-coil formation.

Regarding the **Dex-E**/**Dex-K** and the **E-Dex**/**K-Dex,** although the dextran backbones influence the grafted peptides, only a limited difference was observed. As mentioned in the introduction, coiled-coils formed by peptide **E** and **K** adopt a parallel orientation, thus the same-termini of peptide **E** and **K** are in close proximity.[53] To generate **E**/**K** coiled-coils, peptides **E** and **K** associate at their hydrophobic face (isoleucine and leucine residues at position 'a' and 'd') and are stabilized by electrostatic forces (glutamate resides for peptide **E** and lysine residues for peptide **K** at position 'e' and 'g'). To enable coiled-coils formation between the grafted peptide **E** and **K** in the **Dex-E**/**Dex-K** (or **E-Dex**/**K-Dex**) mixture, the pair of dextran-peptide conjugates need to be close enough to initiate the association between **E** and **K**. Considering the dextran backbones of each binding part are positioned at the same terminus of the conjugated peptide, the backbones of **Dex-E** and **Dex-K** (or **E-Dex**/**K-Dex**) need to be close to each other in a similar direction toward the

peptides to facilitate the parallel coiled-coils formation (Scheme 2A), which may be spatially unfavorable. Presumably, such spatial hindrance between the dextran backbones prevents the conjugates pair **Dex-E**/**Dex-K** (or **E-Dex**/**K-Dex**) from getting close to an effective distance to permit the specific interaction of the grafted peptides **E** and **K**. Therefore we studied another mixture, wherein each bioconjugate has the dextran backbone coupled to the opposite terminus of peptides (i.e. **Dex-E**/**K-Dex** and **E-Dex/Dex-K** mixtures). Here it was assumed that the spatial hindrance between the dextran backbones could be reduced in this manner, see Scheme 2B.

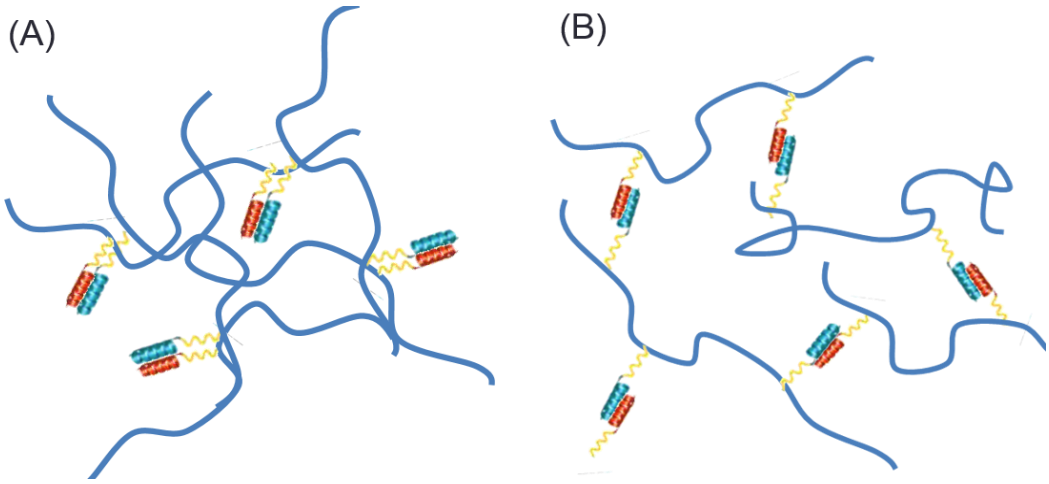

Scheme 2. *Schematic diagram of the potential coiled-coil formation between dextran-peptide conjugates: (A) Dex-E and Dex-K (or E-Dex and K-Dex); (B) Dex-E/K-Dex (or E-Dex/Dex-K).*

Figure 8A/C show the obtained CD spectra of the **Dex-E**/**K-Dex** and **E-Dex/Dex-K** mixtures respectively. Again two minima around 208 and 222 nm were observed and the calculated ellipticity ratios of $[\theta]_{222}/[\theta]_{208}$ were ~1.1 for both mixtures. Similar to the peptide-dextran conjugates discussed above, CD spectra for the mixture were calculated based on the CD spectra of individual peptide-dextran assuming no interaction occurred (Figure 8B/D). It was found that for each of the **Dex-E**/**K-Dex** and **E-Dex/Dex-K** mixtures the ellipticity at 222 nm ($[\theta]_{222}$) and the ellipticity at 208 nm ($[\theta]_{208}$) were greater than the calculated average value, indicating that some intermolecular peptide-peptide interactions occurred.

Figure 9 shows the emission spectra of the **Dex-E**/**K-Dex** and **E-Dex/Dex-K** mixtures respectively. Referring to the **Dex-E**/**K-Dex** mixture, no quenching effect of the donor **Y** in **Dex-E** was observed in presence of **K-Dex**. For the **E-Dex/Dex-K** mixture, almost no quenching effect of tyrosine **Y** in **E-Dex** was observed either. These results indicate that the distance between **Y** of **Dex-E** (or **E-Dex**) and **W** of **K-Dex** (or **Dex-K**) is on the order of or larger than $2R_0$. Thus the relative position of the dextran backbones in the complementary dextran-peptide conjugates does not influence coiled-coil formation between **E**/**K** in the present system.

DLS measurements of the equimolar **Dex-E**/**K-Dex** and **E-Dex/Dex-K** mixtures showed the

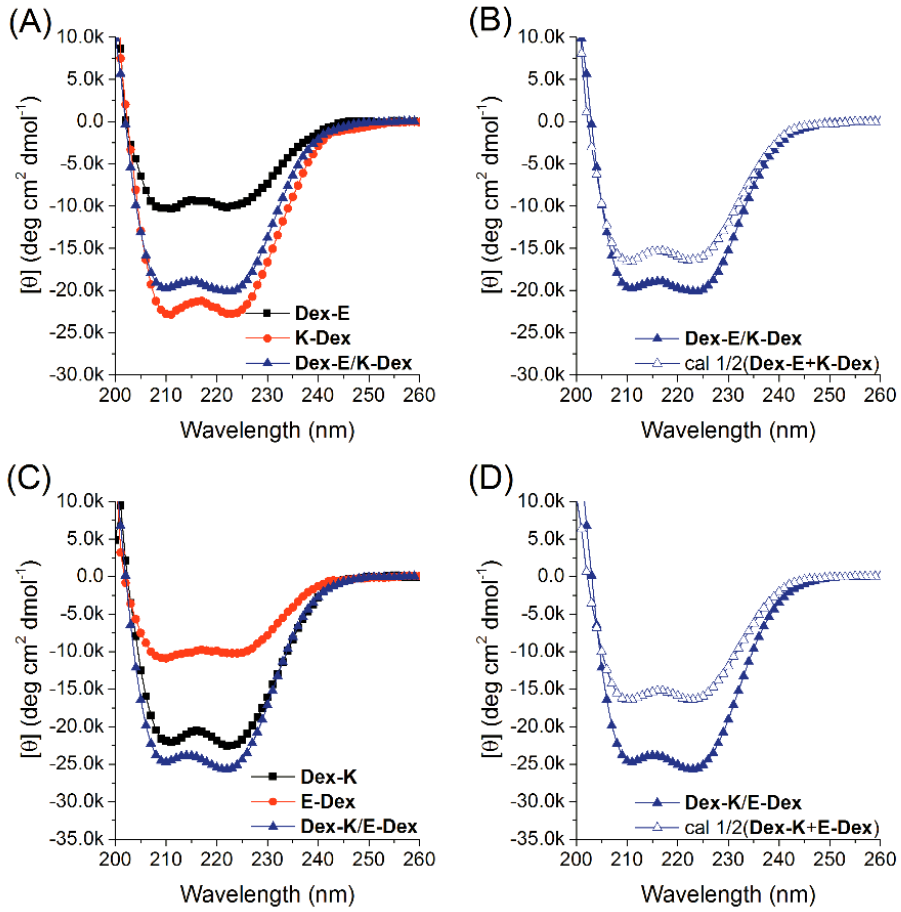

Figure 8. *Circular dichroism spectra at 25 ˚C of (A) Dex-E, K-Dex and the Dex-E/K-Dex mixture; (B) the Dex-E/K-Dex mixture and its estimated diluting curve; (C) E-Dex, Dex-K and the E-Dex/Dex-K mixture; (D) the E-Dex/Dex-K mixture and its estimated diluting curve. All experimental samples were prepared in PBS (pH=7.4) with a total peptide.*

formation of large aggregates in the solution. For both mixtures the peaks of individual dextran-peptide at 10 nm disappeared and large assemblies were observed (Figure 10). The hydrodynamic diameter of the aggregates of **Dex-E/K-Dex** (~58.8 nm) and **E-Dex/Dex-K** (~78.8 nm) were smaller as compared to **Dex-E/Dex-K** (~190.1 nm) and **E-Dex/K-Dex** (~122.4 nm). Thus the relative position of the dextran backbones in the complementary dextran-peptide conjugates influences on the size of the formed aggregates.

In summary, based on the CD, DLS and fluorescence data obtained from our four pairs of complementary dextran-peptide conjugates, formation of large aggregates between dextran-peptide **E** and dextran-peptide **K** were observed but specific coiled-coil interactions of **E/K** may not be the main driving force. It is probable that electrostatic or/and hydrophobic association contributes to the interaction between the peptide **E**-conjugated dextran and the peptide **K**-conjugated dextran and leads to the observed aggregate formation. Neither the linking direction between the peptide

and dextran nor the orientation of the complementary dextran-peptide pair resulted in significant influence on the aggregates. Based on our results and results available from literature, we will discuss the several factors that may play a role in the association of complementary dextran-peptide conjugates.

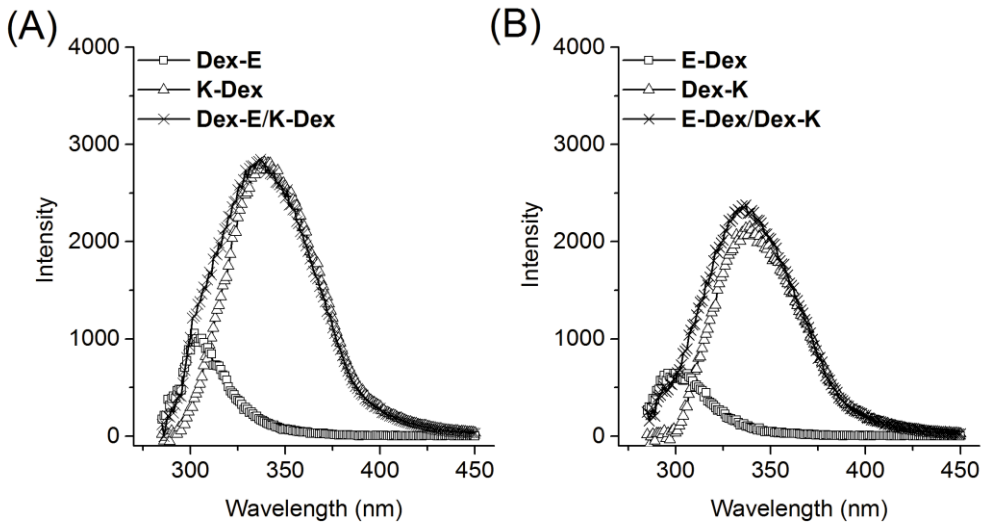

Figure 9. *Fluorescence emission spectra (excitation at 275 nm) of Dex-E (□), K-Dex (⊿), and an equal peptide molar mixture of Dex-E and K-Dex (x); (B) E-Dex (□), Dex-K (⊿) and an equal peptide molar mixture of E-Dex and Dex-K (x) in PBS buffer (pH=7.4) at 25 °C. The peptide concentration was kept at 50 μM.*

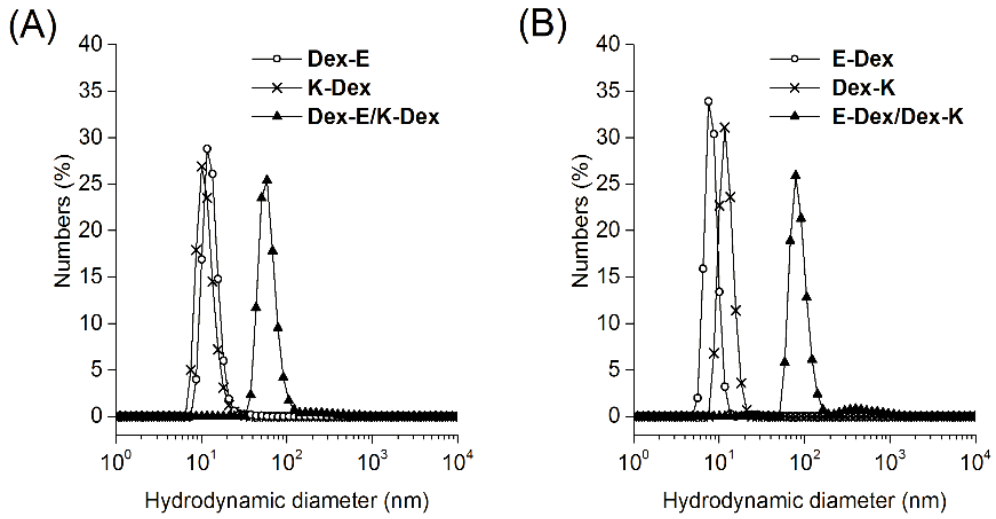

Figure 10. *DLS number distribution for (A) Dex-E, K-Dex and the Dex-E/K-Dex mixture, and (B) E-Dex, Dex-K and the E-Dex/Dex-K mixture in PBS (pH=7.4). In each mixture the peptide segments E and K were mixed in an equimolar ratio and the peptide concentration was kept at 50 μM in each sample.*

First, the conjugation of peptides **K** to dextran polymers induces the formation of homomeric coiled-coils between **K** peptides conjugated to the dextran backbones. Due to the formation of homocoils, an increase of the ellipticity at 222 nm and the ellipticity ratio $[\theta]_{222}/[\theta]_{208}$ was observed in the CD spectra of both **Dex-K** and **K-Dex** conjugates compared to the original peptide **K** (Figure 2B). These intramolecular homomeric coiled-coils seem to inhibit the dextran-peptide **K** conjugates from specific coiled-coil interactions with dextran-peptide **E** conjugates. Our results are in accordance with the finding of Gerling-Driessen et al.[58] They conjugated one or two peptides **K** to polymer backbones respectively to obtain mono-peptide **K** polymer conjugates and divalent peptide **K** polymer conjugates. Here the oligo(amido amine) polymer backbones have well-designed peptide **K** conjugation sites and two glycine resides were introduced as a linker between peptide **K** and the polymer backbone. It was shown that the divalent peptide **K** polymer conjugates formed intramolecular homocoils due to a template effect of the polymer backbone.[52] The grafted peptides are in close proximity to each other triggering intramolecular homocoils formation due to the high local peptide concentration. Formation of homo coiled-coils has also been found in peptide **K** decorated liposome systems, in which multiple peptides **K** were anchored to the surface of the lipidic membrane leading to relatively high local peptide concentration at the lipidic membrane.[37, 51]

Moreover, although homomeric coiled-coils of peptides **K** may transform into heteromeric coiled-coils between **E**/**K**, the accessibility of peptides may be crucial for the transformation process. Upon addition of the complementary peptide **E** with a 1:1 stoichiometry the homomeric coiled-coils of the grafted peptides **K** transformed into heteromeric coiled-coils between **E**/**K**, which is in accordance with the results of Gerling-Driessen et al.[58] However, when the dextran-peptide **E** conjugates (**Dex-E** or **E-Dex**) were mixed as the complementary partner, heteromeric coiled-coil formation was inhibited. Considering the difference in the hydrodynamic volume of peptide **E** and dextran-peptide **E**, it is probably that the access of the grafted peptide **E** on the dextran backbones toward the complementary peptides **K** on the dextran backbones is hampered by steric hindrance.

It is well accepted that even small changes on the design of peptide based molecules, such as adding one methyl group, can alter tertiary and quaternary structure and influence the specificity of biorecognition.[59] The presented data further suggest that dextran polymers are not optimal backbones to couple α-helical (coiled-coil) peptides able to self-assemble into coiled-coil motifs. To our knowledge, till now poly(N-(2-hydroxypropyl) methacrylamide) (polyHPMA) is the most popularly applied polymeric backbones for coupling multiple α-helical (coiled-coil) peptides for biomedical applications.[27, 28, 44, 45, 60-64] The differences between dextran and HPMA polymers may result in distinct effect on supramolecular interactions involved in the coiled-coil formation and the free energy changes upon folding.

The hydrophilic synthetic HPMA polymer family has been continuously developed and studied by Kopecek and co-workers (Scheme 3). For the coiled-coil motifs driven self-assembly systems, multivalent peptides grafted HPMA copolymers were prepared.[64-67] Klok and co-workers reported another synthetic route that includes a first step of synthesis of methacrylated peptides and then copolymerization of HPMA monomers and the methacrylated peptides *via* free radical copolymerization (FRP) or reversible addition-fragmentation chain transfer (RAFT) copolymerization.[60] These synthetic approaches provide straight carbon main chains with a majority of side chains from HPMA and a plurality of side chains terminated in desired peptides, resulting relatively well-defined structure of multivalent peptide-polymer conjugates. Particularly, the amount of peptides grafted to each polymer chain and the theoretical distribution of the peptides on each conjugates can be controlled in the design of the copolymerization. Successful formation of antiparallel and parallel heterodimeric coiled coils between a pair of peptide grafted HPMA copolymers was reported by Yang[44, 45, 61] and Wu.[62] In these studies, conjugation of the peptides did not alter the coiled-coil formation property. For these peptide grafted HPMA conjugates,[44, 45, 61-63] the amide bonds and hydroxyl groups on the side chain of the HPMA polymer were maintained after the copolymerization with other monomers, thus a certain level of hydrogen bonding, both intra- and inter-molecular hydrogen bonding between the side chains of HPMA polymers, can be anticipated in aqueous solutions of the peptide grafted HPMA conjugates.

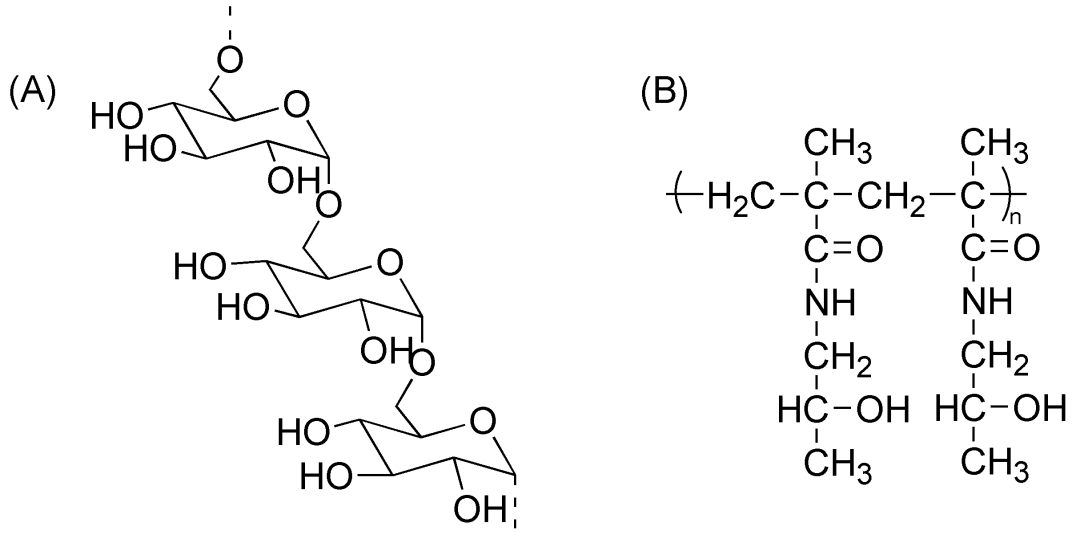

Scheme 3. *Molecular structures of (A) dextran polymers; and (B) HPMA polymers.*

Compared to HPMA, dextran consisting of an α-(1→6) linked D-glucose main chain also adopts a random coil conformation in dilute aqueous solution,[58, 59 68, 69] but dextran exhibits much stronger polymer-solvent interactions. Antoniou et al.[68] studied solvent effects on dextran conformation in various solvents and asserted that hydrogen bonding is the main interaction between dextran polymers and water molecules. Besides these secondary hydroxyl groups of dextran polymers, the

ring oxygens of the glucose unit also contribute to hydrogen bonding with neighbouring water molecules.[68, 70] For dextran-peptide conjugates the grafted peptides are proximal to the dextran backbones, which may result in hydrogen bonding between the dextran backbones and the grafted peptides thereby altering the coiled-coil formation property.

Additionally, the repeating unit of dextran is more compact than that of HPMA, which probably leads to steric hindrance. Wen et al. found that the α-(1→6) linkage of glucose units of dextran causes two adjacent glucose units form an arc instead of lying in a straight line.[71] The α-(1→6) linked architecture results in one hydroxyl group of the first glucose is at the same side of the second glucose and the other two hydroxyl groups locates in the inner side of the arc formed by the adjacent glucose units. Also, these three hydroxyl groups are directly connected to each glucose unit of the dextran polymer, which may also be too close to the glucose unit. Such structural features of the dextran polymer may partially shield the grafted peptides on the dextran backbone by the α-(1→6) linked glucose units, reducing the accessibility of the grafted peptide for further coiled-coil formation.

Last but not least, other features may also be crucial for the coiled coil formation between peptide-grafted polymers. For example, the number of heptad repeats of the conjugated peptide segment, the length and flexibility of the spacer between the peptide and the polymer backbone, the amount of peptide conjugated to each polymer, the ratio of the length of peptide segment to the length of the polymeric backbone. However, the relation between each structural element and the formation of specific coiled-coils has not been revealed yet. In summary, the influence of the conjugation on coiled-coil interaction is more complicated than we initially assumed.

CONCLUSIONS

In this chapter, dextran-peptide conjugates were synthesized by conjugating peptide **E** or peptide **K** to the hydroxyl groups of dextran polymers. Dextran was attached at both the C-terminus and the N-terminus of each peptide to study the effect of linkage on peptide behavior of dextran-peptide conjugates. It was found that the original conformation of peptides was altered after conjugated to the dextran backbone. Particularly, CD spectroscopy revealed homomeric coiled-coil formation in dextran-peptide **K** (both **Dex-K** and **K-Dex**). Although the conformation of the dextran-peptide conjugates in solution behaves different from the peptide, each of the prepared dextran-peptide conjugates maintains coiled-coil formation potential toward its complementary peptide partner, resulting in heterodimeric coiled-coil (i.e. E/K) formation. DLS measurements showed a formation of large aggregates between dextran-peptide **E** and dextran-peptide **K.** However, no conclusion was reached on the specificity of biorecognition between the peptide **E**-conjugated dextran and the peptide **K**-conjugated dextran. Probably, electrostatic or/and

hydrophobic association contributes to the interaction between the peptide **E**-conjugated dextran and the peptide **K**-conjugated dextran instead of the specific coiled-coil interaction. It seems that the coiled-coils formation between the peptide **E**-conjugated dextran and the peptide **K**-conjugated dextran is hampered due to structural features of the dextran backbone.

Although the multivalent conjugation of peptides to a polymer backbone is considered to be a simple but efficient approach for taking the advantageous of both the peptide and the polymer, the multivalent peptides conjugated to one same polymer backbone may increase local concentration of peptides thereby yielding unexpected properties of the polymer-peptide conjugates. In addition, coiled-coil formation is sensitive to the variation of the surrounding environment.[72] Dextran is generally considered as a biocompatible polymer and therefore potentially useful as a scaffold for peptide conjugation; however, the inherent structure of dextran, such as the multiple hydroxyl groups and repeating rigid glucose units, may also influence on the micro-environment of the peptide grafted on the dextran backbone. In order to utilize the coiled-coil motif for developing dextran-based assemblies, the architecture of the dextran-peptide conjugate should be designed more precisely and every building block need to be thoroughly investigated for a better understanding of the complexities of the dextran-peptide conjugates.

EXPERIMENTAL

MATERIALS

Dextran (70 kDa), divinyl sulfone (DVS), sodium hydroxide, 1,2-ethanedithiol (EDT) and triisopropylsilane (TIS), were purchased from Sigma-Aldrich. Fmoc-protected amino acids, Rink Amide resin (0.55 mmol g^{-1}) and O-(1H-6-Chlorobenzotriazole-1-yl)-1,1,3,3-tetramethyluronium hexafluorophosphate (HCTU) were purchased from NovaBioChem. Diisopropylethylamine (DIPEA), piperidine, acetic anhydride, N-methylpyrrolidine (NMP), dimethylformamide (DMF), acetonitrile, and trifluoroacetic acid (TFA) were obtained from Biosolve. All other reagents and solvents used in peptide synthesis were obtained at the highest purity available from Sigma-Aldrich. Phosphate buffered saline (PBS) was composed of 150 mM NaCl, 15 mM K_2HPO_4 and 5 mM KH_2PO_4 in H_2O at pH 7.4.

PEPTIDE SYNTHESIS

Cys-PEG_4-W$(KIAALKE)_3$ and Cys-PEG_4-Y$(EIAALEK)_3$ were synthesized by the following procedure. First, peptides $(KIAALKE)_3$ and Y$(EIAALEK)_3$ were synthesized on a CEM-Libert 1 Single Channel Microwave Peptide Synthesizer using standard Fmoc chemistry.[73] Fmoc-protected Rink amide resin (0.55 mmol g^{-1}) was used to synthesize the peptides on a 0.1 mmol scale. Fmoc

deprotection was performed using 20% (v/v) piperidine in DMF. 4 equivalents of a Fmoc-amino acid, 4 equivalents of HCTU and 8 equivalents of DIPEA in DMF were used for amino acid coupling. Then, 1.5 equivalents Fmoc-NH-PEG_4-COOH, 4 equivalents HCTU and 6 equivalents DIPEA in DMF were added to the resin overnight followed by three times Fmoc deprotection. Next, 4 equivalents of Fmoc-cysteine, 4 equivalents HCTU and 8 equivalents DIPEA in DMF were added to the resin for coupling to the PEG_4 spacer. After one Fmoc deprotection step, the N terminus of each peptide was acetylated using 5% (v/v) acetic anhydride and 6% (v/v) pyridine in DMF. The peptides were cleaved from the resin and side-chain deprotected using a mixture of TFA/water/EDT/TIS=92.5:2.5:2.5:2.5 (v/v) for 1 hour. W$(KIAALKE)_3$-PEG_4-Cys and Y$(EIAALEK)_3$-PEG_4-Cys were synthesized by a similar procedure as described above. Particularly, Fmoc-cysteine was first coupled to the resin manually followed by another manual coupling step of Fmoc-NH-PEG_4-COOH. Then the resin was put into the Peptide Synthesizer for coupling the other amino acid residues.

The cleaved peptides were precipitated in cold diethyl ether and then collected by centrifugation. Purification of the peptides was performed by RP-HPLC using a Shimadzu system including two LC-8A pumps, an SPD-10AVP UV-VIS detector and an ELSD-LTII detector. For UV detection, absorption was measured at 214 and 256 nm. The crude peptides were dissolved in H_2O containing 0.1 vol% TFA and eluted at a flow rate of 15 mL/min with a linear gradient from 20% to 80% of acetonitrile in water with 0.1% TFA (v/v) over 30 minutes. The purification was performed on an EVO C18 reversed phase column (00F-4633-P0-AX, 21.2 mm diameter, 150 mm length, 5 μm particle size). The purified peptides were lyophilized and characterized by LC-MS using a Gemini C18 analytical.

VINYL SULFONE MODIFIED DEXTRAN

Vinyl sulfone modified dextran (Dex-VS) was synthesized based on a reported procedure[74] while the reaction temperature was kept at 0 °C using an ice water bath. Dextran (1 g, 6.17 mmol) was dissolved in 50 mL of a 0.1 M NaOH aqueous solution. The dextran solution was stirred at 1 000 rpm and 2.324 mL of DVS (23.15 mmol) was added. After 1 minute, the reaction was quenched by adjusting the pH to 5 with 5 M HCl. The resulting Dex-VS was precipitated in 300 mL of cold isopropanol.. The precipitate was redissolved in Milli-Q water and then dialyzed against Milli-Q water 5 times over 3 days using a 2 000 MWCO cut-off membrane and subsequently lyophilized. Yield: 1.1 g (80.1%). ^{1}H NMR spectra were recorded on a Bruker AV-400 spectrometer. ^{1}H NMR (400 MHz, D_2O): δ 3.4-4.1 (m, dextran glucopyranosyl ring protons), 4.9 (s, dextran anomeric proton), 5.1 (s, dextran anomeric proton linked to vinyl sulfone substituents), 6.3-6.5 (m, -SO_2CH=CH_2), 6.9 -7 (m, -SO_2CH=CH_2). ^{13}C NMR (400 MHz, D_2O): δ = 97.66, 73.37, 71.38, 70.14, 69.49, 65.50 (dextran C–O), 135.82 (-SO_2CH=CH_2), 131.40 (-SO_2CH=CH_2), 54.13 (-CH_2-

CH_2-SO_2CH=CH_2).

The degree of substitution of the dextran polymer (DS) is defined as the number of vinyl sulfone groups per 100 glucopyranose residues, calculated as 100x/y, in which x is the integral of the vinyl sulfone protons (δ 6.9 -7) and y is the integral of the anomeric proton of dextran (δ 4.9) from the ^{1}H NMR spectra. The DS of the dextran polymer (Dex-VS) synthesized and applied in this work was 4.

SYNTHESIS OF DEXTRAN-PEPTIDES CONJUGATES

The peptide was dissolved in PBS (pH=7.4) at a concentration of 200 μM under a nitrogen atmosphere. A Dex-VS stock solution (10 mg/mL) in PBS was added to the peptide solution dropwise. The final molar ratio of cysteine to vinyl sulfone in the solution was kept at 2. The mixture was stirred at 500 rpm at room temperature under nitrogen protection overnight. The resulting dextran-peptide **E** and dextran-peptide **K** conjugates were purified by Amicon Ultra 4ml centrifugal filters (10 kDa). During the centrifugal purification process, dextran-peptide conjugate stayed in the filter while unreacted peptides passed through the filter with PBS, then fresh PBS buffer was added into the filter for further purification until no UV absorption (280 nm) was detected in the elution using an Agilent Cary 300 UV-Vis spectroscopy. Then the dextran-peptide conjugate was diluted in Milli-Q water and purified by dialysis against Milli-Q water five times over three days (Dialysis float tubing, MWCO 3.5 – 5 kDa) membrane and subsequently lyophilized. The obtained products were stored at -20 °C.

The peptide percentage of each dextran-peptide conjugate was quantified by the following steps and the results are shown in Table 2. First, a stock solution of the obtained dextran-peptide (e.g. 1 mg/mL) was prepared. Next, the molar peptide concentration of the stock solution was determined by UV absorbance at 280 nm using molar extinction coefficients of ε = 1 280 $M^{-1}cm^{-1}$ per tyrosine residue and ε = 5 690 $M^{-1}cm^{-1}$ per tryptophan residue.[75] The weight of peptides in the corresponding dextran-peptide solution was then calculated by multiplying the determined peptide molar concentration and the molecular weight of the corresponding peptide. Thus dividing the weight of peptides by the weight of dextran-peptide conjugates resulted in the peptide weight percent (wt%) of the prepared dextran-peptide conjugate. The number of peptides per dextran polymer was estimated by the following equation:

$$\frac{[weight\ of\ peptide]}{[Mw\ of\ peptide]} \Big/ \frac{[weight\ of\ dextran-peptide]-[weight\ of\ peptide]}{[Mw\ of\ dextran\ backbone]}$$

Table 2. *Quantification of peptide grafted on the prepared dextran-peptide conjugates.*

Sample	Peptide conc.(μM) in 1 mg/mL Dex-peptide solution	Peptide wt% of the dextran-peptide conjugate	Number of peptides per dextran polymer
Dex-E	102.3	24%	9
Dex-K	98.5	23%	9
E-Dex	91.9	21%	8
K-Dex	88.6	20%	8

CIRCULAR DICHROISM SPECTROSCOPY

CD spectra were obtained using a Jasco J-815 CD spectrometer. Wavelength scans were obtained from 260 to 190 nm using a quartz cuvette with 0.1 cm path length, averaging 5 scans with scanning speed 20 nm/s at 25 °C. The ellipticity is given as the mean residue molar ellipticity, $[\theta]$, calculated from $[\theta] = (\theta_{obs} \times MRW)/(10 \times l \times c)$, where $\boldsymbol{\theta}_{obs}$ is the observed ellipticity in millidegrees, MRW is the mean residue molecular weight (i.e. the molecular weight of the peptide divided by the number of amino acid residues), $\boldsymbol{l}$ is the path length of the cuvette in cm and $\boldsymbol{c}$ is the peptide concentration in mg mL^{-1}. The peptide concentration was kept at 50 μM in each sample.

FLUORESCENT SPECTROSCOPY

Fluorescence was measured by a Tecan infinite M1000 pro plate reader with Black Greiner 96-well plates. The excitation wavelength was set to 275 nm, and the emission was recorded in the range of 300 nm to 450 nm. The bandwidth for excitation was 5 nm and the bandwidth for emission was 10 nm. Each peptide concentration was kept at 50 μM. For each measurement, 3 scans at 25 ˚C were performed and averaged.

REFERENCES

1. Pelegri-O'Day E. M., Lin E.-W. and Maynard H. D., Therapeutic protein–polymer conjugates: Advancing beyond pegylation, *Journal of the American Chemical Society*, 2014, **136**, 14323-14332.
2. Klok H.-A., Peptide/protein− synthetic polymer conjugates: Quo vadis, *Macromolecules*, 2009, **42**, 7990-8000.
3. Cobo I., Li M., Sumerlin B. S.*, et al.*, Smart hybrid materials by conjugation of responsive polymers to biomacromolecules, *Nature materials*, 2015, **14**, 143-159.
4. Veronese F. M., Peptide and protein pegylation: A review of problems and solutions, *Biomaterials*, 2001, **22**, 405-417.
5. Khandare J. and Minko T., Polymer–drug conjugates: Progress in polymeric prodrugs, *Progress in Polymer Science*, 2006, **31**, 359-397.
6. Gauthier M. A. and Klok H.-A., Peptide/protein–polymer conjugates: Synthetic strategies and design concepts, *Chemical Communications*, 2008, 2591-2611.
7. Greg T., Academic Press Inc, 2008.
8. Garay R. P., Elgewely R., Armstrong J. K.*, et al.*, Antibodies against polyethylene glycol in healthy subjects and in patients treated with peg-conjugated agents, *Expert Opinion on Drug Delivery*, 2012, **9**, 1319-1323.
9. Schellekens H., Hennink W. E. and Brinks V., The immunogenicity of polyethylene glycol: Facts and fiction, *Pharmaceutical Research*, 2013, **30**, 1729-1734.
10. Basu A., Kunduru K. R., Abtew E.*, et al.*, Polysaccharide-based conjugates for biomedical applications, *Bioconjugate Chemistry*, 2015, **26**, 1396-1412.
11. Day E. M. P., Lin E. and Maynard H. D., Therapeutic protein-polymer conjugates: Advancing beyond pegylation, *Journal of the American Chemical Society*, 2014, **136**, 14323-14332.
12. Bontempo D. and Maynard H. D., Streptavidin as a macroinitiator for polymerization: *In situ* protein-polymer conjugate formation, *Journal of the American Chemical Society*, 2005, **127**, 6508-6509.
13. Heredia K. L., Bontempo D., Ly T.*, et al.*, *In situ* preparation of protein-"smart" polymer conjugates with retention of bioactivity, *Journal of the American Chemical Society*, 2005, **127**, 16955-16960.
14. Ten Cate M. G., Severin N. and Börner H. G., Self-assembling peptide-polymer conjugates comprising (d-alt-l)-cyclopeptides as aggregator domains, *Macromolecules*, 2006, **39**, 7831-7838.
15. Boyer C., Bulmus V., Liu J.*, et al.*, Well-defined protein-polymer conjugates via *in situ* raft polymerization, *Journal of the American Chemical Society*, 2007, **129**, 7145-7154.
16. Liu J., Bulmus V., Herlambang D. L.*, et al.*, *In situ* formation of protein–polymer conjugates through reversible addition fragmentation chain transfer polymerization, *Angewandte Chemie International Edition*, 2007, **46**, 3099-3103.
17. Larsen C., Dextran prodrugs—structure and stability in relation to therapeutic activity, *Advanced Drug Delivery Reviews*, 1989, **3**, 103-154.
18. Mehvar R., Dextrans for targeted and sustained delivery of therapeutic and imaging agents, *Journal of controlled release*, 2000, **69**, 1-25.
19. Heinze T., Liebert T., Heublein B.*, et al.*, in *Polysaccharides ii*, Springer, 2006, pp. 199-291.
20. Richter M., Chakrabarti A., Ruttekolk I. R.*, et al.*, Multivalent design of apoptosis‐inducing bid‐bh3 peptide–oligosaccharides boosts the intracellular activity at identical overall peptide concentrations, *Chem-Eur J*, 2012, **18**, 16708-16715.
21. Morimoto J., Sarkar M., Kenrick S.*, et al.*, Dextran as a generally applicable multivalent scaffold for improving immunoglobulin-binding affinities of peptide and peptidomimetic ligands, *Bioconjugate chemistry*, 2014, **25**, 1479-1491.

22. Tang Q., Cao B., Lei X.*, et al.*, Dextran–peptide hybrid for efficient gene delivery, *Langmuir*, 2014, **30**, 5202-5208.
23. Gaowa A., Horibe T., Kohno M.*, et al.*, Enhancement of anti-tumor activity of hybrid peptide in conjugation with carboxymethyl dextran via disulfide linkers, *European Journal of Pharmaceutics and Biopharmaceutics*, 2015, **92**, 228-236.
24. Shinchi H., Crain B., Yao S.*, et al.*, Enhancement of the immunostimulatory activity of a tlr7 ligand by conjugation to polysaccharides, *Bioconjugate Chemistry*, 2015, **26**, 1713-1723.
25. Lupas A., Van Dyke M. and Stock J., Predicting coiled coils from protein sequences, *Science*, 1991, **252**, 1162-1164.
26. Burkhard P., Stetefeld J. and Strelkov S. V., Coiled coils: A highly versatile protein folding motif, *Trends in cell biology*, 2001, **11**, 82-88.
27. Wang C., Stewart R. J. and Kopecek J., Hybrid hydrogels assembled from synthetic polymers and coiled-coil protein domains, *Nature*, 1999, **397**, 417-420.
28. Kopeček J. and Yang J., Peptide-directed self-assembly of hydrogels, *Acta biomaterialia*, 2009, **5**, 805-816.
29. Adams D. J. and Topham P. D., Peptide conjugate hydrogelators, *Soft Matter*, 2010, **6**, 3707-3721.
30. Apostolovic B., Danial M. and Klok H.-A., Coiled coils: Attractive protein folding motifs for the fabrication of self-assembled, responsive and bioactive materials, *Chemical Society Reviews*, 2010, **39**, 3541-3575.
31. Robson Marsden H. and Kros A., Self‐assembly of coiled coils in synthetic biology: Inspiration and progress, *Angewandte Chemie International Edition*, 2010, **49**, 2988-3005.
32. Boyle A. L. and Woolfson D. N., De novo designed peptides for biological applications, *Chemical Society Reviews*, 2011, **40**, 4295-4306.
33. Petkau-Milroy K. and Brunsveld L., Supramolecular chemical biology; bioactive synthetic self-assemblies, *Organic & biomolecular chemistry*, 2013, **11**, 219-232.
34. Hamley I. W., Peptide nanotubes, *Angewandte Chemie International Edition*, 2014, **53**, 6866-6881.
35. Kopeček J. and Yang J., Smart self‐assembled hybrid hydrogel biomaterials, *Angewandte Chemie International Edition*, 2012, **51**, 7396-7417.
36. Marsden H. R., Korobko A. V., van Leeuwen E. N.*, et al.*, Noncovalent triblock copolymers based on a coiled-coil peptide motif, *Journal of the American Chemical Society*, 2008, **130**, 9386-9393.
37. Robson Marsden H., Elbers N. A., Bomans P. H.*, et al.*, A reduced snare model for membrane fusion, *Angewandte Chemie International Edition*, 2009, **48**, 2330-2333.
38. Zheng T., Voskuhl J., Versluis F.*, et al.*, Controlling the rate of coiled coil driven membrane fusion, *Chemical Communications*, 2013, **49**, 3649-3651.
39. Zope H. R., Versluis F., Ordas A.*, et al.*, *In vitro* and *in vivo* supramolecular modification of biomembranes using a lipidated coiled‐coil motif, *Angewandte Chemie International Edition*, 2013, **52**, 14247-14251.
40. Versluis F., Voskuhl J., van Kolck B.*, et al.*, *In situ* modification of plain liposomes with lipidated coiled coil forming peptides induces membrane fusion, *Journal of the American Chemical Society*, 2013, **135**, 8057-8062.
41. Voskuhl J., Wendeln C., Versluis F.*, et al.*, Immobilization of liposomes and vesicles on patterned surfaces by a peptide coiled‐coil binding motif, *Angewandte Chemie International Edition*, 2012, **51**, 12616-12620.
42. Martelli G., Zope H. R., Capell M. B.*, et al.*, Coiled-coil peptide motifs as thermoresponsive valves for mesoporous silica nanoparticles, *Chemical Communications*, 2013, **49**, 9932-9934.
43. Yu Y. and Chau Y., One-step "click" method for generating vinyl sulfone groups on hydroxyl-containing water-soluble polymers, *Biomacromolecules*, 2012, **13**, 937-942.
44. Yang J. Y., Xu C. Y., Wang C.*, et al.*, Refolding hydrogels self-assembled from n-(2-hydroxypropyl)methacrylamide graft copolymers by antiparallel coiled-coil formation, *Biomacromolecules*, 2006,

7, 1187-1195.

45. Yang J., Wu K., Konak C.*, et al.*, Dynamic light scattering study of self-assembly of hpma hybrid graft copolymers, *Biomacromolecules*, 2008, **9**, 510-517.
46. Kelly S. M., Jess T. J. and Price N. C., How to study proteins by circular dichroism, *Biochimica et Biophysica Acta*, 2005, **1751**, 119-139.
47. Miles A. J. and Wallace B. A., Circular dichroism spectroscopy of membrane proteins, *Chemical Society Reviews*, 2016, **45**, 4859-4872.
48. Gans P. J., Lyu P., Manning M. C.*, et al.*, The helix-coil transition in heterogeneous peptides with specific side-chain interactions: Theory and comparison with cd spectral data, *Biopolymers*, 1991, **31**, 1605-1614.
49. Su J. Y., Hodges R. S. and Kay C. M., Effect of chain length on the formation and stability of synthetic .Alpha.-helical coiled coils, *Biochemistry*, 1994, **33**, 15501-15510.
50. Pandya M. J., Cerasoli E., Joseph A.*, et al.*, Sequence and structural duality: Designing peptides to adopt two stable conformations, *Journal of the American Chemical Society*, 2004, **126**, 17016-17024.
51. Marsden H. R., Korobko A. V., Zheng T.*, et al.*, Controlled liposome fusion mediated by snare protein mimics, *Biomaterials Science*, 2013, **1**, 1046-1054.
52. Mutter M., Altmann E., Altmann K.*, et al.*, The construction of new proteins. Part iii. Artificial folding units by assembly of amphiphilic secondary structures on a template, *Helvetica Chimica Acta*, 1988, **71**, 835-847.
53. Zheng T., Boyle A. L., Marsden H. R.*, et al.*, Probing coiled-coil assembly by paramagnetic nmr spectroscopy, *Organic and Biomolecular Chemistry*, 2015, **13**, 1159-1168.
54. Wu P. G. and Brand L., Resonance energy transfer: Methods and applications, *Analytical Biochemistry*, 1994, **218**, 1-13.
55. Sapsford K. E., Berti L. and Medintz I. L., Materials for fluorescence resonance energy transfer analysis: Beyond traditional donor–acceptor combinations, *Angewandte Chemie International Edition*, 2006, **45**, 4562-4589.
56. Eisenhawer M., Cattarinussi S., Kuhn A.*, et al.*, Fluorescence resonance energy transfer shows a close helix-helix distance in the transmembrane m13 procoat protein, *Biochemistry*, 2001, **40**, 12321-12328.
57. Eftink M. R., in *Methods of biochemical analysis*, John Wiley & Sons, Inc., 2006, pp. 127-205.
58. Gerling-Driessen U. I., Mujkic-Ninnemann N., Ponader D.*, et al.*, Exploiting oligo (amido amine) backbones for the multivalent presentation of coiled-coil peptides, *Biomacromolecules*, 2015, **16**, 2394-2402.
59. Mason J. M. and Arndt K. M., Coiled coil domains: Stability, specificity, and biological implications, *ChemBioChem*, 2004, **5**, 170-176.
60. Apostolovic B., Deacon S. P. E., Duncan R.*, et al.*, Hybrid polymer therapeutics incorporating bioresponsive, coiled coil peptide linkers, *Biomacromolecules*, 2010, **11**, 1187-1195.
61. Yang J., Xu C., Kopeckova P.*, et al.*, Hybrid hydrogels self‐assembled from hpma copolymers containing peptide grafts, *Macromolecular Bioscience*, 2006, **6**, 201-209.
62. Wu K., Yang J., Koňak C.*, et al.*, Novel synthesis of hpma copolymers containing peptide grafts and their self‐assembly into hybrid hydrogels, *Macromolecular Chemistry and Physics*, 2008, **209**, 467-475.
63. Dusek K., Duskovasmrckova M., Yang J.*, et al.*, Coiled-coil hydrogels. Effect of grafted copolymer composition and cyclization on gelation, *Macromolecules*, 2009, **42**, 2265-2274.
64. Pan H., Yang J., Kopeckova P.*, et al.*, Backbone degradable multiblock n-(2-hydroxypropyl)methacrylamide copolymer conjugates via reversible addition fragmentation chain transfer polymerization and thiol-ene coupling reaction, *Biomacromolecules*, 2011, **12**, 247-252.
65. Luo K., Yang J., Kopeckova P.*, et al.*, Biodegradable multiblock poly[n-(2-hydroxypropyl)methacrylamide] via reversible addition−fragmentation chain transfer polymerization and click chemistry, *Macromolecules*, 2011, **44**, 2481-2488.

66. Yang J., Luo K., Pan H.*, et al.*, Synthesis of biodegradable multiblock copolymers by click coupling of raft-generated heterotelechelic polyhpma conjugates, *Reactive & Functional Polymers*, 2011, **71**, 294-302.
67. Kopecek J., Polymer-drug conjugates: Origins, progress to date and future directions, *Advanced Drug Delivery Reviews*, 2013, **65**, 49-59.
68. Antoniou E., Buitrago C. F., Tsianou M.*, et al.*, Solvent effects on polysaccharide conformation, *Carbohydrate Polymers*, 2010, **79**, 380-390.
69. Antoniou E. and Tsianou M., Solution properties of dextran in water and in formamide, *Journal of Applied Polymer Science*, 2012, **125**, 1681-1692.
70. Suzuki T. and Sota T., Improving ab initio infrared spectra of glucose-water complexes by considering explicit intermolecular hydrogen bonds, *Journal of Chemical Physics*, 2003, **119**, 10133-10137.
71. Wen H., Morris K. R. and Park K., Hydrogen bonding interactions between adsorbed polymer molecules and crystal surface of acetaminophen, *Journal of Colloid and Interface Science*, 2005, **290**, 325-335.
72. Rabe M., Aisenbrey C., Pluhackova K.*, et al.*, A coiled-coil peptide shaping lipid bilayers upon fusion, *Biophysical Journal*, 2016, **111**, 2162-2175.
73. Palasek S. A., Cox Z. J. and Collins J. M., Limiting racemization and aspartimide formation in microwave-enhanced fmoc solid phase peptide synthesis, *Journal of Peptide Science*, 2007, **13**, 143-148.
74. Yu Y. and Chau Y., One-step "click" method for generating vinyl sulfone groups on hydroxyl-containing water-soluble polymers, *Biomacromolecules*, 2012, **13**, 937-942.
75. Gill S. C. and von Hippel P. H., Calculation of protein extinction coefficients from amino acid sequence data, *Analytical Biochemistry*, 1989, **182**, 319-326.

SUPPORTING INFORMATION

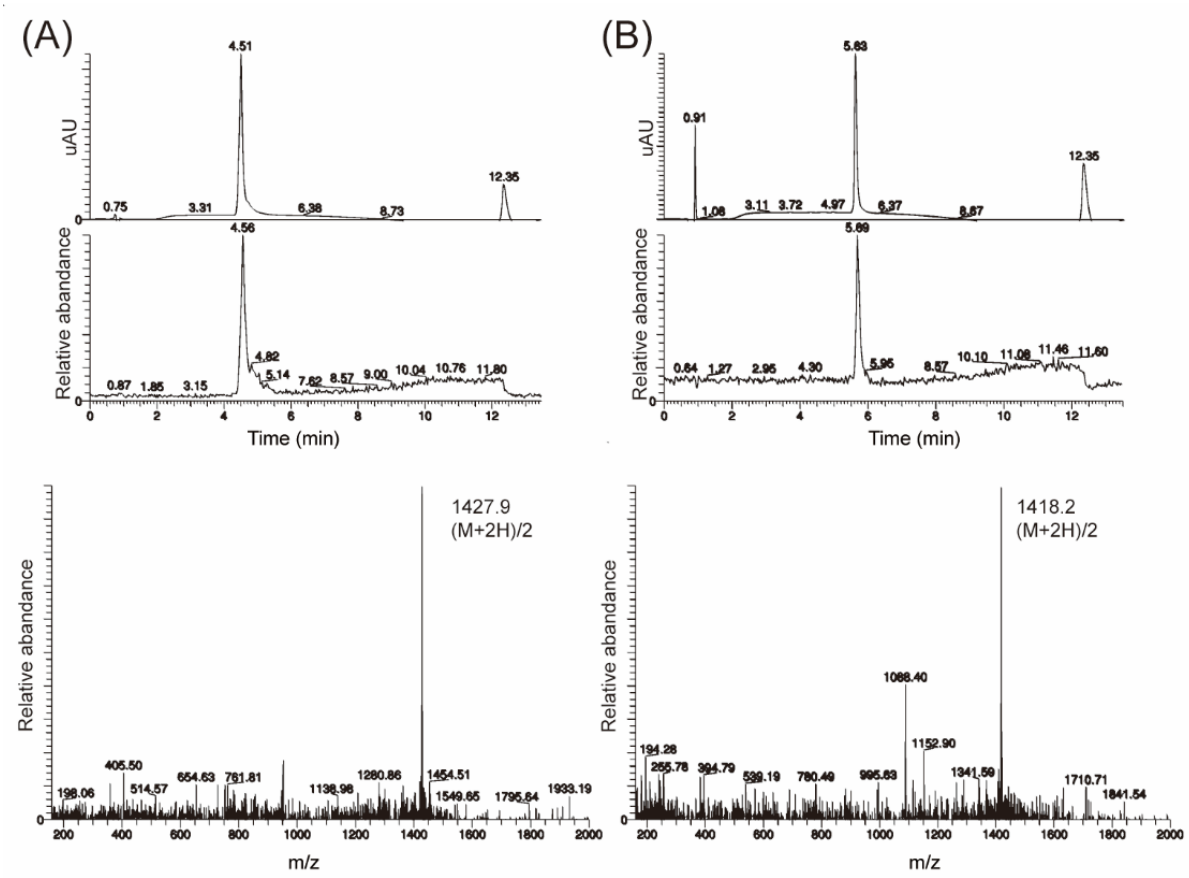

Figure S1. *LC-MS spectra of purified (A) Cys-PEG₄-W(KIAALKE)₃ and (B) Cys-PEG₄-Y(EIAALEK)₃.*

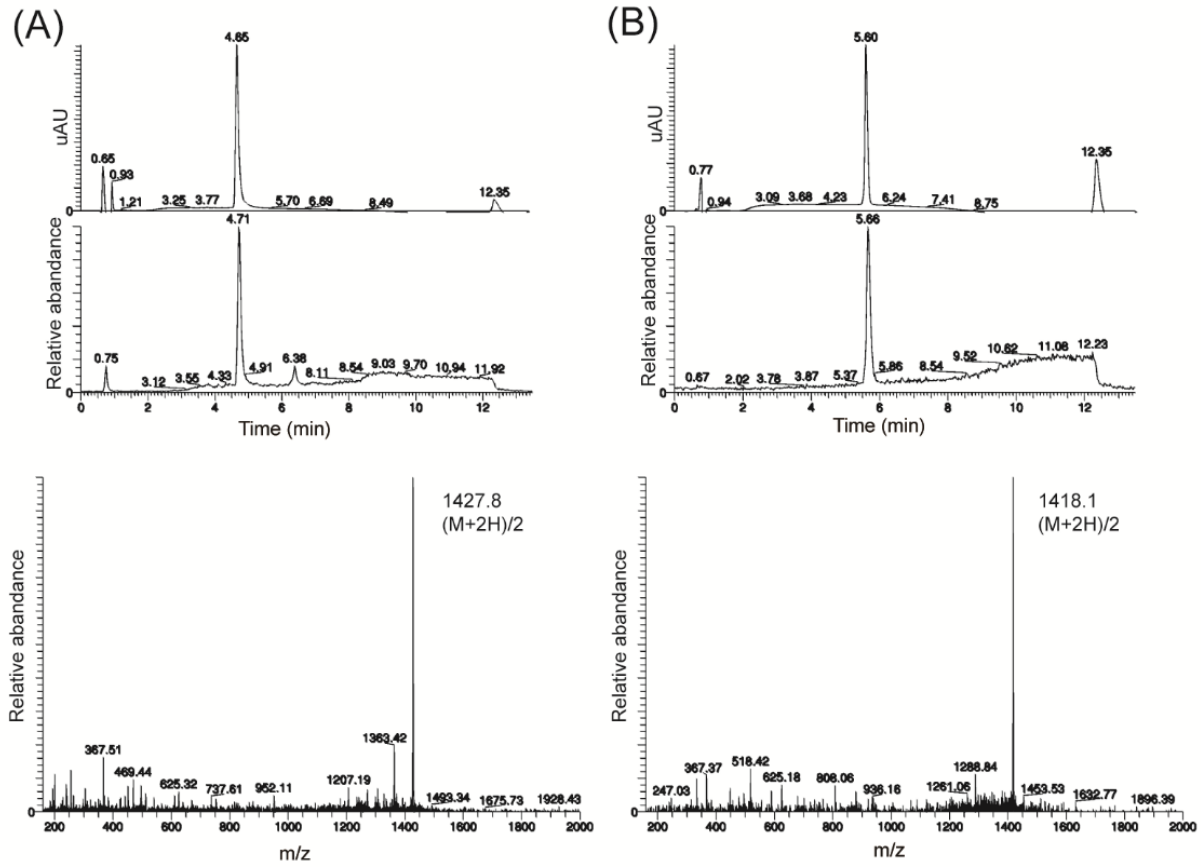

Figure S2. *LC-MS spectra of purified (A) W(KIAALKE)$_3$-PEG$_4$-Cys and (B) Y(EIAALEK)$_3$-PEG$_4$-Cys.*

Chapter 7

Summary and Perspectives

As early as the 1950s, a variety of hydrogels have been designed, characterized and evaluated for biomedical applications. Commercial products based on hydrogels include contact lenses, wound dressings and hygiene products, due to their high water absorption, porosity and unique mechanical properties. In the last two decades, the focus has shifted to explore the potential of hydrogels in the fields of drug delivery and tissue engineering. As a result, the design of hydrogels evolved from relatively simple chemical or physical crosslinked networks to complex multicomponent systems with a high level of spatial and temporal control. The specific demand for multi-functional and well-controlled hydrogels resulted in the development of networks with novel synthetic methodologies and dynamic chemistry/assembly strategies.

In this thesis, new crosslinked hydrogels were designed and applications of these materials in the field of drug delivery were explored. These hydrogels mainly consist of the neutral polysaccharide dextran (Dex) due to its favorable properties like its biodegradable and biocompatible nature, relatively low cost, good water-solubility, and ease of chemical modification.

Inspired by natural systems, novel drug delivery platforms were established in which human serum albumin (HSA) acts simultaneously as an affinity-based drug carrier and crosslinker. **Chapter 2** focuses on the modification of HSA by thiolation, using it to crosslink a maleimide modified dextran (Dex-Mal) polymer, and the sustained delivery of low molecular drugs. To maintain the drug-binding capability of albumin, 2-iminothiolane was used to introduce thiols to albumin, which prevents denaturation by maintaining the surface charge distribution. A further extension of this work on affinity-based drug delivery hydrogels can be to use thiolated albumin in combination with other covalent polymers functionalized with Michael acceptors to gain access to hydrogel materials with a range of properties.

In **Chapter 3**, two approaches were explored to improve the stability and mechanical properties of the dextran-albumin hydrogels. In the first approach, the modification of dextran with vinyl sulfone through an ether linkage to reduce crosslinker hydrolysis was studied. The second approach involved the introduction of a third macromolecular precursor, poly(ethylene glycol) end-functionalized with thiol groups, to the dextran-albumin hydrogel system in order to tune the gelation kinetics and physical properties. The resulting Dex(VS)-sHSA-PEG hydrogels showed improved stability and increased mechanical stiffness making it more suitable for sustained drug delivery applications.

Besides the use of these gels as a drug delivery tool, other applications of these hydrogels were explored in **Chapter 4** and **5**. The uptake of a low molecular weight drug in a zebrafish embryo toxicity assay using the dextran based crosslinked drug carriers was studied in **Chapter 4**. The model drug valproate was solubilized using β-Cyclodextrins conjugated to a dextran-PEG network.

These Dex-CD/PEG carriers (without valproate) were taken up by 4-days post fertilization old (4-dpf) zebrafish embryos into the gastrointestinal tract. Next, 4-dpf zebrafish embryos were exposed to the model drug valproate, which was encapsulated in the drug carrier. As a result, the zebrafish embryos became more sensitive toward valproate strongly suggesting that the Dex-CD/PEG drug carriers are indeed capable of improving its uptake efficiency in the zebrafish embryo toxicity assay. Our results indicate that the Dex-CD/PEG carriers may assist zebrafish embryo-based toxicity assays of any drug that is able to form an inclusion complex with β-cyclodextrin.

Giant unilamellar vesicles (GUV) are used to study membrane biophysics and membrane related processes in general. In **Chapter 5**, a new method to form GUVs using hydrogel film-assisted hydration of a lipid film was established. A thin layer of a hydrogel was formed by a Michael addition reaction between maleimide-modified dextran and dithiol terminated poly(ethylene glycol) on a thiolated glass slide. Covalently linking the hydrogel film to the glass slides ensures that the formed GUVs are not contaminated with polymer fragments. Upon hydration of the polymer film using a buffer of physiological ionic strength, GUVs were formed rapidly in a high yield. The yield and size distribution of the formed GUVs were systematically investigated by varying the hydrogel composition. In order to obtain GUVs with a narrow size distribution in high yield, it was essential that the hydrogel films had a continuous pore structure with a suitable size. Also, the interactions between the lipid components and hydrophilic polymers is an important factor for successful GUV formation. Compared to electroformation methods, this method requires no special equipment and is applicable to any lipid formulation in high ionic strength buffer. This hydrogel film-assisted hydration method generates GUVs within minutes in high yield making it an easy to use method.

In **Chapter 6**, the heterodimeric coiled-coil forming peptides **E** and **K**, were conjugated to dextran in order to direct its self-assembly through non-covalent interactions. The peptides were conjugated either on their C- or N-terminus to dextran, resulting in four multivalent peptide-dextran conjugates. It was observed that the peptide conformation was altered after conjugation to dextran. Formation of large aggregates between dextran-peptide **E** and dextran-peptide **K** conjugates was revealed by dynamic light scattering measurements. However no specific coiled-coil interaction could be observed in fluorescence resonance energy transfer studies. This might be due to homomeric (**K**/**K**) coiled-coil formation in dextran-peptide **K** preventing heteromeric coiled-coil (**E**/**K**) formation. Furthermore, coiled-coil formation may be hampered by steric effects as a result of polymer-peptide conjugation.

In summary, this thesis describes the development of dextran-based hydrogels which can be tuned within a wide range of physicochemical properties for a given application. Moreover, this thesis also explores emerging applications of hydrogels in fields of biophysics and toxicology.

Regarding the use of hydrogels for albumin drug delivery, the binding pockets of albumin were utilized to construct hydrogels for spatial and temporal control over the release of therapeutic agents. Their sustained release was proven with several different drugs in our studies, but further optimization is required. Drug release from these hydrogels involves two stages: the release of the drug from the binding cavities, and subsequent drug diffusion through the insoluble polymer network. Computational simulations of the release process may provide a deeper insight into the release mechanism. From these studies, correlation between drug-albumin binding coefficients and release kinetics from the hydrogel can be established and thus aid in the further design optimization of these materials. Co-delivery of both hydrophobic and hydrophilic therapeutic agents from the various parts of the hydrogel may also be an interesting direction for further investigation.

Regarding the emerging applications of hydrogels described in this thesis, the crosslinked dextran-PEG hydrogel films provide a facile method to prepare GUVs with and without cargo, while the crosslinked Dex-CD/PEG carriers improve the uptake efficiency of low molecular weight compounds like valproate in a zebrafish embryo toxicity assay. It is expected that this method is suited to enhance the uptake of any compound that is able to form host-guest complex with β-cyclodextrin. Besides establishing these new approaches, a fundamental aspect of polymer science is explored in this thesis: orthogonal crosslinking methods in polymer networks and examination of their corresponding physiochemical properties. By careful design of the hydrogel building blocks, defects and inhomogeneities of the polymeric network could be reduced thereby resulting in better performance with respect to reproducibility and application.

Regarding the development of new biomolecule-dextran derivatives, the conjugation between the dextran polymer and biomolecules such as peptides, proteins and nucleic acids seems to be straightforward. However, it becomes apparent that the structure, conformation and functionality of the resulting multivalent biomolecule-dextran conjugates may be more complex than initially expected. Therefore it is necessary in the future to focus on the detailed interactions of biomolecules grafted to dextran backbones as the local environment may interfere with the biomolecule function. The distribution of the polymer grafts on the polymeric backbone and the distance between outer ends of polymer grafts as well as the polymeric backbone may also be important to be able to evaluate these interactions. However designing experiments that could reveal these parameters is not trivial. Nevertheless, a thorough understanding of the newly developed biomolecule-dextran derivatives can assist in their future design.

Tremendous progress was achieved over the years in the design of hydrogels as evidenced by the vast body of literature. Recent developments include the design of multi-component hydrogel systems to meet the needs of increasingly complex scaffolds for a wide range of biomedical applications. To this end, novel hydrogel systems are also designed for facilitating simple and

controllable manipulations such as *in situ* forming and 3D printed hydrogels. By continuing investigation in this research field, new frontiers and lasting contributions to polymer and biomedical sciences are within reach.

SAMENVATTING

Al in de jaren 50 van de vorige eeuw werden verschillende hydrogelen ontworpen, gekarakteriseerd en geëvalueerd voor biomedische toepassingen. Commerciële producten op basis van hydrogelen omvatten onder anderen contactlenzen, wondverbanden en hygiëneproducten, vanwege hun hoge wateropname, porositeit en unieke mechanische eigenschappen. In de laatste twee decennia is de focus verschoven om het potentieel van hydrogelen op het gebied van medicijnafgifte en weefselmanipulatie te onderzoeken. Als gevolg daarvan evolueerde het ontwerp van hydrogelen van relatief eenvoudige chemische of fysisch verknoopte netwerken naar complexe multicomponent-systemen met een hoge mate van ruimtelijke en temporele controle. De specifieke vraag naar multifunctionele en goed gecontroleerde hydrogelen resulteerde in de ontwikkeling van netwerken door gebruik te maken van nieuwe synthetische methodologieën en dynamische chemie en assemblagestrategieën.

In dit proefschrift werden nieuwe gecrosslinkte hydrogelen ontworpen en werden toepassingen van deze materialen op het gebied van drug delivery onderzocht. Deze hydrogelen bestaan voornamelijk uit het neutrale polysaccharide dextraan (Dex) vanwege de gunstige eigenschappen zoals de biologische afbreekbaarheid en biocompatibiliteit, relatief lage kosten, goede wateroplosbaarheid en het gemak van chemische modificatie.

Geïnspireerd door natuurlijke systemen werden nieuwe medicijnafgifte (drug delivery) platforms opgezet waarin humaan serumalbumine (HSA) gelijktijdig gebruikt werd als een affinity-based drug carrier en crosslinker. **Hoofdstuk 2** richt zich op de thiol-modificatie van HSA, om het vervolgens te crosslinken aan een maleïmide-gemodificeerd dextraan (Dex-Mal) polymeer, en de afgifte van laagmoleculaire medicijnen te bestuderen. Om het medicijn-bindend vermogen van albumine te behouden, werd 2-iminothiolaan gebruikt, wat denaturatie voorkomt door de verdeling van de oppervlaktelading te handhaven. Een verdere uitbreiding van deze studie aan hydrogelen op basis van affinity-based drugs kan zijn om gethioleerd albumine te gebruiken in combinatie met andere covalente polymeren die gefunctionaliseerd zijn met Michael-acceptoren om zo hydrogelmaterialen met verschillende materiaaleigenschappen te genereren.

In **Hoofdstuk 3** werden twee methoden onderzocht om de stabiliteit en mechanische eigenschappen van dextraan-albumine hydrogelen te verbeteren. In de eerste benadering werd de modificatie van dextraan met vinylsulfon bestudeerd om de hydrogel stabieler te maken. De tweede benadering bestond uit de toevoeging van een derde macromoleculaire precursor, poly(ethyleenglycol) met thiol eindgroepen, aan het dextran-albumine hydrogel systeem om hiermee de kinetiek van hydrogelvorming en de resulterende fysische eigenschappen beter te controleren. Deze Dex(VS)-sHSA-PEG-hydrogelen vertoonden een verbeterde stabiliteit en

verhoogde mechanische stijfheid, waardoor ze meer geschikt zijn voor langdurige afgifte van medicijnen.

Naast het gebruik van deze gels als drug delivery tool, werden andere toepassingen onderzocht. De opname van een laagmoleculair medicijn in een zebravis-embryo met behulp van de op dextraan gebaseerde geconjugeerde drug carriers werd bestudeerd in **Hoofdstuk 4**. Het geneesmiddel valproaat werd met behulp van β-cyclodextrines ge-encapsuleerd in een dextraan-PEG-netwerk. Deze Dex-CD/PEG-carriers (zonder valproaat) werden succesvol opgenomen in het maagdarmkanaal van 4 dagen oude zebravis-embryo's. Vervolgens werden zebravisembryo's blootgesteld aan valproaat, dat in deze nieuwe materialen was ge-encapsuleerd. Als gevolg hiervan werden de zebravisembryo's gevoeliger voor valproaat, wat laat zien dat de Dex-CD/PEG-carriers de opname van valproaat verbetert. Deze resultaten geven aan dat de Dex-CD/PEG-carriers kunnen helpen bij toxiciteitstesten met zebravis-embryo's van geneesmiddelen die in staat zijn om een inclusiecomplex te vormen met β-cyclodextrine.

Grote unilamillaire vesicles (GUV) worden vaak gebruikt in de membraanbiofysica om membraangerelateerde processen te bestuderen. In **Hoofdstuk 5** wordt een nieuwe methode voor het vormen van GUV's met hydrogelfilm-geassisteerde hydratatie van een lipidefilm beschreven. Een dunne laag van een hydrogel werd gevormd door een Michael-additiereactie tussen maleïmide gemodificeerd dextraan en poly(ethyleenglycol) met thiol eindgroepen op een microscoop glaasje dat voorbehandeld was met thiolgroepen. Het covalent koppelen van de hydrogelfilm aan de glasplaatjes zorgt ervoor dat de gevormde GUV's niet verontreinigd zijn met hydrogel(fragmenten). Na hydratatie van de polymeerfilm met behulp van een buffer van fysiologische ionsterkte werden GUV's snel in een hoge opbrengst gevormd. De opbrengst en grootteverdeling van de gevormde GUV's werden systematisch onderzocht door de hydrogel-samenstelling te variëren. Om een hoge opbrengst van GUV's met eenzelfde diameter te verkrijgen, was het essentieel dat de hydrogelfilms een continue poriestructuur met een geschikte grootte hadden. Bovendien zijn de interacties tussen de lipide-componenten en hydrofiele polymeren een belangrijke factor voor succesvolle GUV-vorming. In tegenstelling tot andere methodes vereist deze methode geen speciale apparatuur en kan toegepast worden op elke lipide-formulering in buffers met hoge ionsterkte. Deze hydrogelfilm-ondersteunde hydratatiemethode genereert binnen enkele minuten GUV's in hoge opbrengst waardoor het een eenvoudig te gebruiken methode is.

In **Hoofdstuk 6** werden de heterodimeer coiled-coil vormende peptiden **E** en **K** gekoppeld aan dextraan om de zelfassemblage te controleren via niet-covalente interacties. De peptiden werden via de C- of N-terminus aan dextraan gekoppeld, wat resulteerde in vier verschillende multivalente peptide-dextraan conjugaten. Door binding aan dextraan veranderde de secundaire structuur van de peptides. Met behulp van dynamische lichtverstrooiingsmetingen werd duidelijk dat er grote

aggregaten tussen dextraan-peptide **E** en dextraan-peptide **K**-conjugaten gevormd werden. Er kon echter geen specifieke coiled-coil interactie worden waargenomen met fluorescentieresonantie-energieoverdracht (FRET). Een mogelijke verklaring is de vorming van homocoil (**K**/**K**) complexen in dextraan-peptide **K** waardoor heteromeer coiled-coil (**E**/**K**)-vorming niet meer mogelijk is. Verder kan coiled-coil vorming belemmerd worden door sterische hindering als gevolg van polymeer-peptide-koppeling.

Samengevat beschrijft dit proefschrift de ontwikkeling van dextraan-gebaseerde hydrogelen waarvan de fysisch-chemische eigenschappen kunnen worden afgestemd voor iedere gewenste toepassing. Bovendien wordt in dit proefschrift ook nieuwe toepassingen van hydrogelen op het gebied van biofysica en toxicologie onderzocht en beschreven.

Met betrekking tot het gebruik van hydrogelen voor medicijnafgifte, werden de bindingspockets van albumine gebruikt om hydrogelen te ontwerpen voor ruimtelijke en temporele controle over de afgifte van therapeutische middelen. Langdurige afgifte werd aangetoond voor verschillende medicijnen in deze studie, maar verdere optimalisatie is vereist. Geneesmiddelafgifte van deze hydrogelen omvat twee stadia: de afgifte van het medicijn uit de bindingsholtes en daaropvolgende geneesmiddeldiffusie door het onoplosbare polymeernetwerk. Computersimulaties van het afgifte-proces kan een dieper inzicht verschaffen in het afgifte-mechanisme. Uit deze studies kan de correlatie tussen geneesmiddel-albuminebindingscoëfficiënten en afgiftekinetiek van de hydrogel worden bepaald en bijdragen aan de verdere optimalisatie van deze materialen. Gelijktijdige afgifte van zowel hydrofobe als hydrofiele therapeutische middelen uit de verschillende delen van de hydrogel kan ook een interessante richting zijn voor verder onderzoek.

Met betrekking tot de nieuwe toepassingen van hydrogelen die in dit proefschrift worden beschreven, bieden de gecrosslinkte dextraan-PEG-hydrogelfilms een gemakkelijke methode om GUV's met en zonder lading te bereiden, terwijl de gecrosslinkte Dex-CD/PEG-dragers de opname-efficiëntie van medicijnen met een laag molecuulgewicht zoals valproaat verbeteren in een toxiciteit test. Naar verwachting is deze methode geschikt om de opname van elke verbinding die in staat is om een inclusiecomplex te vormen met β-cyclodextrine te verhogen. Naast het vaststellen van deze nieuwe benaderingen, werd in dit proefschrift een fundamenteel aspect van de polymeerwetenschap onderzocht: orthogonale methoden voor het crosslinken van polymeernetwerken en onderzoek van de resulterende fysisch-chemische eigenschappen. Door het zorgvuldig ontwerpen van de hydrogelbouwstenen kunnen defecten en inhomogeniteiten van het polymeer netwerk verminderd worden, resulterend in betere prestaties met betrekking tot reproduceerbaarheid en daadwerkelijke toepassing van deze materialen.

Met betrekking tot de ontwikkeling van nieuwe biomolecuul-dextraanderivaten is de conjugatie

tussen dextraan en biomoleculen zoals peptiden, eiwitten en nucleïnezuren eenvoudig. Dit proefschrift laat echter zien dat de structuur, conformatie en functionaliteit van de resulterende multivalente biomolecuul-dextraan conjugaten complexer kunnen zijn dan aanvankelijk werd verwacht. Daarom is het in de toekomst noodzakelijk om de interacties van biomoleculen gekoppeld aan dextraan te bestuderen, aangezien de lokale omgeving invloed heeft op de functionaliteit van de biomoleculen.. Het ontwerpen van experimenten die deze interacties onthullen, is echter niet triviaal. Niettemin kan een grondig begrip van de nieuw ontwikkelde biomolecuul-dextraan-conjugaten helpen bij hun toekomstige ontwerp.

Door de jaren heen is er enorme vooruitgang geboekt in het ontwerp van hydrogelen, zoals blijkt uit de enorme hoeveelheid literatuur. Recente ontwikkelingen omvatten het ontwerp van multicomponent hydrogel-systemen om te voldoen aan de behoeften van steeds complexere materialen voor een breed scala van biomedische toepassingen. Voor dit doel zijn nieuwe hydrogelsystemen ontworpen voor het vergemakkelijken van eenvoudige en regelbare manipulaties zoals *in situ* vormende en 3D-geprinte hydrogelen. Door voortzetting van het onderzoek op dit gebied, liggen nieuwe grenzen en duurzame bijdragen aan polymeer- en biomedische wetenschappen binnen handbereik.

LIST OF ABBREVIATIONS

2-IT	2-iminothiolane
3D	three-dimensional
ATRP	atom transfer radical polymerization
CD	circular dichroism
CDI	1,1'-carbonyldiimidazole
CH	cholesterol
Cryo-SEM	Cryo-scanning electron microscopy
dex-RhoB	rhodamine B labelled dextrans
DIC	N,N'-diisopropylcarbodiimide
DIPEA	diisopropylethylamine
DLS	dynamic light scattering
DMAP	dimethylaminopyridine
DMF	dimethylformamide
DMSO	dimethyl sulfoxide
DOPC	1,2-dioleoyl-sn-glycero-3-phosphocholine
DOPE	1,2-dioleoyl-sn-glycero-3-phosphoethanolamine
DOX	doxorubicin
DPPC	1,2-dipalmitoyl-sn-glycero-3-phosphocholine
DPTS	4-(dimethylamino)pyridinium 4-toluenesulfonate
DT	degrees of thiolation
DTNB	5,5'-dithiobis(2-nitrobenzoic acid)
DVS	divinyl sulfone
DXM	dexamethasone
EDT	1,2-ethanedithiol
ESR	equilibrium swelling ratio
FACS	fluorescence activated cell sorting
FRET	fluorescence resonance energy transfer
G'	storage modulus
G"	loss modulus
GUVs	giant unilamellar vesicles
HCTU	O-(1H-6-Chlorobenzotriazole-1-yl)-1,1,3,3-tetramethyluronium hexafluorophosphate
HSA	human serum albumin
IBU	ibuprofen
kDa	kilodaltons
Mal	maleimide
MSCD	mono-thiolated β-cyclodextrins
NMP	N-methylpyrrolidine
PBS	phosphate buffered saline
PEG	polyethylene glycol
PEG-DT	poly(ethylene glycol) dithiol
POPC	1-palmitoyl-2-oleoyl-sn-glycero-3-phosphocholine
POPG	1-palmitoyl-2-oleoyl-sn-glycero-3-phospho-(1'-rac-glycerol)
PTSA	p-toluene sulfonic acid monohydrate

PTX	paclitaxel
PVA	poly(vinyl alcohol)
RAFT	reversible addition-fragmentation chain transfer
RP-HPLC	reversed-phase high performance liquid chromatography
sHSA	thiolated human serum albumin
TFA	trifluoroacetic acid
TIS	triisopropylsilane
VS	vinyl sulfone

CURRICULUM VITAE

Yue Gao was born on 15th January, 1986 in Changchun City, Jilin Province, China. In 2003, she was enrolled in a four-year bachelor's program of the College of Chemistry of Beijing Normal University. She did her first research internship in the Instrumental Analysis Center of Beijing Normal University to investigate the degradation of gel pen ink under different circumstances. She then chose a specialization in polymer science and conducted her undergraduate thesis project in the Institute of Polymer chemistry and physics, under the guidance of Prof. Huiliang Wang. There she applied aliphatic ketones and aldehydes as water-soluble photoinitiators for photografting and photopolymerization in aqueous solutions. In 2007, she continued her master study under the supervision of Prof. Huiliang Wang. Her master's research focused on the preparation of cross-linked poly(n-vinylpyrrolidone) / poly(acrylic acid) hydrogels by photopolymerization and used compression and tensile tests to characterize the hydrogels' properties. In July, 2010, she graduated with a MSc degree in polymer chemistry and physics.

In September, 2010, with a scholarship from China Scholarship Council, Yue joined the Supramolecular and Biomaterials Chemistry (SBC) group of Prof. Alexander Kros at Leiden University in the Netherlands as a PhD candidate. There, she studied the design and preparation of dextran based hydrogels for drug delivery and explored versatile applications of polymeric cross-linked networks.

Since 2016, she works as a consultant for biotechnology companies in an intellectual property consulting corporation in Shenzhen City, Guangdong Province, China and has obtained her patent agent certificate in 2017.

LIST OF PUBLICATIONS

1. Tu, J.; Bussmann, J.; Du, G.; Gao, Y.; Bouwstra, J. A.; Kros, A., Lipid bilayer-coated mesoporous silica nanoparticles carrying bovine hemoglobin towards an erythrocyte mimic. *International Journal of Pharmaceutics* **2018**, 543 (1), 169-178.

2. Noteborn, W. E. M.; Gao, Y.; Jesse, W.; Kros, A.; Kieltyka, R. E., Dual-Crosslinked Human Serum Albumin-Polymer Hydrogels for Affinity-Based Drug Delivery. *Macromolecular Materials and Engineering* **2017**, 302 (10), 1700243.

3. Mora, N. L.; Gao, Y.; Gutierrez, M. G.; Peruzzi, J.; Bakker, I.; Peters, R. J. R. W.; Siewert, B.; Bonnet, S.; Kieltyka, R. E.; van Hest, J. C. M.; Malmstadt, N.; Kros, A., Evaluation of dextran(ethylene glycol) hydrogel films for giant unilamellar lipid vesicle production and their application for the encapsulation of polymersomes. *Soft Matter* **2017**, 13 (33), 5580-5588.

4. Gao, Y.; Kieltyka, R. E.; Jesse, W.; Norder, B.; Korobko, A. V.; Kros, A., Thiolated human serum albumin cross-linked dextran hydrogels as a macroscale delivery system. *Soft Matter* **2014**, 10 (27), 4869-4874.

5. Lopez Mora, N.; Hansen, J. S.; Gao, Y.; Ronald, A. A.; Kieltyka, R.; Malmstadt, N.; Kros, A., Preparation of size tunable giant vesicles from cross-linked dextran(ethylene glycol) hydrogels. *Chemical Communications* **2014**, 50 (16), 1953-1955.

6. Guo, R.; Gao, Y.; Wu, M.; Wang, H., Aliphatic ketones and aldehydes as water-soluble photoinitiators for the photopolymerization of methacrylic acid. *Polymer* **2013**, 54 (18), 4940-4947.

7. Jin, E.; Xie, M.; Gao, Y.; Wang, H., Effect of Acid and pH Value on the Photografting Initiated by Aliphatic Ketones in Aqueous Solutions. *Journal of Applied Polymer Science* **2011**, 120 (2), 701-709.

8. Liu, Y.-Z.; Yu, J.; Xie, M.-X.; Chen, Y.; Jiang, G.-Y.; Gao, Y., Studies on the degradation of blue gel pen dyes by ion-pairing high performance liquid chromatography and electrospray tandem mass spectrometry. *Journal of Chromatography A* **2006**, 1125 (1), 95-103.